

Hairy Switches and Oscillators
Reconstructing the Zebrafish Segmentation Clock

DISSERTATION

zur Erlangung des akademischen Grades

Doctor rerum naturalium
(Dr. rer. nat)

vorgelegt

der Fakultät Mathematik und Naturwissenschaften
der Technischen Universität Dresden

von

ANNELIE OSWALD

geboren am 29. Mai 1983 in Dresden

Eingereicht am 7. August 2013

Verteidigt am 30. Januar 2014

Gutachter: Prof. Dr. Francis Stewart, BIOTEC TU-Dresden, Germany
Prof. Dr. Andrew C. Oates, UCL, United Kingdom

"What I cannot create, I do not understand."

-Richard Feynman

Summary of Thesis

Formation of segments during vertebrate embryogenesis is regulated by a biological clock. Models and experimental data indicate that the core of this clock consists of a cell-autonomous single cell oscillator. This oscillator likely involves a genetic feedback loop of transcriptional repressors belonging to the *hairy* gene family. In zebrafish, three *her* genes, *her1*, *hes6* and *her7*, have been identified as core oscillator components.

The main purpose of this project was to study the molecular mechanism of the *hairy* gene negative feedback oscillator in single cells. To determine whether a single cell oscillator is part of the zebrafish segmentation clock, a cell dissociation protocol was established to track the expression of Her1 *ex vivo*. Upon dissociation, Her1 expression continued to oscillate for up to three cycles. The period of oscillations was significantly slower than that of the segmentation clock, but appears to speed up in the presence of serum.

To test whether the *hairy* gene interactions are sufficient to generate oscillations in single cells, a protocol was established that uses synthetic biology principles to design, construct and characterize *hairy* gene networks in yeast. First a library of network parts, containing *hairy* genes, promoters and Her binding sites was generated and subsequently assembled into simple devices to test their functionality in yeast. The three core oscillator components, Her1, Hes6 and Her7, were characterized and optimized for expression in yeast. In the SWITCH-OFF assay, the Her1 protein, modified with a MigED yeast repressor domain, was found to function as a transcriptional repressor in yeast, while Hes6 with the same modification can not.

The dissociation of segmentation clock cells provides the first direct evidence that single cell oscillators exist in zebrafish. In this system, oscillator dynamics can be studied without the interactions of higher level clock components. In parallel, establishing a yeast chassis for *hairy* gene networks provides a novel technique to directly test predicted oscillator mechanisms by constructing them 'bottom up'.

Contents

Summary of Thesis	i
List of Figures	vi
List of Tables	vii
List of Abbreviations	viii
1 Introduction	1
1.1 Vertebrate Somitogenesis	2
1.2 The 3 Tiered Segmentation Clock Model	4
1.2.1 BOTTOM Tier: Single Cell Oscillators	5
1.2.2 MIDDLE Tier: Local Regulation via Cell-Cell Oscillator Syn- chronization	8
1.2.3 TOP Tier: Global Regulation of Oscillator Frequency and Arrest within the PSM	10
1.3 The <i>Hairy</i> Gene Oscillator	11
1.3.1 The Zebrafish's Core Oscillator	12
1.3.2 Oscillator Terminology	16
1.4 Open Questions	17
1.5 The Synthetic Biology Approach	18
1.5.1 SynBio from <i>parts</i> to <i>devices</i> and <i>systems</i>	19
1.5.2 Synthetic Oscillators	21
1.5.3 Design Considerations for the SynBio Oscillator	24
2 Aims	28
3 Methods	29
3.1 Fish Care and Preparation	29

Contents

3.1.1	PSM Tissue Explants	29
3.1.2	PSM Cell Dissociation	29
3.2	<i>E. coli</i> Plasmid Transformation	30
3.3	Gateway (GW) Cloning of Yeast Vectors	30
3.3.1	LR and BP reactions, generating <i>Expression</i> and <i>Entry</i> Vectors	32
3.3.2	2-step <i>Entry</i> PCR	33
3.3.3	Generating <i>Destination</i> Vectors	33
3.4	Yeast Plasmid Transformation	34
3.4.1	Yeast Integrative Plasmid Colony Screen	34
3.5	Yeast Storage	35
3.6	Yeast Imaging Preparations	35
3.6.1	ConA Dish Coating & Cell Seeding	36
3.6.2	Protein Degradation	36
3.7	Microscopy	36
3.7.1	Explanted PSM Imaging	36
3.7.2	PSM Cell Imaging	37
3.7.3	Yeast Cell Imaging	37
3.8	Image Processing & Data Analysis	38
3.8.1	Extracting Fluorescent Signals per Cell over Time	38
3.8.2	Generating PSM Kymographs	38
3.8.3	Period Estimate from PSM cells	38
3.8.4	Yeast Reporter Response Measurements	39
3.8.5	Protein Half-Life Estimates	39
3.9	Statistics	40
4	Materials	42
4.1	Chemicals	42
4.2	Enzymes	42
4.3	DNA	42
4.4	Buffers and Solutions	44
4.5	Genetically Modified Organisms	47
4.5.1	Zebrafish Strains	47
4.5.2	Bacterial Strains	47

4.5.3	Yeast Strains	48
5	Results and Discussion	49
5.1	PART1: The Segmentation Oscillator within Isolated PSM Cells . . .	49
5.1.1	Explanted PSM Tissue In Culture	50
5.1.2	Isolated PSM Cells In Culture	52
5.2	PART1: Discussion	54
5.2.1	Explanation of Slowed Oscillator Period in Isolated Cells . . .	54
5.2.2	Isolated PSM cells: applications and future experiments	56
5.3	PART1: Conclusion	57
5.4	PART2: Synthetic Segmentation Oscillator Network in Yeast	58
5.4.1	The Minimal Oscillator Model	59
5.4.2	Part & Device Design	60
5.4.3	Construction	65
5.4.4	Part & Device Characterization	67
5.5	PART2: Discussion	80
5.5.1	Implications of Part Properties on OSCILLATOR Design . . .	80
5.5.2	Synthetic Oscillator Applications and Considerations	86
5.6	PART2: Conclusion	87
	Appendix	89
	Acknowledgements	91

List of Figures

1.1	The Three-Tiered Model	4
1.2	Cyclic Expression Patterns of the Segmentation Clock	6
1.3	Cyclic Genes found in PSM of Mouse, Chick and Zebrafish	7
1.4	Her proteins	11
1.5	Zebrafish Segmentation Clock Oscillator Model	14
1.6	Oscillator Behaviour	16
1.7	Construction Stages of SynBio Networks	20
1.8	Synthetic Oscillator Networks	22
3.1	Gateway Cloning Scheme	31
3.2	Half-Life Decay Curve Fit Model	40
5.1	Extraction of PSM Tissue and Isolation of Cells	49
5.2	Explant PSM of <i>Looping</i> fish	50
5.3	Oscillating PSM Cells	52
5.4	Oscillatory Periods in Explanted PSM and isolated PSM cells	53
5.5	SynBio Experimental Workflow	58
5.6	The Minimal Her1 Oscillator Model	59
5.7	Her SWITCH-OFF Assay	61
5.8	Library of Parts	62
5.9	Final Device Construction	65
5.10	Heterologous expression of <i>hairy</i> genes in yeast	68
5.11	Inducible Promoters: <i>pGAL</i> versus <i>pCUP</i>	71
5.12	SWITCH-OFF: Single Cell Traces	73
5.13	Switch Assay - Reporter Response	75
5.14	SWITCH-OFF in yeast: MigED vs. WRPW	76
5.15	Her Part Degradation Curves	78
5.16	Half Life Values of Her parts.	79

5.17 Her1 Oscillator Model	81
5.18 Effects of Model Parameters on OSCILLATOR expression.	85

List of Tables

1.1 Her proteins associated with zebrafish somitogenesis.	13
4.1 List of Plasmids	43
4.2 List of Oligos and Primers	44
4.3 Buffers and Solution	47
4.4 <i>E.coli</i> Strains	48
4.5 <i>S.cerevisiae</i> Strains	48
5.1 Parameters used for Theoretical Oscillator Model	84

List of Abbreviations

AP	Anteroposterior
BF	Brightfield
bHLH	basic Helix-Loop-Helix
bp	base pairs
CFP	Cyan Fluorescent Protein
CFP-SFC	CFP signal fold change
COI	circle of interest
FGF	fibroblast growth factor
GOF	gain of function
GOI	gene of interest
GW	Gateway
HL	half-life
KD	knock down
L15+	L15 medium with FBS
L15-	serum-free L15 medium
LOF	loss of function
LOI	Line of Interest
NLS	Nuclear Localization Signal
ORF	Open Reading Frame
PA axis	posterior to anterior axis
PCR	Polymerase chain reaction
PSM	Presomitic Mesoderm
RA	retinoic acid
ROI	Region Of Interest
SC	synthetic complete medium
SD	standard deviation
SNR	Signal to Noise Ratio
YFP	Yellow Fluorescent Protein

1 Introduction

The ability to 'tell' time is an important feature of all living things on earth. Internal 'biological clocks' signal when to eat, sleep, wake, mate, hibernate, etc. and thereby coordinate an organism's activity with the natural rhythms in their environment. While these behavioral rhythms are the most obvious outputs of biological clocks, cyclic processes are found in all levels of biological organization from oscillating gene expression (*per* genes of the circadian clock) and molecule concentrations (calcium ions in nerve cells) to coordinated pulsing in tissues (heart beat) and groups of organisms (firefly blinking).

The underlying mechanisms of these biological clocks are complex and not well understood. For example, the vertebrate segmentation clock, which regulates the developmental timing of body axis segmentation in embryos, spans multiple levels of organization from oscillations in single cells to signalling waves at the tissue level. *In silico* theoretical modelling in combination with molecule labelling, gene knock-downs and tissue manipulation suggest that a simple gene oscillator is the core pacemaker unit of this clock. However, definitive proof that this gene network is sufficient to generate timing has not been provided using 'top-down' experimental techniques.

Therefore, we propose a synthetic biology inspired assay to study this specific oscillator network by reconstructing it *de novo*. Instead of progressively breaking the clock using 'top down' experimental techniques, such as gene knock-downs, we can thus study the underlying logic of this network 'bottom-up' using engineering principles to subsequently piece together functional subunits. Building up a network not only tests whether it can function as predicted, but also elucidates how features of network components relate to the clock's overall dynamic properties. Ultimately, the characterization of this synthetic oscillator can be used to improve the parameter space of current segmentation clock models and directly link its structural and functional properties.

In this introduction, I will first review the evidence that somitogenesis in vertebrates is regulated by a biological clock. Then I will describe the current model of the vertebrate segmentation clock in general and the mechanism proposed for the simple segmentation oscillator in zebrafish specifically. And finally, I will examine how a synthetic biology approach can be used to study this biological clock 'bottom-up'.

1.1 Vertebrate Somitogenesis

Somitogenesis is an important and complex event of vertebrate embryogenesis. During development, somitogenesis patterns the embryo's body axis into repeated segments. These structures, called somites, each give rise to a number of different tissues, including skeletal muscle and cartilage. Their formation is crucial for the development of segmented structures in the adult animal, such as peripheral spinal nerves, axial muscle and vertebrae [Saga and Takeda, 2001]. In fact, the mechanism of somitogenesis is conserved between different vertebrate species [Gomez et al., 2008]. However, while the number of somites between individuals of one species is invariant, the number of segments varies greatly between species, from 10 in frogs, 31 in zebrafish and more than 300 in certain snakes. So while these aspects have turned somitogenesis into a hallmark model for segmental patterning processes in embryos, [Baker et al., 2006], somitogenesis has long been of interest to developmental biologists because it involves the coordination of patterning and growth of a tissue by a regularly repeated morphogenetic process [Oates et al., 2012].

Somitogenesis is a dynamic, sequential and rhythmic process. Somites are blocks of cells that form bilaterally on either side of the notochord. The precursors of these cells are derived from the presomitic mesoderm (PSM), the unsegmented tissue at the posterior end of the embryo. As the embryo grows and extends, cells feed into the posterior PSM from the tailbud and are sequestered in discrete time intervals as somites at the anterior. Over time the PSM shrinks until it disappears at the completion of somitogenesis. The time interval between somite formation, termed somitogenesis period, is mostly constant throughout development, only slowing towards the end of somitogenesis when the PSM is diminishing [Schröter et al., 2008]. This period differs between species and depends greatly on temperature [Kimmel

et al., 2005], but varies little within individuals of one species [Schröter et al., 2008]. In zebrafish somitegenesis period is as fast as 18min at 30°C and slows below 55min at 20°C, yet varies less than 2min, equal to 1 standard deviation (SD), between animals at a each temperature. Impressively, somitogenesis seems to be regulated with clock-like precision.

Already in 1976, Cooke and Zeeman proposed that such regularity and rhythmicity could be achieved by the interaction of a biological "clock" in the PSM and a sweeping "wavefront" that moves posteriorly. They suggested that the "clock" is made up of coupled cellular oscillators and that the "wavefront" constitutes a slow moving front that induces a fast switch in cell fate. In combination, the state of oscillators would then periodically adjust the effect of the wavefront on the PSM cells, determining for instance their fate as somite boundary cell. This clock and wavefront model eloquently unifies the somitogenesis mechanism across species, describing differences in somite number as a direct consequence of species specific clock periods and wavefront speeds, which is consistent with varying somitogenesis period and growth rates between species [Cooke and Zeeman, 1976].

Popularity for the clock and wavefront model has greatly increased since the discovery of molecular evidence supporting both the idea of a "wavefront" as well as a "biological clock". Evidence for the "clock" first arose from the discovery of cyclic mRNA patterns of *chairy-1* in the PSM of the chick [Palmeirim et al., 1997], whose waves expression matches the 90min periodicity of chick somitogenesis. Ultimately, not only the expression of *c-hairy1* homologs was found to cycle periodically in mouse [Masamizu et al., 2006] and zebrafish [Holley et al., 2000][Sawada et al., 2000] but eventually a large number of other genes belonging to the Notch, FGF and Wnt pathways were identified [Krol et al., 2011], reviewed in [Oates et al., 2012]. Interestingly, the "wavefront" is linked to signal gradients of FGF and Wnt in the PSM [Dubrulle and Pourquié, 2004], providing a mode of interaction between "clock" and "wavefront" on a molecular level.

However, most important is the ability to verify predicted effects on somitogenesis, when "wavefront" and "clock" mechanisms are altered individually. For example, the application of FGF8 beads unilaterally along the chick PSM pushed the wavefront anteriorly and thereby delayed the determination of cell fate on that side of the PSM [Dubrulle et al., 2001]. Even more convincing is the generation of period

mutants affecting "clock" molecules, where an increase in "clock" period leads to larger segments in zebrafish [Herrgen et al., 2010]. While not all details of the segmentation processes have been clarified, the segmentation "clock" and "wavefront" model remains the basis for somitogenesis models formulated nowadays.

1.2 The 3 Tiered Segmentation Clock Model

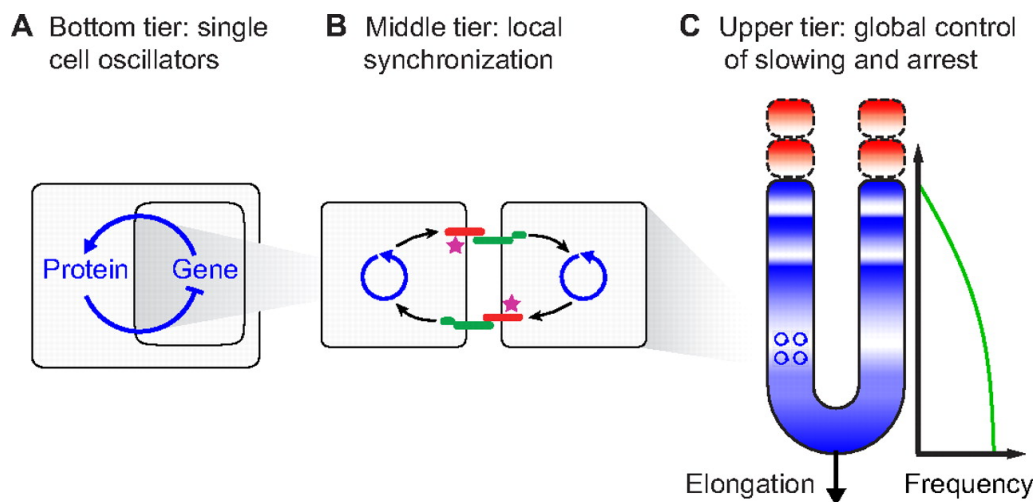


Figure 1.1 The Three-Tiered Model. Three levels of organization give rise to the complex dynamics of the zebrafish segmentation clock. **A.** At the **BOTTOM** tier is a single cell oscillator consisting of genetic negative feedback loops. This intracellular oscillator is the basis for generating timed rhythms in the segmentation clock. **B.** The **MIDDLE** tier is the local synchronization of cellular oscillators and coordinates timing of cyclic gene expression in neighboring cells. **C.** The **TOP** tier consists of global regulatory signals across the PSM that influence oscillator frequency with respect to positioning in the PSM [Oates et al., 2012]

Somitogenesis' mechanisms cross multiple scales, from interaction of cycling genes in individual cells to coordinated cell-fate switching on the tissue level. While the "clock" and "wavefront" model provides a "big picture" view of the segmentation mechanism, the mechanistic details of these processes are dispersed across a multitude of small-scale models [Hester et al., 2011][Oates et al. [2012]. A unifying model, termed the three-tiered segmentation clock model, which integrates these subcomponents, was recently reviewed in Oates et al. [2012].

This model organizes the underlying molecular and cellular mechanisms of the clock into three distinct levels termed bottom, middle and top tiers. At the bottom is

a single cell oscillator consisting of genetic negative feedback loops. This intracellular oscillator is the basis for generating timed rhythms in the segmentation clock. The middle tier is the local synchronization of these oscillators between neighboring cells. Synchronization is achieved by cell-cell receptor ligand interactions that allow cells to communicate the state, or 'time', of their oscillators to one another. This relay of information not only coordinates oscillations in neighboring cells, but also reduces fluctuations in oscillator period in individual cells. The top tier refers to the global control of oscillator frequency and sets the point of oscillator arrest with respect to position within the PSM. The pace at which oscillators tick is influenced by gradients of signaling factors within the PSM, causing them to gradually slow down towards the anterior PSM. The traveling waves of expression across the PSM tissue emerge through the interaction of these three tiers. In the next sections, the biological and mathematical evidence for each tier is described in more detail.

1.2.1 BOTTOM Tier: Single Cell Oscillators

The bottom tier of the segmentation clock defines the smallest rhythm generating unit within the PSM. While an intracellular oscillator was already suggested by Cooke and Zeeman [1976], the pulsatile expression of cyclic genes within chick PSM explants was the first direct evidence of such segmentation clock exclusively located within the PSM [Palmeirim et al., 1997]. These gene oscillations manifest themselves in form of traveling expression waves at both the mRNA and protein level along the PSM's AP axis (Figure 1.2.A/B). Eventually it was shown that small pieces of PSM continue oscillations and that explanted PSM cells display variable transcription [Maroto et al., 2005]. Ultimately, the dissociation of mouse PSM into culture showed that oscillations of cyclic gene products continued in isolated PSM cells [Masamizu et al., 2006] (Figure 1.2.C). These single cell oscillations are slower and noisier than the tissue level segmentation periods [Riedel-Kruse et al., 2007] [Schröter et al., 2008] [Masamizu et al., 2006]. This variability at the cellular level is inherent of biological system [Eldar and Elowitz, 2010] and is compensated at the tissue level by the higher levels of regulation through the middle and top tiers of the clock.

The oscillating components in the PSM are termed cyclic genes and several have been identified in the mouse, chick and zebrafish (Figure 1.3). Most of these genes are associated with the FGF, Wnt and Notch signaling pathways. However, between

1 Introduction

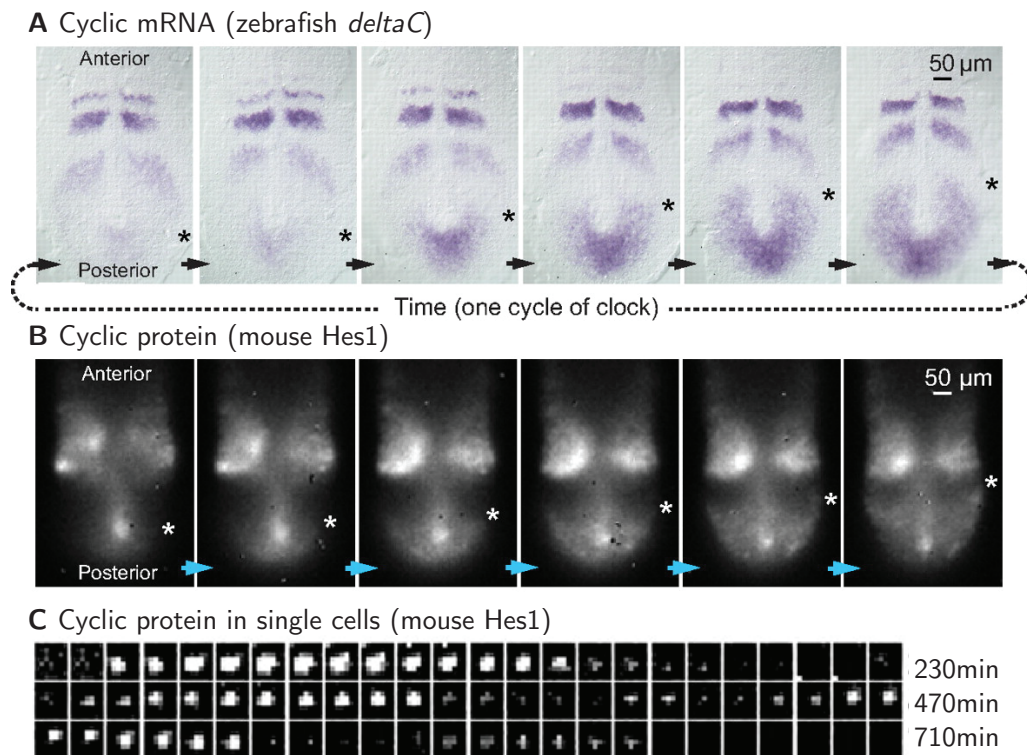


Figure 1.2 Cyclic Expression Patterns of the Segmentation Clock. Several genes are expressed cyclically in the PSM and the corresponding proteins oscillate at both tissue and single cell levels. The typical travelling wave pattern of expression in the PSM consists of a burst of gene expression at the posterior, which becomes thinner as it moves forward (*asterix). **A.** *in situ* staining of *deltaC* mRNA in zebrafish shows three such travelling waves in the PSM at that particular developmental stage [Oates et al., 2012] **B.** Bioluminescence pattern of a Hes1 reporter in mouse PSM tissue shows that oscillations are also present at the protein level. **C.** This bioluminescence signal also cycles in isolated mouse PSM cells and indicates a single cell oscillator is likely the BOTTOM tier of the vertebrate segmentation clock [Masamizu et al., 2006]

species the only overlap consists of the *Hes1* and *Hes5* orthologs, members of the *hairy split enhancer* gene family [Krol et al., 2011]. In zebrafish, *hairy* gene knock-downs result in defective somite formation and disruption of cyclic gene expression, indicating that these genes are essential for clock function [Henry et al., 2002] [Oates and Ho, 2002] [Sieger et al., 2006].

Despite the likelihood of multiple oscillator sub-circuits functioning in parallel in these segmentation clocks [Hirata et al., 2004] [Ferjentsik et al., 2009], the dramatic somitogenesis defects of *Hes7* Null-mice [Bessho et al., 2001] have placed *hairy* genes at the core of the segmentation clock's oscillator. And it has been proposed that in

1.2 The 3 Tiered Segmentation Clock Model

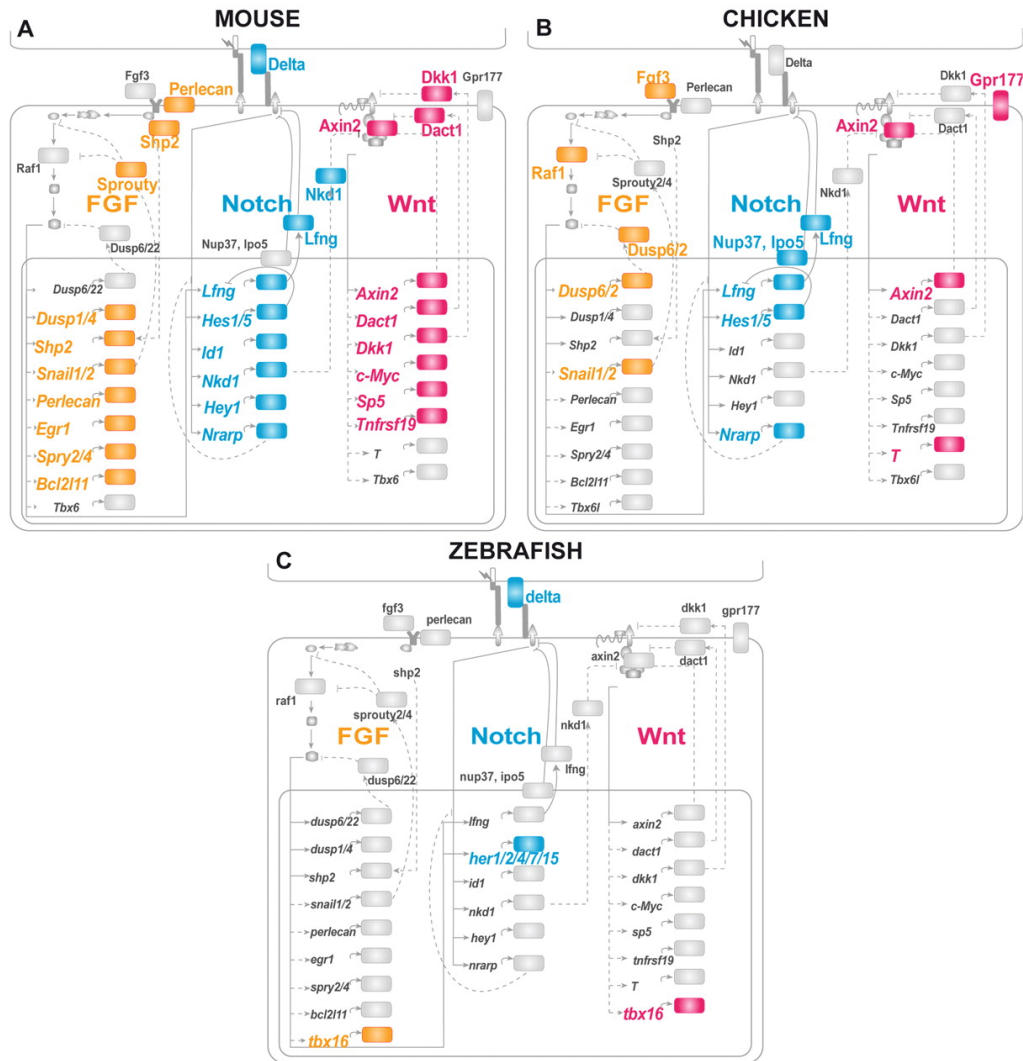


Figure 1.3 Cyclic Genes found in PSM of Mouse, Chick and Zebrafish. Microarray hybridization of RNA expressed during somitogenesis revealed several cyclic genes in the PSM of **A.** mouse, **B.** chick and **C.** zebrafish. Each cyclic gene belongs to either FGF (yellow), Notch (blue) or Wnt (magenta) pathways. Only the orthologs of cyclic genes Hes1 and Hes5 are conserved in all three species and may represent the core oscillator components of the vertebrate segmentation clock. This data revealed a large plasticity in gene patterns, indicating that evolutionary pressure selects for rhythmic activation of the three pathways, rather than individual cyclic genes. [Krol et al., 2011]

contrast to mouse and chick, where multiple cyclic networks appear to interact, *hairy* genes seem to be the core components of the zebrafish's oscillator network. Therefore, zebrafish is the ideal model organism for studying the molecular mechanisms of the core segmentation oscillator. The current models of the zebrafish oscillator mechanism and their biological basis are described in further detail in Section 1.3.

1.2.2 MIDDLE Tier: Local Regulation via Cell-Cell Oscillator Synchronization

The middle tier of the segmentation clock refers to the molecular mechanisms that couple neighboring oscillators to one another. Oscillator behavior, such as phase and amplitude of gene expression (see Section 1.3.2), in cultured PSM cells is noisy and asynchronous [Maroto et al., 2005] [Masamizu et al., 2006]. However, it is clear from the transcriptional wave patterns in Figure 1.2.A/B that oscillators within the PSM are locally synchronized. Therefore, PSM cells are able to relay, or communicate, information about their oscillator state to their neighbors.

In somitogenesis, the prime candidate for such communication is the ligand-receptor interactions of Delta-Notch, a well-studied cell-cell signalling pathway, with functions ranging from development to disease [Lai, 2004]. Both Delta and Notch can be linked directly to somitogenesis, the membrane bound Delta ligand is expressed cyclically [Jiang et al., 2000] and Notch receptor activation appears in traveling waves in the PSM [Huppert et al., 2005]. More specifically, the local overexpression of Delta raises Her expression in neighboring cells [Horikawa et al., 2006]. In addition, Her proteins are targets of Notch signalling [Maroto et al., 2005] and Delta shares the same transcriptional regulatory sites as the *hairy* core oscillator genes [Schröter et al., 2012].

At the cellular level, oscillator coupling to neighboring cells can be described as a short sequence of molecular events. When *hairy* gene expression is off, no Delta is transcribed either. Similarly, once *hairy* gene expression activates, Delta ligand is also expressed and shuttled to the membrane. There it binds with the Notch receptor of the neighboring cell, which leads to the cleavage of the Notch intracellular domain (NICD). The NICD is then free to migrate into to the neighboring cell's nucleus where it targets downstream components, ultimately affecting the expression level of *hairy* and *delta* genes. At the same time, the neighboring cell is signalling back via

the Delta-Notch pathway. Therefore, a continuous exchange occurs between PSM cells with cell-cell contacts.

From a theoretical standpoint, the local regulation of intra-cellular oscillations is important for coordinated cell decisions at the tissue level, since cell-cell coupling compensates for biological noise [Kuramoto, 2003] [Winfree, 1967]. Therefore, when coupling is disturbed during development, the cellular oscillators continue to run but will slowly drift apart in phase, leading to an increasing level of desynchronization between neighboring cells. This is consistent with the posterior segmentation defects associated with Delta-Notch mutants [Holley et al., 2000][Holley et al., 2002][Itoh et al., 2003] [Jülich et al., 2005], where formation of distinct segment boundaries is lost over time. In other words, the loss of coupling results in the deterioration of coherent traveling waves into salt-and-pepper patterns [Jiang et al., 2000] [Oates and Ho, 2002], which has been verified by measurements of disorganization in PSM expression patterns [Herrgen et al., 2010] and tracking of *hairry* genes in Delta/Notch mutants [Delaune et al., 2012].

To date, the delayed coupling theory (DCT) [Morelli et al., 2009] of oscillator synchronization is the most comprehensive model tying together the dynamics of single cell oscillators and local regulations. It considers that production and activation of Delta/Notch signalling pathway components require time and therefore introduce synchronization delay and additional oscillator dynamics. This is consistent with changes in period, segment length and genetic wave pattern when Delta-Notch pathways are compromised [Herrgen et al., 2010]. In other words, the period of segmentation is a multicellular property, where the timing is not only dependent on intrinsic oscillator period but also subject to tuning by Delta-Notch signalling strength. Ultimately, the segmentation period depends on the ratio between intrinsic period of the single cell oscillators and coupling delays. In zebrafish, the coupling delay is believed to speed up tissue-level oscillations [Morelli et al., 2009]. In mouse, coupling delay was predicted to slow down oscillations, which was subsequently shown experimentally [Kim et al., 2011].

1.2.3 TOP Tier: Global Regulation of Oscillator Frequency and Arrest within the PSM

The segmentation model's top tier describes the global mechanisms that control oscillator dynamics along the PSM's AP axis. It is clear from the striped PSM patterns that single cell oscillators not only synchronize locally, but also act in coordination with respect to position in the PSM, progressively slowing down towards the anterior. Most notably, cyclic genes cease to oscillate at the anterior of the PSM [Palmeirim et al., 1997], [Jiang et al., 2000], [McGrew et al., 1998], marking the boundary between formed somite and ticking segmentation clock.

It has been proposed that positional information in the PSM is generated in form of diffusible signalling gradients generated by molecule production and release from the posterior tailbud and the anterior somites. Formation of such morphogen gradients depends on the amount of signal molecules released, their diffusion rate within the tissue, and the degradation of signal over time [Wartlick et al., 2009]. At the tailbud, likely candidates for such gradients are members of the FGF and Wnt pathways that have been linked to the cyclic gene networks of the somitogenesis (Figure 1.3). Indeed, both FGF and Wnt pathway components are expressed in the tailbud and gradients of both FGF8 and β -catenin have been measured in the PSM [Dubrulle and Pourquié, 2004] [Aulehla et al., 2008]. At the anterior PSM, retinoic acid (RA) is synthesized in somites and gradients of RA response have been observed in mouse [Vermot et al., 2005].

Similarly to the Notch pathway, FGF, Wnt and RA are major signalling pathways that play a role in other aspects of development such as axis elongation. Therefore, it is difficult to separate effects of the somitogenesis clock from morphologic defects. Nonetheless, temporary perturbations of these pathways show that RA appears mutually antagonistic to the opposing gradients of FGF and Wnt. For instance, a loss in either FGF or Wnt leads to longer somites, the same effect as is observed for an increase in RA [Sawada et al., 2001] [Aulehla et al., 2003][Moreno and Kintner, 2004] [Dubrulle et al., 2001]. In turn, due to the direct relationship between somite size and somitogenesis timing, the change in somite length indicates that FGF/Wnt and RA affect the period of oscillations.

As a result, the current model for a global regulation of oscillations in the PSM involves a frequency gradient, generated by the opposing signalling gradients of

FGF/Wnt and RA. While high levels of FGF/Wnt signals at the posterior PSM permit fast oscillations in cells [Aulehla and Pourquié, 2010], the high levels of RA at the anterior PSM have the opposite effects causing oscillator frequency to decrease. Therefore cells can use these opposing gradients to determine their position along the PSM. While it is unclear whether one gradient is dominant over the other, it is believed that at some position in the PSM a threshold of either too low FGF/Wnt or high enough RA is passed where single cells arrest oscillations. This threshold position is called the maturation front, the location at which the oscillator fate is determined.

1.3 The *Hairy* Gene Oscillator

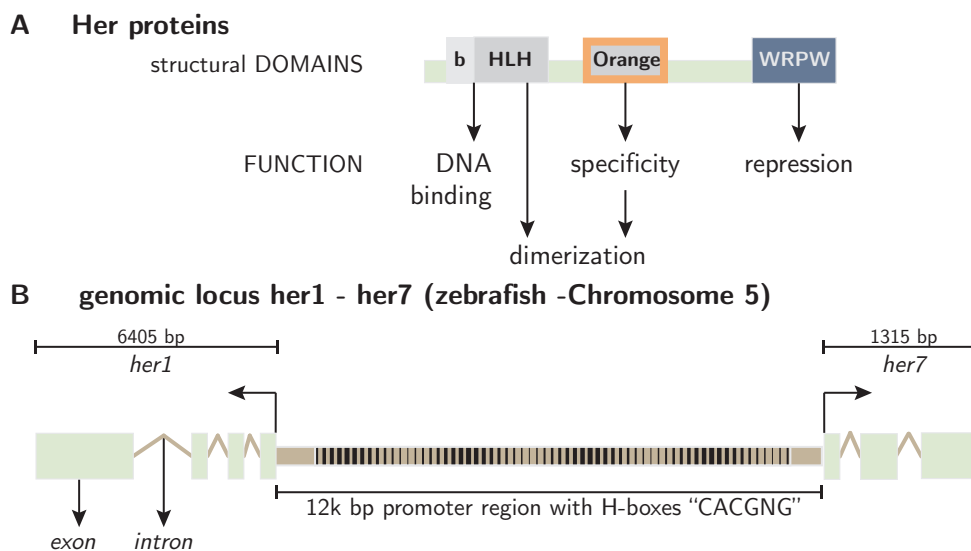


Figure 1.4 Her proteins. Her (or Hairy) proteins are bHLH transcription factors. **A.** A schematic shows the conserved Her protein domains. Her proteins contain a basic domain, associated with DNA binding, a Helix-Loop-Helix (HLH) dimerization domain, Orange domain, lends binding partner specificity and a WRPW repressor domain. The C-terminal WRPW domain recruits Groucho as co-repressor. **B.** Schematic of the genomic region containing *her1* and *her7* in zebrafish. The two genes sit back to back on chromosome 5 and share a 12k bp promoter region. This promoter region contains H-box motifs, the binding sites of Her genes. *her1* has 3 introns and *her7* contains 2.

Since the discovery of cyclic PSM genes by Palmeirim et al. [1997] the conserved *hairy*, or *her*, genes have remained at the core of the single cell oscillator model. Her proteins are basic helix-loop-helix (bHLH) transcription factors that contain

DNA binding, dimerization and repressor domains (Figure 1.4.A). The basic domain and part of the N-terminal helix of the HLH domain bind H-box sites with the "CACGNG" DNA motif. Dimerization is mediated by the HLH domain. In addition, Her proteins contain the "Orange" protein domain, which influences the specificity of dimer formation. Lastly, the "WRPW" amino acid motif at the C-terminus of Her proteins is the domain responsible for recruiting the co-repressor Groucho to the DNA site [Fisher and Caudy, 1998]. Therefore, Her proteins fulfill the requirements needed to partake in a transcriptional negative feedback loop, the gene network suggested to regulate oscillations in segmentation [Lewis, 2003][Bessho et al., 2003].

1.3.1 The Zebrafish's Core Oscillator

In zebrafish, nine *her* genes have been linked to the segmentation clock through overexpression, knock-down and mutant analysis (summarized in Table 1.1). Not all, but many of these cause somitogenesis defects. However, loss of function (LOF) phenotypes identify Her1, Hes6 and Her7 as the major clock components, while the other Hers are likely part of redundant oscillator networks. Of the three only *her7* and *her1* are cyclic genes and their deleterious effect on somitogenesis was first discovered in a mutant missing the genomic region where *her7* and *her1* are located [Henry et al., 2002]. On this locus, the two genes sit back to back, sharing the same 12k bp promoter region and therefore the same regulatory elements (Figure 1.4.B) [Gajewski et al., 2003][Schröter et al., 2012][Trofka et al., 2012]. Importantly, this genomic locus contains several H-box sites indicating that these *hairy* genes can indeed physically bind to their own promoter region. Consequently, it is probable that Her proteins interact in an auto-regulatory negative feedback loop.

In combination with the somite defects observed for Her1/Her7 knock downs and *her1-her7* double mutant [Holley et al., 2000][Henry et al., 2002][Oates and Ho, 2002], the previous results form the basis of initial oscillator models, in which either Her1 monomers [Monk, 2003] or Her1-Hes7 heterodimers [Lewis, 2003] inhibit transcription of the *hairy* genes. Besides the negative feedback loop, these networks require sufficient time delay, non-linearity and balanced timescales of reactions in order to oscillate [Novak and Tyson, 2008]. In the Her network, time delay can be generated by non-instantaneous molecular events such as transcription and splicing

name	PSM expression	somitogenesis defects	LOF?
Her1	cyclic[Holley et al., 2000][Krol et al., 2011]	mRNA injection, fused somites (GOF)[Takke and Campos-Ortega, 1999] morpholino injections, anterior defects (LOF)[Holley et al., 2002][Henry et al., 2002][Oates and Ho, 2002]	yes
Her2	cyclic[Krol et al., 2011]	none	no
Her4	stripes[Takke et al., 1999], cyclic[Shankaran et al., 2007][Krol et al., 2011]	mRNA injection, fused somites(GOF)[Takke and Campos-Ortega, 1999]	no
Hes5	cyclic[Krol et al., 2011]	none	no
Hes6	gradient[Kawamura et al., 2005]	morpholino, worsens Her1 phenotype (LOF), improves Her7 phenotype (GOF)[Sieger et al., 2006] mutant, slowed somitogenesis period[Schröter et al., 2012]	yes
Her7	cyclic[Oates and Ho, 2002] [Krol et al., 2011]	morpholino, posterior defects (LOF)[Henry et al., 2002] [Oates and Ho, 2002] mutant, posterior defects (LOF)[Schröter et al., 2012] mRNA injection, boundary defects (GOF)[Shankaran et al., 2007]	yes
Her11	cyclic[Sieger et al., 2004]	none	no
Her12	cyclic[Shankaran et al., 2007]	mRNA injection, boundary defects (GOF)[Shankaran et al., 2007]	no
Her15	cyclic[Shankaran et al., 2007][Krol et al., 2011]	mRNA injection, boundary and morphological defects (GOF)[Shankaran et al., 2007]	no

Table 1.1 Her proteins associated with zebrafish somitogenesis. The first column shows Her expression patterns in the PSM. The second column lists the loss of function (LOF) and gain of function (GOF) phenotypes obtained from mutants, knockdown morpholinos or mRNA injection of each Her. The Her proteins with LOF phenotypes, listed in the last column, are likely key components of the oscillator's molecular network.

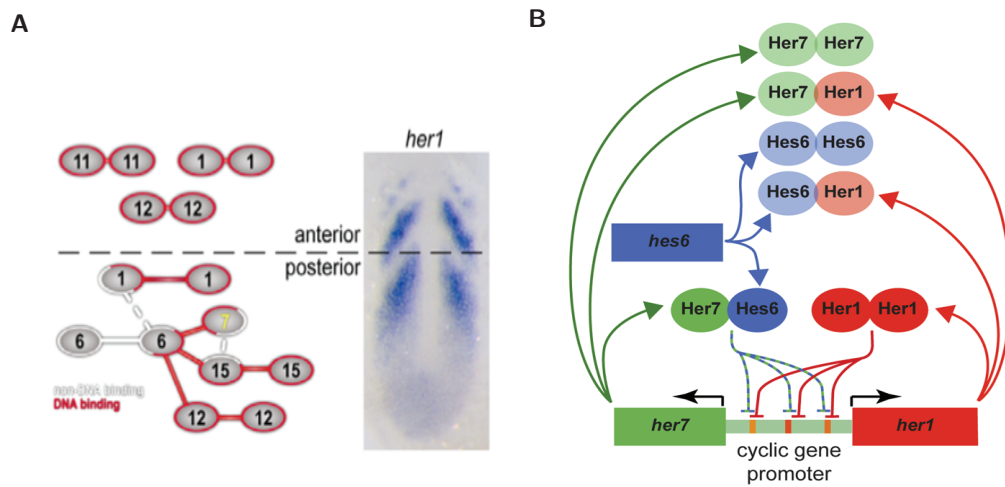


Figure 1.5 Zebrafish Segmentation Clock Oscillator Model. **A.** An illustration of dimer network and DNA binding activity of segmentation clock associated Her proteins in zebrafish. [Trofka et al., 2012] **B.** The molecular model of the core Her1-Hes6-Her7 oscillator network inferred from dimerization and DNA binding affinity as well as segmentation defects of Her knock-downs and mutants.[Schröter et al., 2012]

[Takashima et al., 2011], as well as translation, subcellular transport and protein maturation. Non-linearity results from cooperativity or multimerization events, such as DNA binding and dimer formation of Her proteins. Finally, balanced timescales mean that molecular dynamics and Her life-times are comparable. In the case of the zebrafish segmentation clock, the short 30min period of oscillations implies that Her molecules have similarly short half-lives, which is a reasonable assumption as Her mRNA and protein concentrations quickly fall below detectable limits in the absence of transcriptional activation [Oates and Ho, 2002].

Recently, dimerization and DNA binding affinities of zebrafish Her proteins have been investigated rigorously by Trofka et al. [2012] and Schröter et al. [2012]. While there were some inconsistencies between *in vitro* and *in vivo* experiments, both studies showed that Her proteins dimerize promiscuously with other Her proteins, forming either homo- or hetero-dimers. Both studies investigated Her dimer binding to H-boxes found within the endogenous promoter regions of zebrafish cyclic genes, several of which are found upstream of *her1*, *her7* and *dlc*. They found that only a subset of dimer pairs is able to bind to the "CACGNG" DNA motifs and that binding affinity depends largely on the flanking DNA bases. Ultimately, only Her1 homodimers and Her7-Hes6 heterodimers were identified as DNA binding partners.

This not only eliminates the Her1-Her7 dimer inhibition model proposed by Lewis [2003], but also places Hes6, a non-cyclic PSM gene that was investigated as a link to FGF signalling, at the hub of the segmentation oscillator's dimer network (Figure 1.5). The effects of double knock-downs involving *her1*, *her7* and *hes6* are in agreement with this finding. In these, the anterior defect phenotype of Her1 deficient fish is drastically worsened in the double knockdown with Hes6, resulting in a complete loss of properly formed segment boundaries. In contrast, the double knockdown of Hes6 with Her7 restores all defects [Sieger et al., 2006]. While both DNA-binding dimers Her1-Her1 and Her7-Hes6 are disrupted in the first case, the removal of Hes6 in addition to Her7 leaves Her1 dimers functional in the second case. This also indicates that the presence of Hes6 interrupts Her1 homodimer function in the Her7 knockdowns.

On the basis of the binding assays in combination with the observed knockdown phenotypes the molecular oscillator model was expanded to include interaction networks between Her1, Hes6 and Her7 proteins (Figure 1.5). In the current molecular model of the single cell oscillator mechanism, the H-box containing genetic locus from which both *her1* and *her7* are transcribed, builds the core of the network. Upon expression, both Her1 and Her7 form dimers promiscuously with themselves and other Her proteins, but only Her1 homodimers and Her7-Hes6 heterodimers are able to bind to H-boxes in the promoter regions of *her1* and *her7* and in turn result in repression of both genes. The remaining dimers interact in this network by sequestering monomers of Her1 and Her7 and thereby affect the concentration of available DNA-binding repressors.

The dynamics of these simple dimer interactions is not intuitive and can mask underlying features of genetic networks. For instance, the Her7 mutants show significant somitogenesis defects despite the presence of an intact Her1 loop, indicating that Her1 alone cannot generate stable oscillations. On the other hand, zebrafish mutants lacking Hes6 protein end up with regular segment boundaries indicating that Her1 is sufficient after-all. This result is contradictory considering both mutations affect the same Hes6-Her7 oscillator loop, but the molecular model shows that this effect is a natural consequence of the dynamics arising from competing dimer-partners [Schröter et al., 2012]. Furthermore, despite the lack of obvious somite defects, a subtle increase in somite length of Hes6 mutants reveals that Hes6

1 Introduction

changes somitogenesis period, which in turn results from changes in the effective life-times of its binding partners, Her1 and Her7. Therefore, both precise models and proper measurements are essential for providing insight into somitogenesis clock function.

1.3.2 Oscillator Terminology

A number of terms can be used to describe the dynamic properties of the single cell oscillator. In general, oscillators are rhythm generating mechanisms associated with repetitive variations in time. Oscillations are best described by the movement of a pendulum, a weight attached to a string that continuously swings back and forth. The pendulum's swinging motion can be mapped on a position versus time graph (Figure 1.6.B). The resulting graph describes a sinusoidal curve, a series of smoothly connected *peaks* and *troughs*. The position between these two extreme positions, where the pendulum would rest when it is not oscillating, is its *equilibrium* value.

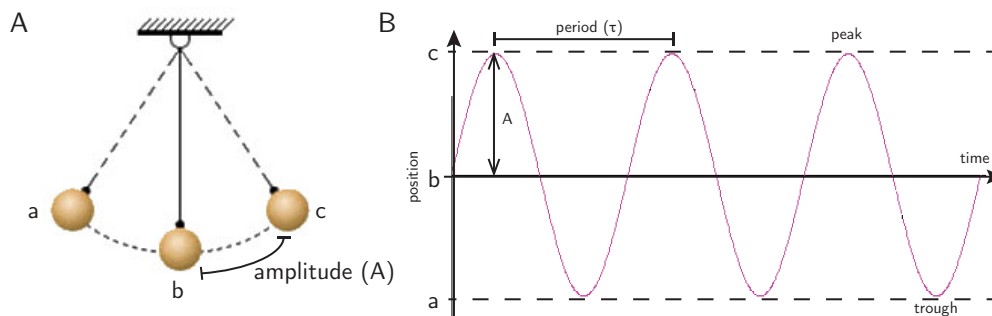


Figure 1.6 Oscillator Behaviour. Oscillations are characterized by their amplitude (A), period (τ), phase (a,b,c) and stability. **A.** The repetitive swinging motion of a pendulum is an example of a simple oscillator. The amplitude of oscillations is the maximum deviation of the pendulum from the center position, b , on each swing ($A = b-a$ or $c-b$). The period is the time the pendulum needs to swing once through its full range of motion (from a to b to c and back to a). Correspondingly, the frequency, f , of oscillation is the number of cycles per unit time or the inverse of the period ($f = \frac{1}{\tau}$). The phase can be thought of the position of the pendulum along its oscillatory path. For instance, position b and c would be the 'center' and 'right' phases, respectively. **B.** The graph shows stable oscillations as a function of position vs. time. Stability means that measurable parameters do not vary over time.

The term *period* describes how long an oscillator takes to pass through one cycle of this repetitive motion and is effectively the peak-to-peak distance of the curve. In turn the *frequency* of oscillations is the inverse of the period. In the graph, the

amplitude is the vertical distance between the mid-line and the extreme positions and describes how strongly the oscillator varies from its equilibrium. The phase of an oscillator describes its position along each cycle of repetition. Oscillators can either be *stable*, with uniform period and amplitude over extended stretches of time, or *unstable*, and fluctuating in amplitude or period or both. A special case of instability are *damped* oscillations, when the amplitude of fluctuations decreases over time until the variations around the equilibrium are undetectable.

To describe biological systems it is useful to exclude properties that are susceptible to biological noise, such as absolute numbers of molecules per cell. Therefore, biological oscillators are frequently described by characteristics such as *periodicity*, *robustness* and *entrainment*. While periodicity is a direct measurement of timing in the system, an oscillator's robustness describes whether it is stable over a wide range of conditions and entrainment refers to the processes whereby independent oscillators with different periods are able to synchronize. A good example of entrainment is the circadian clock, where an animal's internal clock synchronizes to the 24 hour day-night rhythm. The internal period of a clock will be referred to as *intrinsic period* of the clock or oscillator. In addition, biological oscillators are typically *unstable* and have steady-state values different from the resting position between peak and trough. Together, these terms describe the *behaviour* of an oscillator.

1.4 Open Questions

It is widely accepted that the single cell oscillator is the underlying pace-maker of the zebrafish segmentation clock. This hypothesis is consistent with both computational approaches and top down molecular biology techniques, such as gene knock-down and molecule labelling. However, an oscillator has never been shown to cycle autonomously in single zebrafish PSM cells. The imaging of three isolated mouse PSM cells by Masamizu et al. [2006] suggests that single cell oscillators exist. However, it is not clear whether the low number of reported oscillating cells is due to technical difficulties of the mouse experimental model or a general lack of such oscillators altogether. And if the latter is true, whether this is a general property in vertebrate somitogenesis or a special feature of the mouse segmentation clock.

To investigate these questions, we propose to study the single cell oscillator in zebrafish. Similar to Masamizu et al. [2006], this approach requires the "real-time" tracking of clock genes in dissociated PSM cells, thereby eliminating the effects of the middle and top tiers of clock regulation. At the start of this project, the first transgenic zebrafish lines for tracking fluorescently tagged Her1 during somitogenesis, generated by Daniele Soroldoni (MPI-CBG), were becoming available in the lab. This presents a great improvement over previous labelling techniques, such as mRNA *in situ* or immuno-staining, which required fixing embryos at concrete time-points and is particularly impractical for dynamic studies in single cell.

While a single cell oscillator seems to be at the core of the segmentation clock, the Her proteins seem to be at the core of the oscillator mechanism. However, it is not clear how molecular interactions between the components of *her* gene networks generate the period of the single cell oscillators [Oates et al., 2012]. Knock-downs and molecular models indicate that two redundant genetic feedback loops involving Her1-Hes6-Her7 build the core mechanism in zebrafish. What then is the role of the other cyclic *hairly* genes oscillating and dimerizing in the PSM? Are these integral components of the core oscillator or simply redundant pathways and secondary read-outs relaying temporal information to other processes in the cell? Ultimately, it is not even certain that a Her1-Hes6-Her7 feedback is the core of oscillations or merely a secondary read-out of another underlying oscillator altogether.

Therefore, the question remains whether a negative feedback involving any or all of the Her1-Hes6-Her7 proteins is not only *essential* but also *sufficient* to generate oscillations. While establishing the single cell dissociation technique is useful in studying oscillator dynamics in the absence of tissue-level phenomena it is not sufficient in abolishing overlapping intra-cellular network interactions. For these reasons, we propose to use a bottom-up approach to sequentially build up this oscillator network in the absence of interacting networks.

1.5 The Synthetic Biology Approach

In contrast to traditional molecular biology and biochemical techniques, synthetic biology offers a unique design driven approach to investigate molecular models. The segmentation oscillator network is a perfect example where a simplified model is

difficult to test in traditional experimental set-ups. While in whole-embryos many molecular players can potentially influence the oscillator, *in vitro* biochemical studies lack the necessary complexity inherent of eukaryotic cells. In other words, both top-down whole embryo and bottom-up *in vitro* experiments do not match the level of abstraction used in the models to be tested. In synthetic biology the advantages of bottom-up and top-down approaches are combined to match the necessary level of complexity required by starting with simple networks and building up complexity gradually in the natural environment provided by the host organism. Therefore, both network-components and host organism can be chosen to match the requirements of the proposed system, in this case a simple segmentation clock oscillator.

1.5.1 SynBio from *parts* to *devices* and *systems*

In order to design and construct increasingly complex yet well-defined biological systems, synthetic biology combines techniques from biology and engineering disciplines. It is best to design synthetic systems, which can not only be predicted *in silico*, but also be measured *in cellulo* through pre-defined input and output variables. Therefore, novel networks should be constructed using logical networks, standardized building blocks and defined environments (host organism). In practice, the generation of functioning synthetic networks involves three stages: 1. design & modeling, 2. construction, 3. characterization & optimization, this workflow iterates until the network behaviour matches design requirements and model predictions (Figure 1.7).

In the design stage, synthetic networks are broken down into several layers of abstraction, called *parts*, *devices* and *systems*. At the heart of these networks are genetic parts with simple, yet well-defined, biological function. These *parts* can range in size from small non-transcribed DNA motifs to multi-domain proteins. Even individual protein domains can be considered parts if they have a defined function and modular properties. Any number of parts can be assembled to form biological devices that have defined input and output signals. Ultimately, individual devices are hooked up to one another to form more complex systems. The assembly of parts into devices and systems falls in the construction phase.

A major aim of synthetic biology is to make engineering of biological systems easy and reliable. Therefore, by design each level of abstraction should be independent

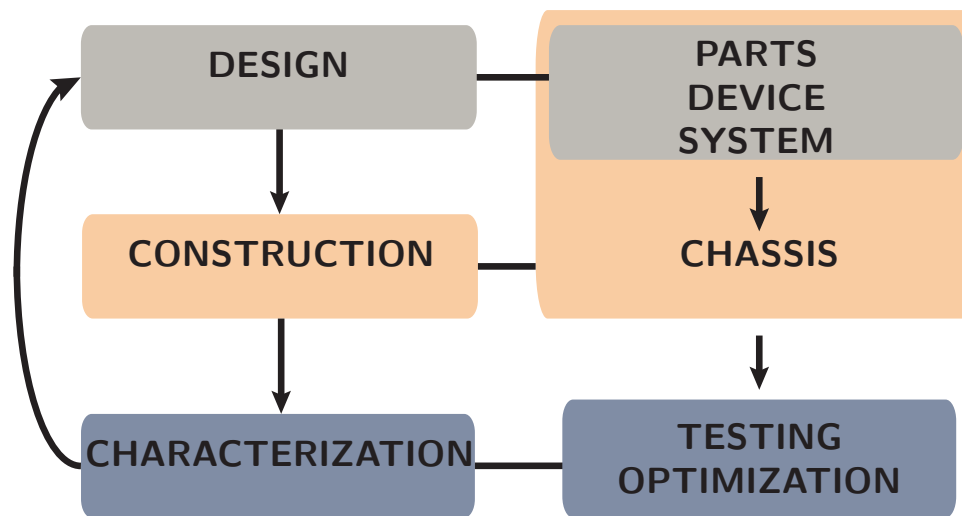


Figure 1.7 Construction Stages of SynBio Networks. Synthetic biology uses abstraction and standardization to systematically build up reliable and well-defined biological networks. In SynBio the desired network is considered to be a system made up of functional subunits called parts and devices. In the design stage, the parts and devices of the system are identified and a blue-print of the system is generated based on the functional properties of available parts. The next stage involves the physical assembly of the parts, devices and system as well as placement into an appropriate chassis. In the final stage, each constructed system is characterized and analyzed using standard measurement techniques. This information is then used to optimize the system and redesign the blueprints if need be.

from each of the other levels. In other words, the assembly of *devices* should not require the redesign of individual *parts*, but rather be guided by standard plug-and-play standards [Endy, 2005]. To this aim, a number of cloning techniques have been established that standardize the use of *parts* and *devices*. These include modular assembly standards that refer to the physical links between *parts*. The first standard assembly technique is a digest-ligation of defined flanking BioBrick sequences, the format of *parts* stored in the largest library of biological building blocks [Shetty et al., 2008]. Besides general inconveniences of the digest-ligation procedure, the major disadvantage of this method is the 5bp scar that is created at the joints of *parts*, which would result in frameshifts of protein domain fusions. Therefore, alternate techniques such as the PCR based Gibson assembly are gaining popularity [Gibson et al., 2009]. However, with the ever decreasing prices of gene synthesis, the need for standardized assembly of small devices might become obsolete.

Ultimately, the constructed *systems* are placed in a host organism, called *chassis*. By definition, a *chassis* is an internal framework that supports a man-made object

in its construction and use. In electronic devices this refers to the metal frame onto which circuit boards and their components are mounted. Similarly, in synthetic biology the *chassis* is thought of as an empty box onto which a biological system can be mounted and activated. Besides supplying energy it provides the machinery to run basic cellular processes such as transcription and translation. The most widely used *chassis* is the bacterium *E. coli*; however, other bacteria, eukaryotic cells and cell-free systems have been investigated for their suitability as a container for *parts* and *devices*. The main criteria is the ready uptake of the system components. However, it is also important that the interaction between *chassis* and *system* is either inert or can be separated from the *system's* measured output. It is imaginable that one day, a completely synthetic organism with all its components defined, designed and characterized will be the standard chassis.

Initially, assembled systems need to be tested to determine whether network components function as predicted. In this characterization stage, measurement standards are used to evaluate and compare *parts* to one another. This typically involves measuring the *part's* RNA and protein response curves over time and extensively testing *system* prototypes to predict behavior of final *system* design [Cantone et al., 2009].

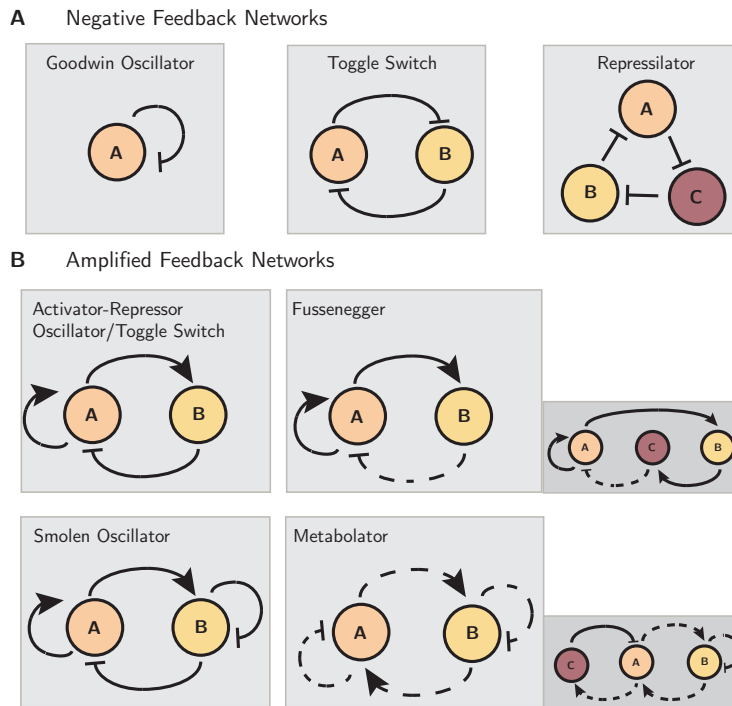
The final optimization stage aims to improve undesired *system* properties by altering either network design or swapping *parts*. This illustrates the importance that has been placed on accumulating large libraries of characterized *parts*, such as the partsregistry for BioBricks (partsregistry.org). An alternative to design and construction improvements is the approach of directed evolution to push a system to a certain network parameter space. In fact, many synthetic biologists believe that the combination of synthetic design-construction with directed evolution will generate more robust systems.

1.5.2 Synthetic Oscillators

While the segmentation clock oscillator has never been reconstructed bottom up, synthetic biologists have succeeded in generating a number of gene regulatory networks involving negative feedback (summarized in Figure 1.8). The complexity, stability and robustness of these oscillators varies greatly, revealing some basic features required for reliable and tunable oscillations in biological systems [Purcell

Figure 1.8 Synthetic Oscillator Networks

that were successfully constructed using **A.** negative feedback links only or **B.** combining both negative and positive feedback links. One notable exception to oscillator networks is the bistable Toggle Switch. Three component versions of the Fussenegger and Metabolator networks are shown in the small, darker, boxes. The solid lines are direct transcriptional control processes, while the dotted lines are non-transcriptional processes such as protein sequestration due to binding or proteolysis.



et al., 2010]. Although these networks are artificial constructs, they not only provide design considerations for synthetic oscillators but also aid in understanding the qualitative characteristics of natural oscillators. Therefore, though many of these synthetic oscillators have been studied exclusively in prokaryotes, parallels can be drawn to eukaryotic systems in general and the construction of the segmentation oscillator specifically.

The simplest negative feedback network, called the *Goodwin oscillator*, consists of a single gene repressing its own transcription (Figure 1.8.A) and was first constructed in bacteria by Stricker et al. [2008]. Mathematical models revealed that this network relies heavily on sufficient time delays and non-linearity in its molecular interactions to enlarge the parameter space in which oscillations occur [Stricker et al., 2008][Bratsun et al., 2005]. Time delay is a result of non-instantaneous molecular events such as transcription, splicing or translocation between sub-cellular compartments and Swinburne et al. [2008] used intron splicing to generate pulsed expression in mouse cells. While these events are common to all eukaryotes, in bacteria they are fast or non-existent, and therefore non-linearity, which results from cooperativity and multimerization, may be more important. Indeed, a single negative feedback loop in

which the repressing molecules formed dimers instead of tetramers, nonlinearity was not sufficient and the network settled into a homeostatic steady-state rather than generating fluctuations [Becskei and Serrano, 2000]. It was found that the Goodwin Oscillator generates irregular oscillations and requires careful parameter tuning in bacteria, including strong, yet tightly regulated promoters as well as short repressor half-lives.

Two further synthetic networks using only negative feedback regulation, have been constructed in bacteria. One is the *toggle switch* [Gardner et al., 2000], consisting of two negative feedbacks. It cannot generate oscillations, but instead results in a bistable system, again highlighting negative feedback as a tool to promote homeostatic transcription. The other one is the *repressilator*, the first ever synthetic oscillator, which consists of three genes that sequentially repress each others transcription [Elowitz and Leibler, 2000]. Similar to the Goodwin Oscillator, the repressilator requires strong, tightly regulated promoters and short-lived repressors and its oscillatory regime is enlarged through noise in the biological system. Nonetheless, negative feedback oscillations are neither stable nor robust and as a result the effect of positive regulation has been studied on these systems.

These amplified-negative feedback oscillators vary in their levels of complexity; however, their topologies can all be represented as two-component networks with at least one negative feedback connection (Figure 1.8.B). The simplest two-component oscillator, the *amplified negative feedback oscillator*, consists of two genes, where one gene activates its own transcription and that of the other gene. In turn, the other gene represses the transcription of the first gene. Depending on specific design choices, this network is either a toggle switch or a damped oscillator *in vivo*, which is consistent with biologically relevant parameters [Atkinson et al., 2003]. This type of network requires fast amplification and significantly slower repression, which is equivalent to adding time delay into the negative feedback loop [Purcell et al., 2010].

This concept has been implemented in the *Fussenegger oscillators*, where sense-antisense regulation was used to generate delay in the negative feedback loop [Tigges et al., 2009]. In contrast to the Atkinson et al. [2003] amplified-negative feedback network, this oscillator was constructed in mammalian cells and was the first oscillator to use non-transcriptional regulatory elements. The Fussenegger oscillator generates stable and undamped oscillations and can be tuned via gene dosage. However,

significant cell to cell variation exists in this system and model predictions cannot explain this variance.

Another two-component oscillator is the *Smolen Oscillator*. It uses one activating gene, which amplifies its own transcription and that of gene number two, and one repressor gene, which represses both itself and the activator gene. The Smolen Oscillator is a robust oscillator resulting in stable oscillations and is tunable using small molecules as transcriptional activators [Stricker et al., 2008]. This type of oscillator topology has subsequently been used to study synchronization and entrainment effects on oscillator amplitude and intrinsic period [Danino et al., 2010] [Mondragón-Palomino et al., 2011].

The *Metabolator* is distinct from the previously discussed two-component oscillator networks in two ways. On one hand, it uses metabolites and non-transcriptional regulation for all network links. Secondly, instead of one activator and one repressor gene, each gene in this network activates the other and represses itself [Fung et al., 2005]. While this oscillator is not particularly robust or stable, its dynamics can be tuned using external metabolite sources.

These experiments verify that negative feedback loops can generate oscillations and that time-delay and non-linearity are important properties for oscillator behavior. Even though time-delay, through the intra-cellular processes of transcription, translation, protein maturation and transport between sub-cellular compartments, is a natural feature of eukaryotes, prokaryotes have been the choice of chassis for most synthetic networks. This is a result of their relative simplicity in comparison to eukaryotes, which allows for more accurate network models and in turn more predictable oscillator behavior. Other issues of synthetic oscillator design are robustness and elimination of interference with cellular processes such as cell growth, cell cycle or other cellular clocks.

1.5.3 Design Considerations for the SynBio Oscillator

We want to build an oscillator, where the synthetic *system* is designed based on the network models proposed for the zebrafish oscillator. Therefore, the choice of both *parts* and *devices* will closely mimic their endogenous structure in the zebrafish. In turn, the choice of *chassis* depends on the basic framework required by the *system* to function. This includes the cellular machineries that control transcription, trans-

lational and protein modification. However, the availability or absence of certain cellular structures and other molecular components are equally important factors. Importantly, the *system's* subcomponents need to be compatible with this framework.

In the case of constructing the segmentation clock's single cell oscillator a *hairly* transcriptional feedback loop should be build up in the absence of redundant circuitry, local synchronization or global period regulation. Essentially this means, keeping the molecular machinery present in isolated PSM cells while eliminating all *hairly* genes. Therefore, the *chassis* for a *Hairy Oscillator* needs to fulfill the following requirements:

1. eukaryotic cell (transcription, translation, sub-cellular compartments)
2. single cells (eliminate effects of middle and top clock tiers)
3. lack of *hairly* gene homologues

The prime candidate for this project (and synthetic biology in general) is the well-studied model organism *Saccharomyces cerevisiae*. It is a simple unicellular eukaryote, containing sub-cellular compartments such as the nucleus, but is also capable of post-translational modifications linked to higher eukaryotes. While yeasts do not have homologues of *hairly* genes, they do contain other bHLH proteins, indicating that they are capable of this type of transcriptional regulation. This is important, since Her proteins interact with the co-repressor Groucho in zebrafish and will rely on homologous mechanisms to function in the yeast. Indeed, Groucho has a structural homologue that functions as corepressor in yeast, called Tup1, and whose propeller like domain interacts with DNA-binding transcription factors [Malavé and Dent, 2006].

Besides the time-delays introduced during transcription, translation, and Her protein translocation between cytoplasm and nucleus, other time-factors, such as molecular turn-over rates, are important constraints of the oscillator dynamics. In zebrafish, both mRNA and proteins of *hairly* genes have fast turn-over rates [Oates and Ho, 2002]. Her proteins are ubiquitinated and degraded by the cell's proteasomes [Hirata et al., 2002]. It is possible that the corresponding ubiquitin-proteasome degradation pathway operates on similar timescales in *S.cerevisiae*. In contrast, the

1 Introduction

degradation mechanisms for *hairly* mRNA are not known, however, mRNA turn-over is found to be generally fast, especially for transcription factors [Miller et al., 2011].

The natural properties of *S.cerevisiae* make it a suitable *chassis* for DNA assembly of synthetic systems. Its genome has been sequenced completely and large amount of information is available for many of its genes, gene products, their functions and interactions. In addition, the ease of genetic manipulation of yeasts is especially useful. Foreign and synthetic genetic materials can be transformed directly into yeast and many options are available that control copy number and transcription levels of heterologous gene expression. The workload associated with screening large gene libraries in this model organism has resulted in streamlined and largely standardized technologies. This includes standard sets of shuttle vectors with low or high copy numbers, different selection markers and expression cassettes with characterized promoter sequences. Furthermore, the ability of yeast to stably integrate exogenous DNA pieces into its genome through homologous recombination allows site-specific genomic manipulation in this organism.

An integral element of synthetic network construction is the characterization of *part* and *device* function within the *chassis*. This typically involves linking the network output to a reporter and measuring its gene expression levels. In yeast enzymatic assays that measure color changes (*lacZ*) or bioluminescence (luciferase) are available. However, the most frequently used reporters are fluorescent proteins, since they offer improved spatial and temporal resolution in comparison to other methods. Reporters can be linked to *systems* either through network regulated promoters or by direct protein-fusion to network *parts*. The expression of the reporter can be measured at the population level, for individual cells (flow cytometry), and even with sub-cellular precision (single-cell microscopy).

Based on reporter measurements the *system's* functionality can be assessed and optimized. For example, zebrafish derived *parts* may function differently in yeast, displaying properties that could not be predicted *ad hoc*. Therefore, testing prototype *systems* can help debug faulty networks, leading to redesign of networks or exchange with more suitable *parts*. Likely options include changing basal transcription levels by switching between different strength promoters. While there is no extensive *part* library available for yeast, yet, documentation of expression and

functionality of investigated endogenous and heterogenous protein domains can be used as a basis for alternate part design.

The optimization of the oscillator's subcomponents not only determines whether given *parts* can function in the proposed networks but also provide insight into which extend each *part* contributes to the dynamics of this network. In the specific case of the *hairly* network, the role of protein decay rates, external activation cues and binding site number can be addressed in this way. This will not only help design oscillators with particular dynamic properties in yeast, but can also provide valuable insight into the zebrafish's segmentation oscillator. The SynBio *Hairy* OSCILLATOR could therefore be used as an assay to directly test the single cell models proposed for the zebrafish. Ultimately, it may be possible to reconstruct an artificial PSM tissue, where each scale of the segmentation clock is designed, characterized, optimized and essentially understood. In other words, proving the segmentation clock mechanism by building it up based on the proposed theoretical and biological blueprints.

2 Aims

The goal of this thesis is to study the minimal oscillator network of the zebrafish segmentation clock. However, prior to verifying the proposed mechanism of the *hairy* gene oscillator, the existence of an autonomous oscillator in single cells of the zebrafish's PSM needs to be confirmed. Although it seems clear that a negative feedback loop of the *hairy* genes could generate cell-autonomous oscillations, it is difficult to show, which network is sufficient for generating oscillations, using top-down whole embryo approaches. Therefore, an approach is needed that excludes the effects of other underlying oscillators as well as redundant molecular components that mask the dynamics of the core mechanism.

Specifically, this thesis addresses the following open questions:

1. Do PSM cells contain a cell-autonomous segmentation oscillator?
2. Can a minimal network, based on *hairy* gene interactions, oscillate?

In order to investigate these questions, I aimed to:

1. Establish a cell dissociation technique for zebrafish PSM cells to track oscillator behaviour in individual cells.
2. Develop a novel approach for studying the segmentation oscillator outside the zebrafish embryo.
3. Determine whether *hairy* genes can be used as functional building blocks in such networks.

3 Methods

3.1 Fish Care and Preparation

All fish used for these experiments were raised based on standard fish care-taking techniques as described in Westerfield [1993].

Embryos for PSM extraction and dissociation experiments were obtained by crossing two heterozygous *Looping1* fish. The embryos were raised in clear E3 (without methylene blue) at 28°C until shield stage and then shifted to 20°C. At approximately the 4 somite stage, embryos were selected under a fluorescent stereoscope for the brightest YFP signal in the PSM region. Therefore, the *Looping1* embryos used in this study were homozygotic for the transgenic reporter insert.

3.1.1 PSM Tissue Explants

For intact PSM tissue microscopy, the PSM of selected *Looping1* embryos was explanted using dissection techniques described in Picker et al. [2009]. More specifically, the embryos were dechorionated and transferred to L15- medium. Then they were cut in half along the dorsoventral axis with a scalpel, separating head and tail regions. The initial step of injecting AMP-PNP was omitted since yolk cell contractions are not problematic if the dissection is carried out rapidly. Upon cleaning the tail piece from yolk debris and epidermal layer, the nonsegmented tissue at the posterior end was detached using a tungsten wire and transferred to fresh L15- medium. In these experiments, the entire PSM tissue was transferred into a round glass bottom imaging dish filled with L15- medium.

3.1.2 PSM Cell Dissociation

In order to isolate individual segmentation clock cells, the PSM tissue is first explanted from selected *Looping1* embryos and then dissociated by trypsin digestion and physical agitation (Masamizu et al. [2006], Maroto et al. [2005]). To minimize

cell loss arising from pipetting and transferral steps, the entire procedure is carried out in the glass bottom imaging dish. The explanted PSM is transferred into a drop of L15- medium, then trypsin solution is added in 1:5 ratio and the digest is allowed to proceed for 5min at 37°C. The trypsin solution is then removed and the cells are washed with small amounts of L15- medium. In this step, the fluid flows are utilized to physically agitate, separate and disperse PSM cells on the glass-bottom surface. Finally, the wash solution is replaced by imaging medium, either L15- or L15+FBS.

3.2 *E.coli* Plasmid Transformation

Standard transformation protocols were used to amplify plasmids into chemo-competent *E.coli* cells. Plasmids containing the *ccdB* death cassette were transformed using DB3.1 *ccdB* resistant cells. All other plasmids were amplified in the DH5 α strain. For transformation into HIP-competent DH5 α cells, a 100 μ l DNA mix containing the plasmid DNA, 20 μ l 5xKCM and H₂O was prepared. First cells are thawed on ice and then added in 100 μ l aliquots to the desired plasmid DNA. The DNA/cell mix is incubated on ice for 5-30min, then heatshocked at 42°C for 45sec and then returned to ice for 5min. Then, 1ml of room temperature SOC was added, followed by a 1 hour recovery at 37°C prior to plating onto selection agar plates. Colonies can be screened after over night incubation at 37°C. Due to the high efficiency GW cloning, it was sufficient to amplify two colonies using QIAGEN mini-preps and checking positive clones using sequencing.

3.3 Gateway (GW) Cloning of Yeast Vectors

The design of all yeast vectors used in this study is based on the standardized gateway (GW) cloning strategy [Invitrogen, 2003]. In this cloning scheme libraries of genes, or network parts, can be assembled via reversible, single enzyme, cloning reactions. At the base of this scheme are four types of vectors, DESTINATION, ENTRY, EXPRESSION and DONOR, and two types of reactions, LR and BP. The LR reaction, catalysed by LR clonase, transforms ENTRY and DESTINATION vectors into EXPRESSION and DONOR vectors and BP clonase catalyses the reverse reaction (Figure 3.1).

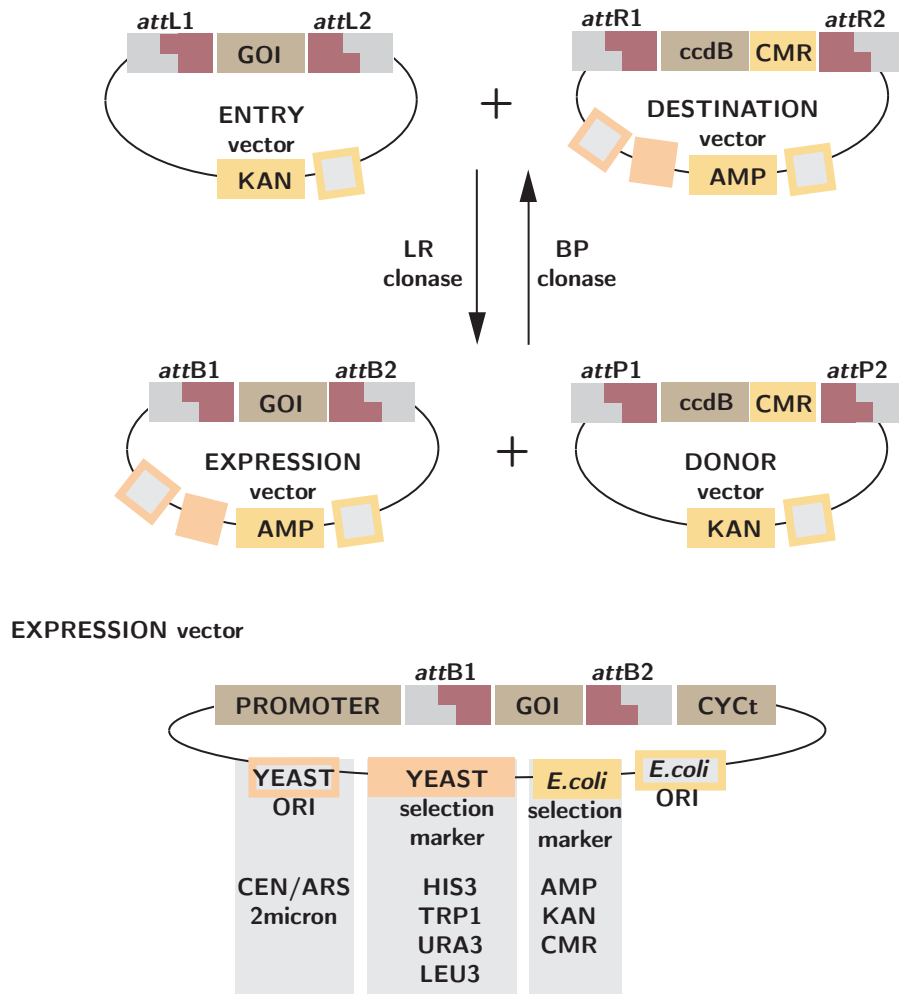


Figure 3.1 Gateway Cloning Scheme. The LR reaction transforms ENTRY and DESTINATION vectors into EXPRESSION and DONOR vectors. The reaction is reversible using BP clonase. A modular EXPRESSION vector design was used for all synthetic yeast devices in this thesis. The genes of interest (*GOI*) were inserted between a promoter region and the *CYC1* terminator sequence resulting in *attB1* and *attB2* scars between these elements. The EXPRESSION vectors further included selection markers for growth in yeast and bacteria as well as origins of replication (ORI) in both organisms.

The λ clonases recombine specific *att* sites, namely L and R sites to form B and P sites and vice versa. These sites flank the interchanging regions of each vector. In the ENTRY vector the gene of interest (*GOI*) is flanked by *attL* sites. In the DESTINATION vector a selectable death cassette, *ccdB*, is flanked by *attR* sites between a promoter and terminator sequence. After the LR cloning reaction, the resulting EXPRESSION vector contains the *GOI*, flanked by *attB* sites, between the promoter and terminator sequences. These standard EXPRESSION vectors are the target design of all synthetic yeast devices.

In this project, the *GOIs*, including ORFs of *Her* parts and *2xCFP* reporter, were obtained in ENTRY vector form (named pE-'*GOI name*'), either through the inclusion of *attB* flanking sites during synthesis design or via 2-step ENTRY PCR. To generate Her EXPRESSION vectors, ENTRY vectors of Her parts were cloned into the DESTINATION vectors *413pGAL-ccdB* and *413pCUP-ccdB* using the LR reaction. The *413pGAL-ccdB* plasmid was obtained from Simon Alberti. It is a CEN/ARS, low copy, yeast replicative plasmid with a HIS3 auxotrophic selection marker and contains the GAL promoter (*pGAL*) and CYC terminator (*tCYC*). The *413pCUP-ccdB* was generated through standard digest and ligation protocols, replacing the *pGAL* in *413pGAL-ccdB* by *pCUP* from the *pMK-pCUP-HMY* plasmid obtained from Genart.

For the SWITCH-OFF assay, the reporter cassette *100BSpTEF-2xCFP* was synthesized by Genart and cloned into the MCS of pRS304, a yeast insertion plasmid that contains the TRP1 selection marker, using digest and ligation. From this, the DESTINATION vector *304-100BSpTEF-ccdB* for switching reporter genes was generated using BP reactions and selection.

3.3.1 LR and BP reactions, generating *Expression* and *Entry* Vectors

LR and BP reactions were prepared in 2.5 μ l reaction volumes, containing approximately 20fmol of each plasmid. Stock solutions of plasmids are typically between 200 and 500 ng/ μ l, thus 1:4 dilutions of each plasmid were used. For LR reactions 1 μ l of ENTRY and DESTINATION vectors were combined with 0.5 μ l of LR clonase. The reactions were incubated at 25°C over night and transformed into DH5 α *E.coli* (Section 3.2). The bacteria were grown on ampicillin (AMP) agar plates to select for the EXPRESSION vector, positive colonies were amplified and purified using the

QIAGEN mini-prep kit. Similarly, BP reactions used 1 μ l of each EXPRESSION and DONOR vectors plus 0.5 μ l of BP clonase and over night incubation. The reaction product was transformed into DH5 α *E.coli* and the ENTRY plasmid containing cells were selected on kanamycin (KAN) agar plates.

3.3.2 2-step *Entry* PCR

The 2-step PCR amplification protocol was obtained from the Alberti Lab (MPI-CBG) and uses nested PCR to amplify short gene sequences (<2kb) from genomic or plasmid DNA with gene-specific primers and adds flanking *attB* using universal primers in the second PCR. The standard PCR protocol uses *Pfx* polymerase and 50ul reaction volumes. The final product is PCR purified and cloned in a BP reaction with the pDONR plasmid to generate an ENTRY vector containing the amplified gene.

3.3.3 Generating *Destination* Vectors

The DESTINATION vector *413pCUP-ccdB* vector was generated by replacing the *pGAL* in *413pGAL-ccdB* with the *pCUP* from *pMK-pCUP-HMY*. The primers CUPp-RNheI and CUPp-L were used to amplify *pCUP* in a standard PCR and then cut in a double restriction digest using SacI and NheI. In parallel the *pGAL* was removed from *413pGAL-ccdB* in a double digest using SacI and SpeI. Since SpeI and NheI generate the same sticky ends, the *pCUP* peptide was ligated into the linearized *413-ccdB* backbone. Each DNA fragment was gel purified prior to ligation and positive transformants were screened using cmR3-away and T3 primers and then verified via sequencing.

The protocol for generating the DESTINATION vector *304-100BSpTEF-ccdB* was adapted from Cheo [2004] and can be used as a general protocol for DESTINATION VECTOR cloning. For this the *attB* flanked *2xCFP* in *304-100BSpTEF-2xCFP* was swapped with the *ccdB* cassette from the pDONR plasmid using the BP reaction. In fact, the resulting DESTINATION vector is considered a byproduct of the BP reaction and therefore needs special care for positive selection. The key step is to minimize unwanted background transformants by linearizing all reactant vectors first. *304-100BSpTEF-2xCFP* was digested in its *GOI* using EcoRI and pDONR was digested

in its backbone using EcoRV. The DNA products were precipitated by adding 3M NaAc and 100% Ethanol and resolved in TE buffer prior to running the BP reaction. The final plasmid is transformed into DB3.1 cells and plated onto AMP/CMR plates to maintain the *ccdB* cassette.

3.4 Yeast Plasmid Transformation

A standard LiAc/PEG transformation protocol was used for both replicative and insertion plasmids (*413xxx* and *304xxx*, respectively). In short, the target yeast strain is collected from an $OD_{600} \approx 0.5$ culture and resuspended in 0.1M LiAc. The transformation mix consists of salmon sperm ssDNA, plasmid DNA, yeast cells in LiAc solution, PEG/LiAc and DMSO. Upon heatshock, cells are either allowed to recover in YPD medium, for integrative plasmids and drug resistance selection, or plated directly on selective media, for replicative plasmids. Transformed colonies were picked after 2 days and respread on fresh selective plates.

In this thesis, the auxotrophic markers *URA3*, *TRP1*, *HIS3* and *LEU2*, which are nonfunctional in the target yeast strain W303 ADE+, were used for selecting both replicative and integrative plasmids. For integrations, *URA3* and *TRP1* plasmids were linearized by cutting within the auxotrophic markers using digestive enzymes ApaI and Bsu36I respectively.

3.4.1 Yeast Integrative Plasmid Colony Screen

Integrative plasmids can be inserted into the yeast genome by linearizing within the selection marker. Yeast cells then insert the entire plasmid at a site of homology, thereby introducing a functional copy of the selection marker at the target site. Both multiple and single insertion events are possible and depend on the amount of plasmid DNA used. To verify the number of insertion events, I used a PCR screening scheme provided by Julie Valastyan. There are four primers available for each marker, 30x A/B/C/D.

The primer pairs A-B and C-D produce products for plasmids inserted at the locus and primer pair B-C is used to determine whether tandem repeats are present. Of course, this approach only distinguishes between single and multiple insertions.

A basic yeast colony PCR protocol was used to check for both proper insertion and tandem events. For this, a small amount of freshly grown yeast colony is resuspended in 25ul PCR mastermix, containing the desired primer pair, and run at 95°C for 10 min followed by 35 cycles of

1. 95°C, 30 sec
2. 50°C, 30 sec
3. 72°C, 1.5 min

and followed by another 3 min at 72°C.

3.5 Yeast Storage

For long term storage, yeasts are suspended in YPD with 17.5% glycerol and can be kept at -80°C indefinitely. For short term storage, yeasts are kept at 4°C on selective media plates (replicative plasmids) or YPD plates for up to 3 weeks. After this time, fresh plates were streaked from frozen stock.

3.6 Yeast Imaging Preparations

For visual screening of yeast cultures, small amounts (3-4 μ l liquid volumes) of cells were sandwiched between a clean microscope slide and cover slip. For this, cells were either picked from media plates and diluted in PBS or obtained from liquid cultures. To obtain liquid cultures for long-term imaging, small amounts of yeast were picked from plates and resuspended in the applicable SC growth medium supplemented with the desired carbon source (glucose, galactose or raffinose). These cultures are grown overnight on shakers at 25°C, then strongly diluted and grown for another 3-5 hours until mid-log phase ($OD_{600} \approx 0.4$). For long-term imaging yeast cells were seeded on ConA coated imaging dishes.

All systems that contain constitutively expressing promoters or pCUP devices exclusively were cultured in 2% glucose SC media. To induce transcription of pCUP devices, copper sulfate (1000x $CuSO_4$) was added to the imaging medium to a final concentration of 1mM. For galactose induction of devices containing *pGAL*, yeast cells were cultured in 2% raffinose SC medium over night. To induce transcription,

the raffinose medium was exchanged with 2% Galactose SC at the start of imaging (long-term microscopy) or two hours prior (for screening and transcription block).

3.6.1 ConA Dish Coating & Cell Seeding

All coating steps were carried out at room temperature. First glass-bottom imaging dishes are pre-treated with 1M NaOH for 1 hour, followed by two rinses with H₂O. Then the entire glass-bottom is covered ConA Coating solution, incubated for at least 20min, and again rinsed twice with H₂O. At this point, dishes are ready for cell seeding. The dish's bottom should stay covered by water until the experiment, but no longer than 12 hours.

First all H₂O is removed from imaging dish. Then diluted yeast culture is added in a drop covering the glass-bottom of the dish. The cells are allowed to settle onto the glass surface in a 5 min incubation. Then all cell-containing medium is suctioned away and quickly replaced with imaging medium (applicable SC medium).

3.6.2 Protein Degradation

To stop protein expression using cycloheximide to block translation, the regulatable pMET REPRESSOR devices were used. To induce Her transcription these devices were grown in 2% glucose SC-MET medium. Immediately prior to imaging, translation was blocked by adding a small volume of cycloheximide (35 μ g/ml final concentration) directly to the medium.

3.7 Microscopy

3.7.1 Explanted PSM Imaging

An inverted Zeiss Axiovert 200M microscope with motorized stage and Andor iXon 888 EM-CCD camera was used. This system contains standard brightfield optics for transmitted light imaging and uses mercury lamp excitation for fluorescent imaging. For time lapse imaging a 60x objective and YFP bandpass filter was used. A fluorescent image as well as brightfield reference image were taken in multiple z-planes for each explanted PSM and the best focus plane was determined manually. For the

nuclear localization images, the 60x objective was used in combination with YFP bandpass and mcherry longpass filter.

3.7.2 PSM Cell Imaging

In addition to the Zeiss system described in the previous section, a Bachhoffer chamber was mounted on the motorized stage for temperature control of single PSM cells at 28°C. For time lapse imaging both 100x (NA) and 60x objectives in combination with a YFP bandpass filter and standard brightfield optics were used.

Upon PSM cell dissociation (Section 3.1.2) the imaging dishes were transferred to the microscope and multiple imaging fields were identified manually. Cells within the imaging fields had to be well dispersed and in part YFP positive. Typically, microscopy set and thus the time between cell dissociation and start of imaging lasted 30 to 45 min. Time lapse movies were recorded with 1.5 to 4 min time point intervals for 3 hours. Image sequences were saved in a single .tiff stack for each imaging field.

3.7.3 Yeast Cell Imaging

The DeltaVision Core system used for yeast single cell microscopy consists of an inverted Olympus - IX71 microscope and Photometrics Cool Snap HQ2 camera with Applied Precision motorized stage and weather station black environmental control box. The system uses an LED as transmitted light source and an SSI-lumencor for fluorescent imaging. All experiments used Delta Vision CFP/YFP Live Cell filter sets and were carried out at 25°C. For time lapse imaging, Olympus UPlanSApo 100x 1.4oil or Olympus PlanApo N 60x 1.42oil objectives were used.

After yeast cell seeding (Section 3.6), imaging dishes were transferred to the microscope and multiple imaging fields were selected. Typically 5 fields were recorded for each experimental condition, resulting in approximately 20 imaging fields per 4 compartment dish. Additives, such as transcriptional inducers galactose and copper sulfate, were added immediately prior to setting the initial z-focus. Each imaging set consisted of an image-based autofocus, using the BF channel, z-stacks of each applicable fluorescent channel and a reference BF image.

Image sequences were exported in single .dv files for each imaging field.

3.8 Image Processing & Data Analysis

3.8.1 Extracting Fluorescent Signals per Cell over Time

All single cell images were processed using Fiji, an open source image processing package that recognizes a large number of image types including both .tiff stacks and .dv files. First, the image sequences of different channels (BF, YFP and CFP) were separated and a max projection of fluorescent images was obtained using the "Grouped Z Project" plugin. Individual cells were tracked manually by marking circular regions, corresponding to the perimeter of cells, on BF images and saving these to a ROI list. To track fluorescent signals per cell over time, Johannes Schindelin generated a custom "Circle Interpolator" plugin, which is able to interpolate size and position between user-defined oval regions in these ROI lists over several frames and subsequently calculates pixel values within all regions. I wrote an additional Fiji macro, which applies the "Circle Interpolator" with the current ROI list to all applicable projections and summarizes explained data into a single table. The values from this table, including region area and mean fluorescent signal per region, were stored in Excel.

3.8.2 Generating PSM Kymographs

The PSM kymograph was generated using Fiji. For this a segmented line of interest (LOI) was specified along the PSM on one side of the notochord, using BF images as reference, for several images in a time series. The 'LOI Interpolator' plugin, customized by Johannes Schindelin, was then used to calculate the position of LOIs for remaining images in the time series. The plugin also calculated the signal along the length of the LOI, by averaging across the line width, and generated a kymograph by plotting these linegraphs sequentially in a 2D image.

3.8.3 Period Estimate from PSM cells

To estimate periods for single cell oscillations, I measured peak to peak and trough to trough distances of the explained mean fluorescent signal for each cell track using hand curation and MATLAB. To eliminate the detection of intermediate peaks, each cell track was first normalized to its minimum and maximum values and then

smoothed with a 7-point smoothing average. Then a peakfinding function detected peaks, based on the constraints that the minimum peakdistance is 40 min and that the minimum peak height was 30% of the maximum height. To find trough to trough distances the datasets were inversed, through multiplication with -1, prior to running the peakfinding algorithm. The detected values were then manually verified before an average period was calculated per cell.

3.8.4 Yeast Reporter Response Measurements

To quantify the reporter response in the yeast SWITCH-OFF assay the cell tracks' CFPp signal fold change (CFP-SFC) over time was calculated using MATLAB. For this the final CFPp signal measurement was divided by the initial signal measurement for each tracked cell. Due to the inhomogeneities in Her part induction across cells of a single culture, a measure for successful Her part induction was calculated. For this, the signal to noise ratio (SNR) for YFPp induction in each cell was estimated by dividing the mean signal YFPp of each cell by the standard deviation of noise calculated from the cell tracks of non-expressing cells. Only cell tracks with SNR values above those of non-expressing cells were considered in further analysis. To compare reporter response between independent experiments, each CFP-SFC was normalized to the mean values calculated for non-expressing cells in each experiment.

3.8.5 Protein Half-Life Estimates

To quantify half-life (HL) of fluorescently tagged proteins in yeast, I measured the decay of fluorescence signal per cell over time using PRISM. Each cell trace was fit with the built in "plateau followed by one phase decay" function using automatic outlier elimination. This method uses robust nonlinear regression on each data set to determine a best-fit curve, shown in Figure 3.2, which fits the following equation:

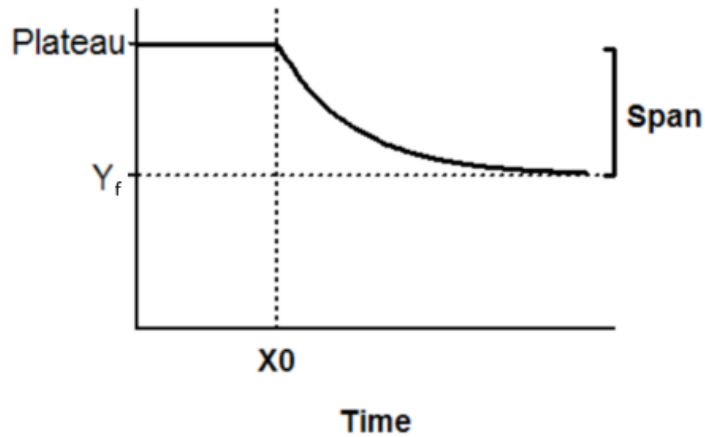
$$\begin{aligned}
 Y(x) &= Plateau && \text{for } x < X0 \\
 &= Y_f + Span * e^{-K*(x-X0)} && \text{for } x > X0
 \end{aligned}
 \tag{3.1}$$

The initial *Plateau* represents the signal before the effects of treatment, such as cycloheximide, take affect. $X0$ is the timepoint at which the signal intensity drops

3 Methods

and the effects of treatment are detectable. The final value, Y_f , is the detected signal at the end of the decay and the *Span* is the difference between *Plateau* and Y_f . K provides the rate of decay from which HL can be computed, as $HL = \ln(2)/K$.

Figure 3.2 Half-Life Decay Curve Fit Model. Her protein degradation curves were fit in PRISM using the 'plateau followed by one-phase decay' model. The decay equation is: $Y(x) = Y_f + Span * e^{-K*(x-X_0)}$ for $x > X_0$. The half-life is then computed from $HL = \frac{\ln(2)}{K}$, where K is obtained from the decay fit.



To estimate half-life from oscillating *pCUP* expression data, the first expression peak of each cell trace was shifted to the initial time point. This aligns all traces to $X_0 = 0$. In addition, each data trace was truncated before the signal increase of a subsequent expression peak.

Half-life measurements were only recorded for cells whose nonlinear regression converged to a best-fit curve. This typically excluded cell traces with low signal to noise values. To compare HL between different samples, the mean HL of independent experiments was calculated.

3.9 Statistics

All data sets were analyzed using PRISM and all measurements are referenced as $MEAN \pm SD$, unless otherwise stated. To compare oscillator periods in single cells and explanted PSM tissue, the data points of each independent experiment were analyzed using the Kruskal-Wallis multiple comparison test (unpaired, nonparametric). Their mean measurements were then pooled, unless they were found to be significantly different. Each mean value therefore represents one independent experiment and n gives the total number of independent experiments. Different samples were then compared using the Welch's t-test (unpaired, unequal variance).

Similarly, both the SWITCH-OFF assay's CFP-SFC values as well as the HL values were analyzed using the Kruskal-Wallis multiple comparison test. Again, the non-significant experiments were pooled and the mean value of each independent experiment was used in subsequent statistical analysis (Kruskal-Wallis multiple comparison test). For the SWITCH-OFF assay, CFP-SFC values of each sample were compared against the CFP-SFC of negative cells. For HL measurements, all samples were compared to one another.

All statistically analyzed samples were visualized using box plots that show the median, 25th and 75th percentiles as horizontal lines of the box with whiskers extending from the smallest to largest value. In addition, the graphs show all data points of all pooled experiments as well as the p-value and number of independent experiments obtained from statistical analysis.

4 Materials

4.1 Chemicals

All used chemicals are technical grade and obtained from companies listed in the Appendix List of Companies.

4.2 Enzymes

Restriction enzymes and DNA modifying enzymes, as well as their corresponding buffers, were obtained from Fermentas. Gateway cloning enzymes, LR and BP clonase, were obtained from Invitrogen.

4.3 DNA

All plasmids were amplified using the QIAGEN mini-prep kit.

There are two types of plasmids that are generated in gateway (GW) cloning reactions: 1. DONOR and DESTINATION vectors and 2. ENTRY and EXPRESSION clones. DONOR and DESTINATION vectors contain the *ccdB* cassette at the locus where a gene of interest (*GOI*) can be inserted. The integration of *GOIs* via LR or BP reactions results in ENTRY and EXPRESSION clones, respectively. The DONOR vector as well as a majority of DESTINATION vectors were obtained from the Alberti lab [Alberti et al., 2007]. All plasmids used in this thesis and their source are listed in Table 4.1. In addition to GW generated plasmids this list also includes commercially synthesized genes and DNA constructs that were obtain from Genearth and Eurofins.

Primers (Table 4.2) were also synthesized using either Invitrogen, for short oligos, or Biomers, for long or modified oligos.

Name	Description	Source
pDONR221	DONOR vector	Invitrogen
413pGAL-ccdB	DESTINATION vector with GAL promoter	SAP
413pGPD-ccdB	DESTINATION vector with GAL promoter	SAP
413pCUP-ccdB	DESTINATION vector with CUP promoter	AO
413pMET-ccdB	DESTINATION vector with MET promoter	SA
304-100BSpTEF-ccdB	DESTINATION vector with TEF promoter preceded by 6 Her1 BS	AO
pE-H1Y	zebrafish cDNA derived 5'- <i>HER1</i> - <i>WRPW</i> - <i>VYFP</i> -3'	PK
pE-H6Y	zebrafish cDNA derived 5'- <i>HES6</i> - <i>WRPW</i> - <i>VYFP</i> -3'	PK
pE-H7Y	zebrafish cDNA derived 5'- <i>HER7</i> - <i>WRPW</i> - <i>VYFP</i> -3'	PK
pE-HWY	yeastized gene sequence of 5'- <i>HER1</i> - <i>WRPW</i> - <i>VYFP</i> -3'	Geneart
pE-HYW	yeastized gene sequence of 5'- <i>HER1</i> - <i>VYFP</i> - <i>WRPW</i> -3'	Geneart
pE-YHW	yeastized gene sequence of 5'- <i>VYFP</i> - <i>HER1</i> - <i>WRPW</i> -3'	Geneart
pE-HMY	yeastized gene sequence of 5'- <i>HER1</i> - <i>MIGED DOMAIN</i> - <i>VYFP</i> -3'	AO
pE-H6MY	yeastized gene sequence of 5'- <i>HES6</i> - <i>MIGED DOMAIN</i> - <i>VYFP</i> -3'	Geneart
pMK-pCUP-HMY	<i>pCUP attB1-HMY-attB2</i>	Geneart

Table 4.1 List of Plasmids. PK-Phillip Knyphausen (Oates Lab, MPI-CBG), SA-Simon Alberti Lab (MPI-CBG), SAP-published in [Alberti et al., 2007], AO-Annelie Oswald (Oates Lab, MPI-CBG)

4 Materials

name	sequence
CUP-RNhel	GCT TAG GCT AGC TTT ATG TGA TGA TTG ATT GA
CUP-L	TAG TTC GAG CTC TAC CGA CAT TTG GGC GCT ATA CGT
T3p	ATT AAC CCT CAC TAA AGG GA
304-A	GCTGACAGGGAAATGGTCAG
304-B	CGA TTT CGG CCT ATT GGT TA
304-C	GGC TTA ACT ATG CGG CAT CAG AGC
304-D	CCC CCT GCG ATG TAT ATT TT
5'-gene-specific	A GGA GAT AAC AAA ATG <i>gene-specific sequence</i>
3'-gene-specific	CAA GAA AGC TGG GTC <i>gene-specific sequence</i>
5'-universal	GGGG ACA AGT TTG TAC AAA AAA GCA GGC TTC GAA GGA GAT AAC AAA ATG
3'-universal	GGGG AC CAC TTT GTA CAA GAA AGC TGG GTC

Table 4.2 List of Oligos and Primers

4.4 Buffers and Solutions

Name	Composition
E3 clear	5 mM NaCl 0.17mM KCl 0.33 mM CaCl ₂ 0.33 mM MgSO ₄
L15-	500 ml Leibovitz's L-15 (Invitrogen nr.21083027) without phenol red 5 ml Penicillin + Streptomycin (PAA nr.P11-010)
L15+ FBS	500 ml Leibovitz's L-15 (Invitrogen nr.21083027) without phenol red 5 ml Penicillin + Streptomycin (PAA nr.P11-010) 10% FBS (Invitrogen nr.10270106)
1xPBS	137 mM NaCl 2.7 mM KCl 10 mMNa ₂ HPO ₄

Continued on next page

4.4 Buffers and Solutions

Name	Composition
	pH 7.4
Trypsin Solution	0.25% Trypsin, EDTA (PAA L11-004)
5xKCM	500 mM KCl 150 mM CaCl ₂ 250 mM MgCl ₂
1.step PCR (1rxn)	0.4 μ l Pfx Polymerase $\frac{2.5U}{\mu l}$ 5 μ l 10x PCR buffer 5 μ l 10x PCR enhancer 26.1 μ l H ₂ O 1.5 μ l 10mM dNTP 1 μ l 50mM MgSO ₄ 1 μ l 100 $\frac{ng}{\mu l}$ DNA template 10 μ l 10 μ M gene-specific primer mix
2.step PCR (1rxn)	0.4 μ l Pfx Polymerase $\frac{2.5U}{\mu l}$ 3 μ l 10x PCR buffer 3 μ l 10x PCR enhancer 16.5 μ l H ₂ O 1.5 μ l 10mM dNTP 0.6 μ l 50mM MgSO ₄ 20 μ l 1.step PCR reaction 5 μ l 5 μ M universal primer mix
yeast PCR mastermix (1rxn)	0.5 μ l TAQ Polymerase $\frac{5U}{\mu l}$ 2.5 μ l 10x PCR buffer 0.5 μ l 10mM dNTP 5 μ l 10 μ M primer1 5 μ l 10 μ M primer2 11.5 μ l H ₂ O

Continued on next page

4 Materials

Name	Composition
LiAc	0.5 ml 1M LiAc (C ₂ H ₃ LiO ₂) 4.5 ml H ₂ O
PEG/LiAc	4 ml PEG 3350 0.5 ml 1M LiAc (C ₂ H ₃ LiO ₂) 0.5 ml H ₂ O
YPD	10 g Bacto Yeast Extract (BD nr.212720) 20 g Bacto Peptone (BD nr.211820) 20 g Dextrose H ₂ O to final Volume of 1000 ml
SC w/ 2% sugar	50 ml 10% Difco-Yeast Nitrogen Base w/o AA (BD nr.291940) 0.345 g CSM (MP-Bio nr. 114500022) 50 ml 20% sugar (Raffinose/Glucose/Galactose) H ₂ O to final Volume of 500 ml
SC-HIS3 w/o sugar	50 ml 10% Difco-Yeast Nitrogen Base w/o AA (BD nr.291940) 0.345 g CSM-HIS (MP-Bio nr. 114510322) H ₂ O to final Volume of 450 ml
SC-MET w/o sugar	50 ml 10% Difco-Yeast Nitrogen Base w/o AA (BD nr.291940) 0.345 g CSM-MET (MP-Bio nr. 114510712) H ₂ O to final Volume of 450 ml
SC-HIS3 w/ 2% sugar	450 ml SC-HIS3 w/o sugar 50 ml 20% sugar (Raffinose/Glucose/Galactose)
200mM Phosphate Buffer	87.7 ml 0.2 M sodium phosphate, mono salt 12.3 ml 0.2 M sodium phosphate, di salt 100 ml H ₂ O pH 6

Continued on next page

Name	Composition
ConA Coating solution	250 μ l 5 $\frac{mg}{ml}$ ConA
	125 μ l 200 mM phosphate buffer (pH 6)
	2.5 μ l 1M CaCl ₂
	5 μ l Sodium Azide 10%
	2117 μ l 1x PBS

Table 4.3 Buffers and Solution

4.5 Genetically Modified Organisms

4.5.1 Zebrafish Strains

For both PSM extraction and dissociation experiments, the transgenic zebrafish line *Looping1* was used. This line was generated by Daniele Soroldoni in the lab and contains a 20kb gene segment of the endogenous *her1/her7* gene locus and the sequence of the yellow fluorophore Venus added to the ORF of *her1*. Therefore, the YFP signal generated in this mutant correlates with endogenous expression levels of HER1 protein. Secondly, a nuclear marker line was used to check for the localization of Her1-Venus within PSM cells. This line was obtained from Gabby Krens of the Heisenberg Lab and expresses a red fluorophore, mcherry, fused to the histone H2A.

4.5.2 Bacterial Strains

The DH5 α strain was used for all standard plasmid amplification protocols. The DB3.1 strain was used for propagating plasmids containing the *ccdB* operon, also known as death cassette.

4 Materials

name	genotype
DH5 α	<i>F- endA1 glnV44 thi-1 recA1 relA1 gyrA96 deoR nupG Φ80dlacZΔM15 Δ(lacZYA-argF)U169, hsdR17(r_K^- m_K^+), λ^-</i>
DB3.1	<i>F- gyrA462 endA1 glnV44 Δ(sr1-recA) mcrB mrr hsdS20(r_B^-, m_B^-) ara14 galK2 lacY1 proA2 rpsL20(Sm^r) xyl5 Δleu mtl1</i>

Table 4.4 *E.coli* Strains

4.5.3 Yeast Strains

The W303 ADE2+ strain was chosen as chassis for all generated gene networks discussed in this thesis. It is a derivative of the common W303 wildtype strain and was chosen for its extensive properties. Most importantly, the additional ADE2+ mutation eliminates the accumulation of red pigment. This reduces autofluorescence of cells and makes this strain suitable for fluorescence microscopy applications. The TC strain contains a stably integrated copy of the reporter construct (*100BS_pTEF_2xCFP*) and is used for testing the repressor function of various *hairry* derived genes.

name	chassis	genotype	origin
W303 ADE2+	W303	<i>his3-11/15 trp1-1 leu203/112 ura3-1 ADE2+ can1-100</i>	Alberti Lab
TC	W303 ADE2+	<i>ura3-1::URA3-100BS-pTEF-2xCFP</i>	AO

Table 4.5 *S.cerevisiae* Strains

5 Results and Discussion

5.1 PART1: The Segmentation Oscillator within Isolated PSM Cells

In order to determine whether a cell-autonomous oscillator exists, I first needed to isolate the oscillator from the local and global regulatory machinery of the segmentation clock. More specifically, the cells of the PSM needed to be separated from one another, to disrupt cell-cell communication via Delta-Notch signaling, and grown in an environment lacking diffusible signaling factors (Figure 5.1). First, I explanted PSM tissue of 8-12 somite stage zebrafish embryos using the flat-mount tissue dissection protocol from [Picker et al., 2009]. Then, I adapted the dissociation protocols previously used for chick and mouse embryos [Maroto et al., 2005],[Masamizu et al., 2006] to physically dissociate cells for an *ex vivo* culture in serum free L15 medium (L15-). In order to track the expression of clock genes, I used the transgenic zebrafish line *Looping*, in which Her1 is tagged with a yellow fluorescent protein (YFP).

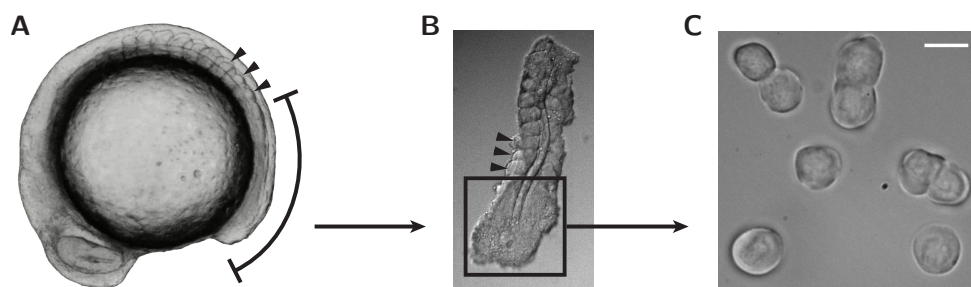


Figure 5.1 **Extraction of PSM Tissue and Isolation of Cells.** For explanted PSM tissue experiments the segmentation clock containing PSM was explanted from 8 to 12 somite stage embryos. Isolated PSM cultures were obtained by physically dissociating explanted PSM with trypsin and pipetting. **A.** The unsegmented PSM tissue of a dechorionated embryo is marked by the solid bar and the 3 last formed somites are marked by arrows. **B.** The dorsal view of explanted PSM tissue is shown with the last formed somites marked by arrows. **C.** Single cells were obtained exclusively from the unsegmented PSM (area in box) and maintained in L15- medium.

5 Results and Discussion

5.1.1 Explanted PSM Tissue In Culture

In order to test whether the segmentation clock remains functional in explanted PSM tissue, I cultured PSM tissue in L15- medium and imaged YFP expression for up to 6 hours. During this time the explanted PSM tissue continues to undergo morphological changes (Figure 5.2.A.). It extends along its anteroposterior axis (AP) and shrinks mediolaterally. These convergent extension movements indicate that the explanted PSM tissue continues typical tail-development in culture medium.

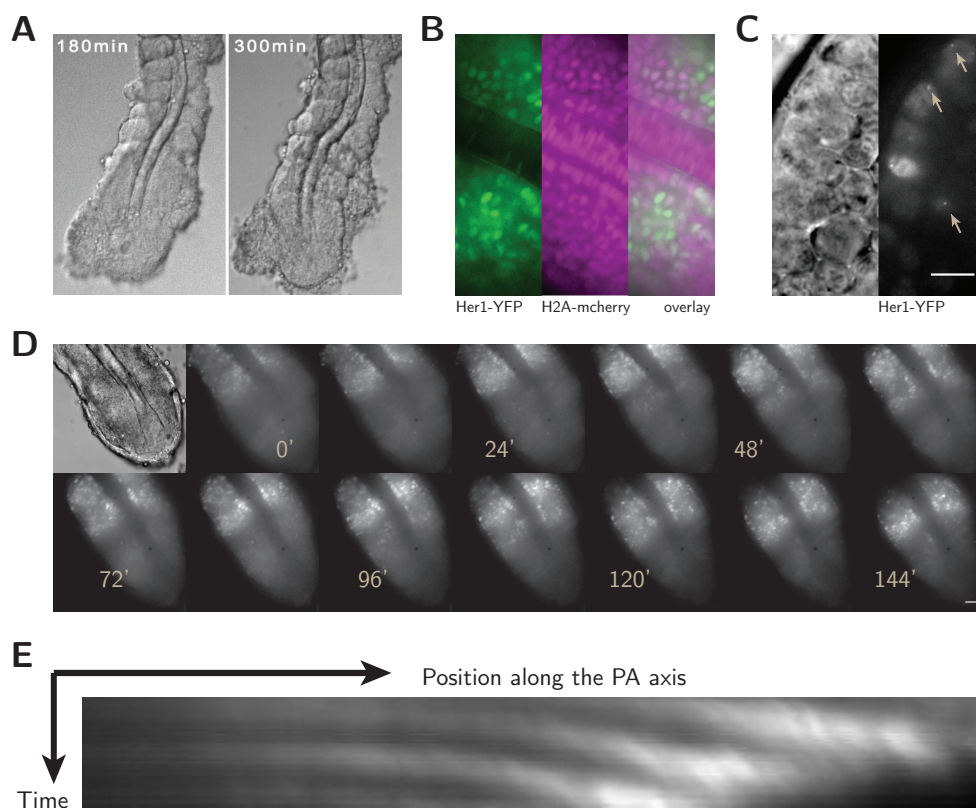


Figure 5.2 Explanted PSM of *Looping* fish. **A.** Explanted PSM tissue continues to form somites and displays convergent extension movements when cultured in L15- medium. **B.** The Her1-YFP reporter protein (green) localizes to the fluorescently tagged nucleus (magenta). **C.** Her1-YFP reporter accumulate in nuclear spots (arrows). **D.** The YFP reporter is expressed cyclically in the PSM and displays the typical traveling wave pattern over time. **E.** A kymograph, plotting protein expression over time, shows the propagation of waves from the posterior to anterior end of the PSM [Soroldoni and Oates, 2011].

More importantly, the explanted tissue also continues to form somites and to cyclically express Her1-YFP in L15- medium. Similarly to observations in whole embryo

imaging of the *Looping* line, the traveling waves of YFP expression stripes are clearly visible and the peak fluorescence intensity is greater in cells at the PSM's anterior end (Figure 5.2.D.). In Figure 5.2.E., a kymograph plotting protein expression over time along the PA axis shows the typical curved expression patterns observed for segmentation clock reporters reviewed in Soroldoni and Oates [2011]. This indicates that the segmentation clock remains functional in the cultured tissue.

Unfortunately, due to the absence of cellular markers and limited resolution, the oscillators of single cells within the tissue cannot be tracked over time. However, based on the DCT model, the intrinsic period of these oscillators is tightly linked to the tissue level period of oscillations and ultimately to somite formation over time. Therefore, the segmentation period of explants serves as an estimate of global oscillatory period, P_g , which in turn provides an estimate of single cell oscillator periods within these cultured tissues.

To estimate the period of somite formation in these tissues, I counted the number of somites formed during the imaging interval for 7 explants. The average segmentation period in these tissues is 35 ± 8 min and ranges from 29 min to 50 min. This distribution is comparable to endogenous somitogenesis periods recorded at physiological temperatures between 20 °C and 26 °C [Schröter et al., 2008]. Since the explanted PSMs were not grown in a temperature controlled environment, some variation due to fluctuations in room temperature at the microscope are reasonable.

In contrast to whole embryo imaging [Soroldoni and Oates, 2011], the microscopy of explanted PSM improves the spatial resolution of YFP signal, which is not uniformly distributed in the cell. In order to verify the nuclear localization of Her1-YFP in PSM cells, I crossed *Looping* with a transgenic line that constitutively expresses mcherry tagged histones (Figure 5.2.B). This shows that the YFP signal is spatially localized to cells in the unsegmented PSM tissue on either side of the notochord. Therefore, the YFP signal is a suitable marker for PSM cells and can be used in single cell experiments to distinguish these from other cell-types. Interestingly, at high magnification subnuclear spots are clearly visible within the expressing cells (Figure 5.1.C). Whether these spots are DNA binding sites where YFP tagged Her1 is accumulating or whether they are aggregation sites of non-functional protein has not been investigated.

5.1.2 Isolated PSM Cells In Culture

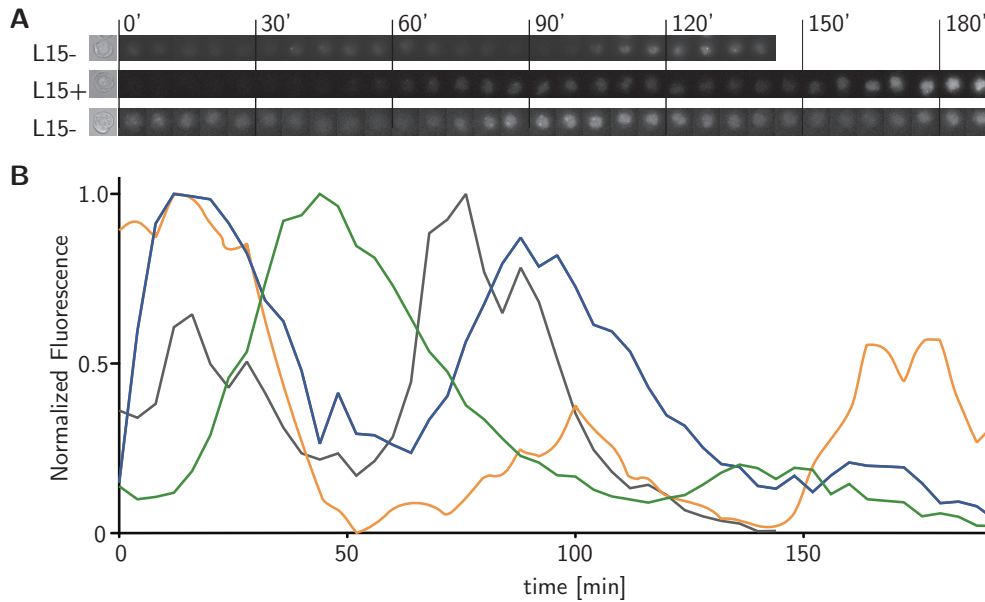


Figure 5.3 Oscillating PSM Cells. Imaging of dissociated PSM cells of Her1-YFP from *Looping* embryos shows that Her1-YFP expression fluctuates cyclically in individual PSM cells. **A.** Images of the YFP signal oscillations from dissociated PSM cells cultured in either L15- or L15+ medium over time. **B.** Normalized cell tracks of individual PSM cells. Tracks were obtained by quantifying the mean YFP signal per cell at each time point. For comparison, each cell track was normalized to its maximum and minimum values.

To study the segmentation clock’s oscillator in single cells, I dissociated up to three PSM explants (Method 3.1.2) in a single imaging dish and cultured them in L15- medium. This dissociated cell culture contained not only PSM cells, but also cells originating from the notochord and possibly some remnants of the epidermis and yolk. Therefore, I specifically selected imaging fields containing YFP expressing cells, which originate exclusively from the PSM (Figure 5.1.B.&C.), and recorded both fluorescence signals and brightfield images for up to three hours. Three types of expression patterns were observed in isolated cells:

1. cells without any detectable YFP signal
2. cells whose YFP signal degraded over time
3. cells with one or more peaks of YFP expression

In the last group, up to 3 peaks of expression were observed, which corresponds to 2 cycles of oscillations. Therefore, a subset of PSM cells is able to continue oscillatory

5.1 PART1: The Segmentation Oscillator within Isolated PSM Cells

expression in serum-free culture conditions. Neither expression patterns nor timing of peaks was coordinated in cells from individual experiments (Figure 5.3). Thus, oscillations are considered unsynchronized in the dissociated cell cultures.

Next, I wanted to determine the period of cyclic gene expression in cells with oscillating YFP expression. For analysis (Section 3.8), I used the corresponding brightfield images to track isolated cells, defined as cells not forming contacts with other cells, and calculated the mean fluorescence per cell at each time-point using the FIJI COI interpolator macro written by Johannes Schindelin. Then, I used MATLAB to estimate peak-to-peak, as well as trough-to-trough intervals, for each cell track and averaged all values to obtain an approximate period of oscillation per cell, hereafter defined as period per cell. In total, I analyzed 50 cell tracks stemming from 4 independent experiments. The oscillatory periods ranged between 53 min and 110 min and were not significantly different between experiments. The average period per cell for all pooled measurements is 77 ± 12 min.

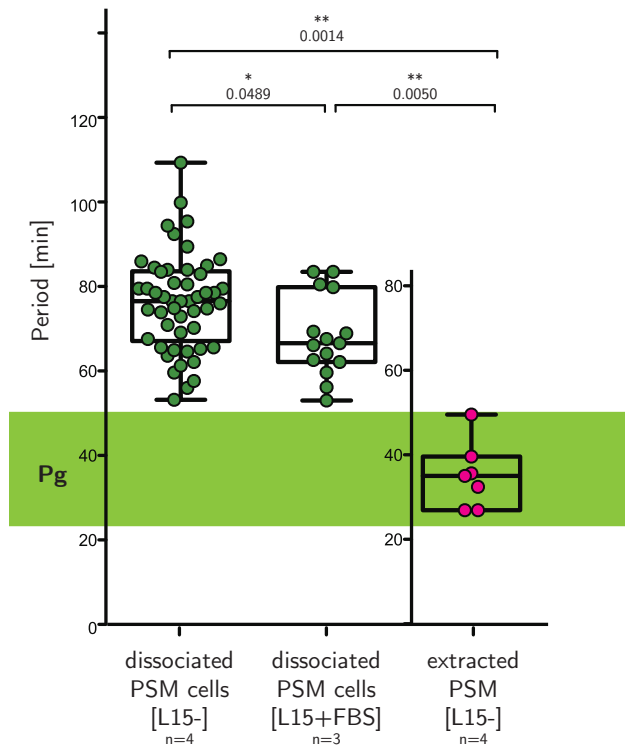


Figure 5.4 Oscillatory Periods in Explanted PSM and isolated PSM cells. The shaded bar shows the range of global somitogenesis periods, P_g , of zebrafish embryos at room temperature ($20^\circ\text{C} - 28^\circ\text{C}$) [Schröter et al., 2008]. Explanted PSMs were grown at room temperature and their segmentation period is 35 ± 8 min (magenta datapoints) and was estimated from the rate of segment formation in BF images. Isolated cells were cultured at 28°C . The oscillator periods per cell were estimated by averaging the duration between consecutive peaks and troughs of fluorescent signal (green datapoints). The period of cells grown in L15+ was 69 ± 10 min and that of cells cultured without FBS was 77 ± 12 min. The segmentation period of explanted PSMs is comparable to global somitogenesis, while Her1 oscillations in dissociated cells was significantly slower. The p values between sets of independent experiments is given at the top.

The current segmentation clock model postulates that diffusible regulatory factors determine oscillator period in individual PSM cells. In zebrafish, the growth

factor FGF is linked to maintaining sustained high-frequency oscillations in the posterior PSM. Therefore, the addition of growth factors to dissociated cell cultures is expected to either speed up oscillations or extend the duration of the oscillatory regime. To test this hypothesis, I added FBS, which contains numerous growth factors, to dissociated PSM cells and tracked their YFP fluorescence signal. For these dissociated cells in L15+FBS, the same range of expression patterns as for non-serum treated cells was observed and for oscillatory expression a maximum of 3 consecutive YFP peaks was recorded. The periods per cell were calculated as described above. In total, I analyzed 15 cells from 3 independent experiments and the periods for FBS treated cells range from 53 to 84 min and average at 69 ± 10 min. Thus, oscillations in FBS treated cells are slightly faster ($p = 0.0528$) than those of cells grown in L15-.

5.2 PART1: Discussion

5.2.1 Explanation of Slowed Oscillator Period in Isolated Cells

Similarly to its chick and mouse homologs, *c-hairy1* [Maroto et al., 2005] and *Hes1* [Masamizu et al., 2006] respectively, the zebrafish clock gene *her1* oscillates in PSM fragments and dissociated PSM cells. These studies confirm that the segmentation period in explanted PSM fragments is comparable to the embryo's global segmentation period and that oscillations in isolated cells are not synchronized.

While *c-hairy* oscillations in dissociated chick cells were not tracked over time, Masamizu et al. [2006] observed that *Hes1* oscillates in isolated PSM cells at similar rates as the global segmentation period of explanted PSM tissues. In contrast, the oscillator periods per cell of both L15- and L15+FBS experiments are significantly slower than the segmentation period estimated from explanted PSMs (Figure 5.1.2). Based on the DCT model [Morelli et al., 2009], which relates frequencies of the individual oscillators to that of the global segmentation clock frequency, we expect that the frequency cellular oscillators does not differ more than 30% from the global segmentation frequency. At growth temperatures of 28°C , where the global period, P_g , equals 23.5min , the intrinsic period, p_i , can be estimated as follows:

$$\begin{aligned}
.7 * \omega_i &< \Omega_g < 1.3 * \omega_i \\
.7 * \frac{2\pi}{p_i} &< \frac{2\pi}{P_g} < 1.3 * \frac{2\pi}{p_i} \\
.7 * 23.5min &< p_i < 1.3 * 23.5min
\end{aligned}$$

We therefore expect an intrinsic period between 16min and 31min. These values lie well below all periods of single cell oscillations recorded in this study. If the DCT model holds then it is possible that the measured periods in the isolated zebrafish cells are not the true intrinsic oscillator periods, p_i . In other words, they may be measurements of slowing oscillators that are either already arresting or lacking required factors for sustained high-frequency oscillations.

As predicted by the frequency profile, oscillators are slowing down towards the anterior of the PSM before arresting completely. Indeed, the imaged cells might originate from this area, since PSM cells were selected based on the presence of YFP fluorescence. It is possible that due to the increase of YFP signal in the anterior PSM of the *Looping* these slowing oscillators were preferentially captured for subsequent analysis. This issue can easily be resolved by using tailbut tissue exclusively for future dissociation experiments.

Our current model proposes that the slowed single cell oscillations towards the anterior of the PSM result from signaling gradients of growth factors in the PSM and it has been shown that FGF can maintain PSM cells in an immature, oscillatory state, *in vivo* [Sawada et al., 2001]. Therefore, we propose that the addition of serum improves oscillator stability in cells regardless of their origin within the PSM. While Masamizu et al. [2006] found that mouse PSM cells sustain oscillations upon serum treatment, oscillations were not drastically changed with serum in isolated zebrafish PSM cells with respect to untreated cells. It is possible that the concentration of FBS was too low to cause an effect in these experiments, however it may also be the case that FBS growth factors are not properly recognized in zebrafish cells. Therefore, it would be interesting to not only test the increase of serum concentration but also other forms of growth factors (fish serum derived or purified FGFs) and whether these are able to sustain oscillations in the cultured cells.

Only recently, it has been shown that Her1 within PSM cells in fact oscillates with the same period as somitogenesis [Delaune et al., 2012]. While this is not indicative

of the intrinsic period of isolated oscillators, it does show that the period of cellular oscillators matches the global period of segment formation. Delaune et al. [2012] also looked at Her1 oscillations Notch pathway mutants and showed that these are indeed important for synchronization of neighboring oscillators. Interestingly, upon visual inspection it appears that not only are cells less synchronized, but their oscillatory periods are also considerably longer than in the wild type reporter. In this case, the slow periods measured in cultured cells could also be a direct consequence of lacking Delta-Notch signaling.

5.2.2 Isolated PSM cells: applications and future experiments

"A major scientific goal is to understand how oscillatory behavior of the segmentation clock at the tissue level relates to molecular oscillations in single cells." [Soroldoni and Oates, 2011] In terms of our 3 tier model, this means understanding how the global and local regulatory machineries interact with individual oscillators [Oates et al., 2012]. In this thesis, I showed that it is possible to dissociate single PSM cells into culture and track the cellular oscillators using an appropriate reporter line, such as the *Looping1*. With this new approach, we are able to measure the core oscillator's dynamics and test the effects of extracellular cues on its frequency, stability and robustness.

The global regulatory machinery comprises signalling gradients of FGF, Wnt and retinoic acid (RA) that determine the frequency of oscillators along the PSM as well as the point of oscillatory arrest [Aulehla and Pourquié, 2010] (reviewed in [Oates et al., 2012]). In culture, different concentrations and combinations of these signalling factors can easily be tested. Therefore, concentration regimes of sustained, slowed and arrested oscillations can be determined in this assay. And the interplay of FGF, Wnt and RA with respect to PSM cell maturation can be measured directly and the following questions can be addressed:

1. Which concentrations of FGF/Wnt/RA allow for sustained oscillations?
2. Does any one gradient have the dominant effect?
3. Are external maturation cues reversible? Can arrested cells restart segmentation clock oscillations?

The local regulatory machinery consists of the cell-cell communication pathway Delta-Notch that synchronizes oscillators of neighboring PSM cells. In contrast to the global signaling factors described above, Delta ligands need to be immobilized to induce Notch signaling and thus cannot be added to the medium directly [Varnum-Finney et al., 2000]. However, the effects of cell-cell communication can be studied indirectly in cultured cells that have formed adhesions between one another. Undesired cell-cell interactions in dissociated cell cultures showed a number of interesting oscillatory behaviors (data not shown). For instance, two touching cells can undergo anti-phase oscillations and rows of connected cells tend to send waves of expression along their 1D axis. In combination with micropatterning techniques, various cell-interaction geometries could be generated and the arising oscillatory patterns studied to understand how synchronization scales up to the tissue level.

5.3 PART1: Conclusion

In the first part of this thesis, a protocol for dissociating zebrafish PSM cells was introduced to isolate the core oscillator from the remaining segmentation clock components. This has not been possible before and allows the study of the segmentation clock at an intermediate level, filling the gap between 'bottom up' and 'top down' approaches. I showed, for the first time in dissociated PSM cells, that Her1 proteins continue to oscillate at the single cell level and thereby verified that a cell-autonomous oscillator exists in the zebrafish segmentation clock. This technique can also be applied to other transgenic lines to track the dynamics of clock components at the single cell level. In addition, this system makes individual cells highly accessible to the external control of their signalling molecules. Therefore, the established cell dissociation protocol is the core element of future experiments studying the oscillator dynamics in individual cells and its interplay with the local and global regulatory machineries of the segmentation clock.

5.4 PART2: Synthetic Segmentation Oscillator Network in Yeast

In the first part of this thesis, the existence of a segmentation oscillator in single zebrafish PSM cells was verified. This confirms that in the zebrafish the bottom tier of the segmentation clock model consists of an autonomous single cell oscillator. In this section, I introduce the synthetic biology approach for studying the components of this single cell oscillator, by rebuilding a minimal *hairy* gene network outside the zebrafish, in yeast cells. For this purpose, I established a six step experimental workflow, summarized in Figure 5.5, which follows the three construction stages of SynBio networks.

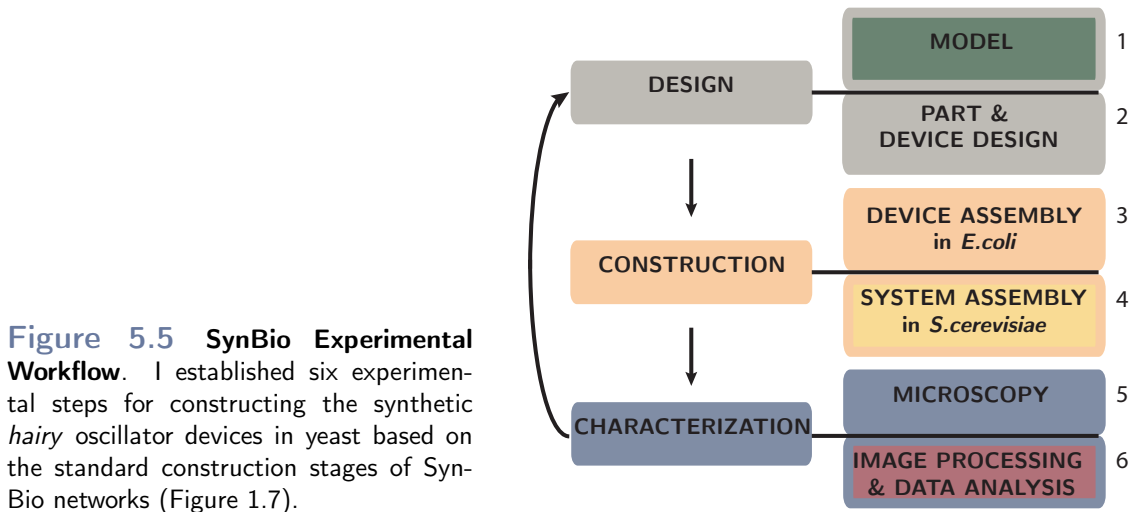


Figure 5.5 SynBio Experimental Workflow. I established six experimental steps for constructing the synthetic *hairy* oscillator devices in yeast based on the standard construction stages of SynBio networks (Figure 1.7).

For the first stage, I introduce the minimal *hairy* gene oscillator model and describe the parts and device designs derived for this system. For the second stage, I briefly discuss the standardized strategies established for device and system assembly in *E.coli* and *S.cerevisiae*, respectively. For the third stage, I discuss the results of characterizing oscillator parts and devices using single cell microscopy and image analysis. Finally, I conclude on the optimization strategies of the current system design.

5.4.1 The Minimal Oscillator Model

The simplest model of a genetic network oscillator is the Goodwin Oscillator, consisting of a single negative feedback loop (Figure 5.6.A), in which a single gene product represses its own transcription [Novak and Tyson, 2008]. Current models propose that the zebrafish segmentation oscillator consists of redundant networks involving Her1 and Her7, which are both transcriptional repressor proteins [Cinquin, 2007][Lewis, 2003][Oates and Ho, 2002]. However, recent studies show that, of the two, only Her1 is able to bind within its promoter region without other interaction partners [Schröter et al., 2012] [Trofka et al., 2012]. Therefore, we propose that the minimal oscillator network could be a single component negative feedback loop, in which Her1 periodically binds to its promoter region and represses its own transcription (Figure 5.6.B).

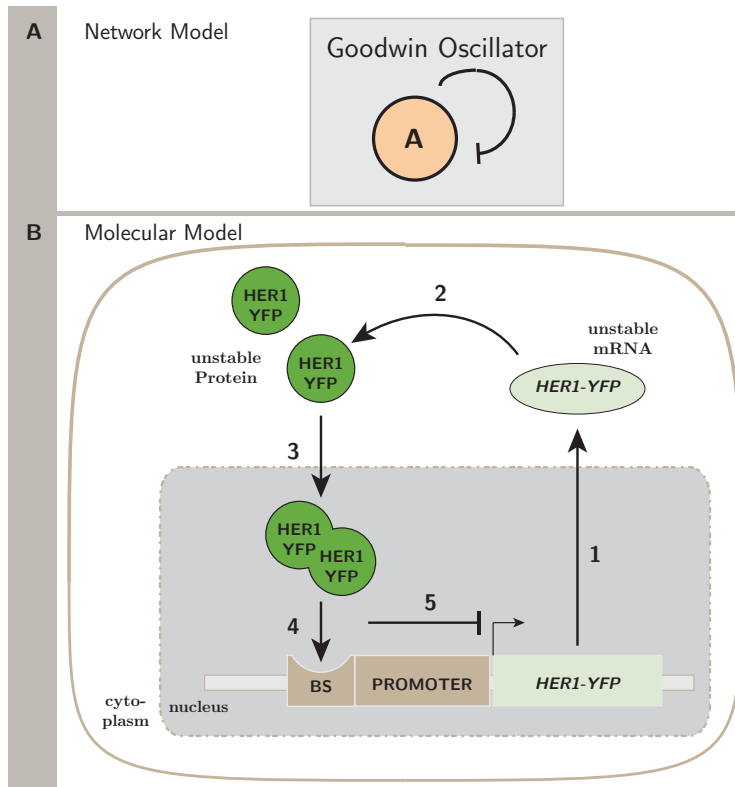


Figure 5.6 The Minimal Her1 Oscillator Model. **A.** The simplest negative feedback oscillator network is the Goodwin Oscillator, which consists of a single gene component repressing its own expression. This network is the basis for the initial design of the synthetic Her1 oscillator. **B.** In the molecular model of this network *her1* is transcribed to mRNA (1), translated into protein (2), transported to the nucleus (3) where it binds, as a dimer, to its promoter region (4) and represses its own transcription (5). The oscillator's dynamics depend on the time delay resulting from steps 1-3, nonlinearities introduced in steps 4 and 5, as well as the time-scales of mRNA and protein degradation.

The dynamics of this network arise from five successive molecular events. In the absence of Her1 protein the promoter region is active, transcribing *HER1* into mRNA (1). This mRNA is then translated into Her1 proteins (2), which can sub-

sequently dimerize and translocate back into the nucleus (3). There these dimers bind upstream of the promoter to Her1 binding sites (4) and block transcription by recruiting co-repressors (5). As a result, the unstable *HER1* mRNA and protein molecules disappear from the cell until the Her1 dimer concentration is too low to generate repression. At this point the cycle starts over.

It is easy to see how oscillations of *HER1* mRNA and protein molecules are generated in such a network. However, modelling and construction of synthetic Goodwin Oscillators has demonstrated that the time-scales and non-linearity of the molecular events specifically, and thus building part properties in general, determine whether such networks can indeed oscillate. Since we want to build an oscillator using the zebrafish's segmentation clock components, rather than previously used components, the first objective of this project was to generate a library of suitable building blocks and characterize their functionality in the yeast chassis.

5.4.2 Part & Device Design

The eukaryote *S.cerevisiae* was chosen as a 'black box' chassis, in which the oscillator network is sequentially pieced together using 'building blocks' from the zebrafish segmentation oscillator. To build the minimal oscillator network in yeast (Figure 5.8.A), three genetic parts are needed:

1. a constitutively active promoter
2. a gene encoding the Her1 repressor
3. a Her1 binding site

The design of each part is inspired by its endogenous properties in the zebrafish, but modulated for use in yeast. In order to measure the behavior of this synthetic network in single yeast cells, we decided to tag the Her1 repressor with a fluorescent protein. The YFP tag, used as a reporter for tracking oscillations in isolated PSM cells, was also chosen as a live-reporter in yeast networks.

In contrast to previously generated synthetic oscillators, the zebrafish derived parts have not been characterized for standardized "construction" in yeast cells. Therefore, we designed an additional system, the SWITCH-OFF assay (Figure 5.8.B), to test oscillator parts individually. The SWITCH-OFF system consists of two devices, the REPRESSOR and REPORTER. The REPRESSOR device contains

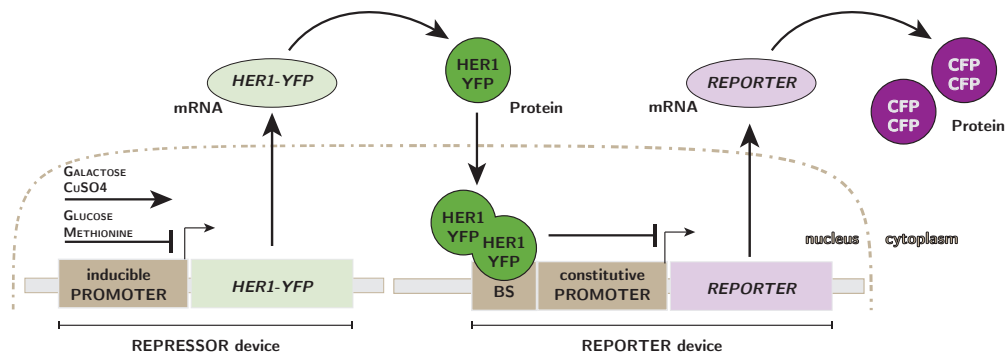


Figure 5.7 Her SWITCH-OFF Assay. This schematic shows the REPRESSOR and REPORTER devices introduced into the yeast cells to test the Her parts' function as transcriptional repressors in yeast. In an uninduced state only the reporter gene will be transcribed off the constitutive promoter of the REPORTER device and CFP fluorescence accumulates in the cell. The induction of the REPRESSOR device will result in the accumulation of the tagged Her parts in the cells. If the Her part is functional, both able to bind to the DNA binding sites and recruit the yeast's repression machinery, then the expression of the reporter gene will be terminated and CFP fluorescence will decrease over time.

the Her1 repressor part and a controllable yeast promoter to regulate transcription levels of Her1 parts (1). On the other hand, the REPORTER device contains a fluorescent reporter preceded by the Her1 binding sites and the constitutive yeast promoters (2). Each device can be tested individually to verify basic properties of the yeast promoter parts. In combination, this assay functions like a switch, if the Her1 part can function as a repressor then reporter expression and consequently the reporter's fluorescent signal is "switched-off".

Her1 repressor parts

In the zebrafish, Her1 is transcribed from a 6406 bp long ORF, which contains three introns, one of which is longer than 4000 bp (Figure 1.4). In yeast, introns are not only rare but also short, between 100bp and 400bp in length, and typically only one intron is present in a gene [Spingola et al., 1999]. It is unclear whether the yeast's splicing machinery is able to remove multiple and long introns. Therefore, we decided to use the intron free cDNA sequence of *HER1* for yeast expression. For visualization, the Venus-YFP, also used for tracking Her1 in the single PSM cell experiments, was linked at the C-terminus. In fact, the *HER1-YFP* cDNA was derived directly from the transgenic *Looping1* lines used in the single PSM cell

5 Results and Discussion

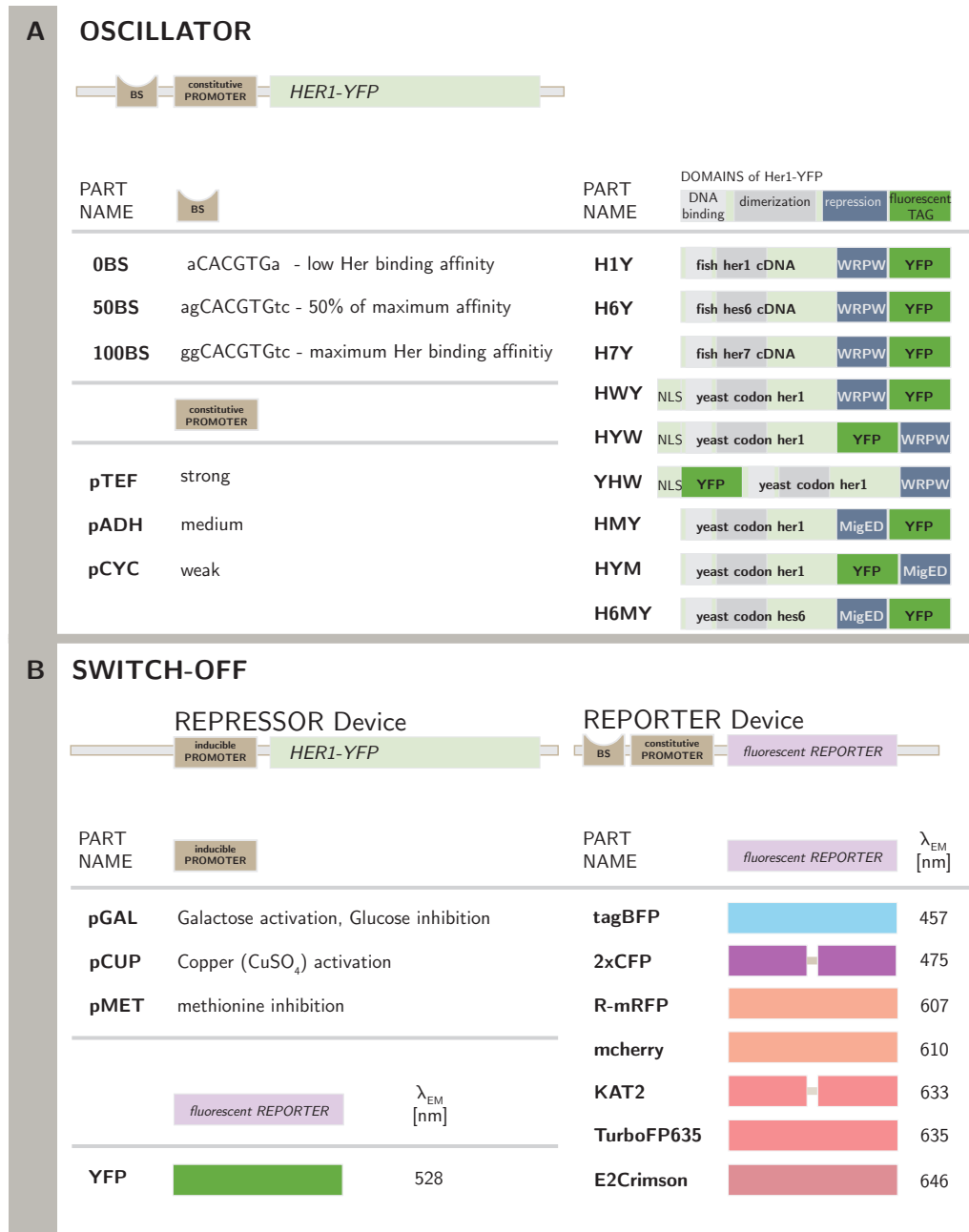


Figure 5.8 Library of Parts. A complete list of genetic building blocks accumulated for the devices used in **A.** the OSCILLATOR and **B.** SWITCH-OFF assays. All coding sequences, such as Her parts and fluorescent reporters, are stored as genes of interest (GOI) in ENTRY vectors. The regulatory components, such as binding sites (BS) and promoters were incorporated into DESTINATION vectors (see Method Section 3.3)

study described in Section 5.1. The *HER1-YFP* part, named H1Y, was obtained from Phillip Knyphausen (MPI-CBG) in the lab.

To address potential translation deficiencies arising from incompatible codon usage between yeast and zebrafish coding sequences, a synthesized yeast-codon optimized *HER1-YFP* version, named HWY, was obtained from Genart. In addition, the parts *HER1-YFP-WRPW*, named HYW, and *YFP-HER1-WRPW*, named YHW, were designed and synthesized to explore the effect of YFP position on part expression and function.

Initially it was unclear whether the endogenous Her1 nuclear localization signal is recognized in yeast. Therefore, I added a *SV40-NLS* sequence, a standardized nuclear localization signal (NLS) adapted for yeast http://partsregistry.org/Part:BBa_J63008, at the 5' end of the ORF of repressor parts HWY, HYW and YHW. However recently, Schröter et al. [2012] successfully used Her1 in a yeast one hybrid assay, where the NLS within Her1 was sufficient for nuclear localization (since the attached GAL-AD is known to lack NLS sequences [Silver et al., 1988]). Therefore, the addition of *SV40-NLS* was omitted in the design of further Her1 repressor parts.

Besides proper expression and localization, Her1 also needs to function as a transcriptional repressor in yeast. In the zebrafish the WRPW domain at the N-terminus of Her1 recruits Groucho, a transcriptional co-repressor. Groucho is structurally and functionally similar to the co-repressor Tup1 in yeast [Buscarlet and Stifani, 2007][Sekiya and Zaret, 2007]. While Tup1 interacts with the N-terminal domains of other transcription factors, such as Mig1 [Ostling et al., 1996], in yeast it has not been shown to interact with the Her1 WRPW domain. Therefore, I designed a Her1 repressor part that can interact with Tup1, named HMY, in which the WRPW domain is exchanged by the Mig1 effector domain (MigED).

In addition to Her1 derived repressor parts, I included Her7 and Hes6, Hairy transcription factors closely associated with the zebrafish segmentation oscillator, in this 'building block' library. These parts are used as negative controls when testing for Her1 repressor function, since neither Hes6 nor Her7 are able to bind DNA as homodimers. Similarly to H1Y, the parts H6Y and H7Y were obtained from Phillip Knyphausen (MPI-CBG) and consist of the zebrafish derived cDNA sequence of *HES6-YFP* and *HER7-YFP*, respectively. In addition, a yeast codon

optimized sequence *HES6-MIGED-YFP*, named H6MY, was obtained as a control part for the Tup1 interacting HMY.

Yeast Promoters

The endogenous promoter region of *HER1* in zebrafish includes both transcription activation cues as well as Her binding sites [Schröter et al., 2012][Trofka et al., 2012]. In yeast, however, foreign transcriptional promoters typically lead to aberrant initiation or are inactive altogether. Therefore, yeast derived promoters are generally used for foreign gene expression [Romanos et al., 1992]. For this purpose, several yeast promoters have been identified and characterized in terms of their expression rates and sensitivity to regulating factors [Mumberg et al., 1995][Mumberg et al., 1994]. Furthermore, several yeast promoters have been characterized specifically for the use as standardized parts in synthetic gene networks [<http://partsregistry.org/Promoters/Catalog>].

In order to mimic the basal transcription activity of the endogenous *HER1* promoter, several constitutive yeast promoters of varying expression strengths were selected from these studies. This list includes the *pCYC*, *pADH*, and *pTEF*, hereafter referred to as the low, medium and strong expressing promoter parts respectively. For the REPRESSOR device, the Galactose and copper inducible promoters *pGAL* and *pCUP*, as well as the methionine repressible promoter *pMET* were selected.

Her1 binding sites

The Her1 binding site used in this toolbox is CACGTG, a 6-mer of nucleic bases derived from the H-box consensus binding sequence for Hes/Her proteins. It was shown that the DNA affinity of Her1 proteins also depends on the bases flanking the core hexamer [Schröter et al., 2012]. From this data I derived three different binding sites for the part library with low (0%), medium (50%) and high (100%) binding affinity with respect to the highest affinity measured in the MITOMI. These binding sites are named *0BS*, *50BS* and *100BS*, respectively.

Fluorescent reporters

For the SWITCH-OFF system several reporter fluorophores were designed. Since venusYFP, a yellow fluorescence protein, is used to track Her1 repressor parts, reporter proteins need to be either blue or red fluorophores. Besides emission wavelengths and yeast codon optimization, the main concerns for reporter design in yeast include brightness of signal, fast-turnover (short half-life) and fast maturation of fluorophore. The list of screened reporters includes tagBFP, mcherry, the dimers 2xCFP and tdKatushka2, the N-degron destabilized R-mRFP (R stands for the N-terminal arginine), as well as TurboFP635, E2Crimson.

5.4.3 Construction

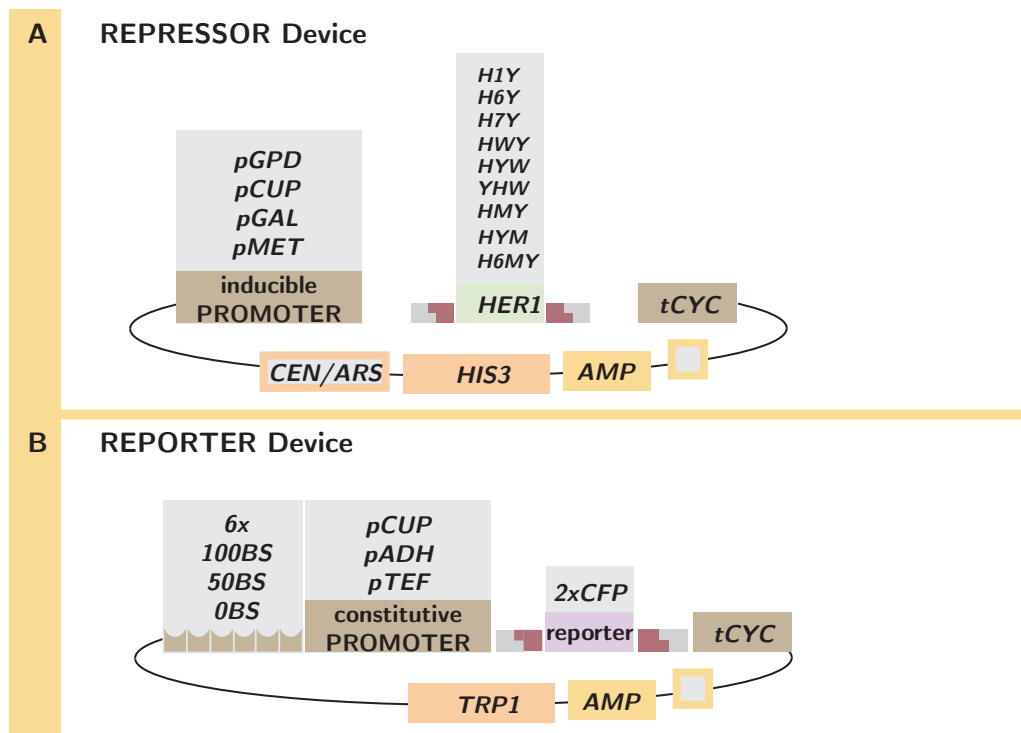


Figure 5.9 Final Device Construction. In the final construction stage for **A. REPRESSOR** and **B. REPORTER** devices a number of different promoter and GOI parts were assembled into a library of EXPRESSION vectors. This device library was subsequently screened for functionality, which led for instance to the selection of 2xCFP as core fluorescent reporter for the SWITCH-OFF assay network.

For the first stage of construction, the gateway (GW) cloning strategy was used to systematically assemble network parts and devices. GW cloning uses site specific

recombination and can insert DNA fragments, our defined parts, at specific locations along a predefined sequence array, while maintaining their orientation. The insertion site simply depends on the flanking sequences of the DNA fragments and since the reactions are reversible the parts can easily be swapped in and out. GW cloning is quick and efficient and the resulting genetic arrays can be amplified using standard *E.coli* transformation and culturing. Therefore, this is a reliable cloning system for generating part and device libraries.

I used single site GW cloning for initial network assembly of each device (for definitions of GW terminology, see Method Section 3.3). Therefore, I generated a library of ENTRY vectors containing all Her1 repressor and fluorescent reporter parts. For the REPRESSOR devices, I generated a library of low and high copy DESTINATION vectors, containing the yeast CEN/ARS and 2μ origins of replication (ORI), respectively, as well as one of the yeast auxotrophic selection markers *HIS3*, *TRP1*, *URA3* or *LEU3*. Each of these vectors contains either the constitutive promoter, *pGPD*, or one of the controllable promoters, *pGAL*, *pCUP* or *pMET*, upstream of the insertion site and a standard yeast transcription terminator sequence, *tCYC*, downstream of the insertion site. For the REPORTER device, yeast integrative DESTINATION vectors, lacking yeast ORIs, containing the *TRP1* or *URA3* selection markers were obtained. Here, six consecutive Her1 binding site parts and one of the constitutive yeast promoters, *pCYC*, *pADH* or *pTEF*, were placed upstream and a *tCYC* downstream of the insertion site. Essentially, the final REPORTER and REPRESSOR devices, shown in Figure 5.9, are EXPRESSION vectors obtained by combining specific DESTINATION and ENTRY vectors.

In the second stage of construction, I inserted REPORTER devices into the W303 ADE⁺ yeast genome, utilizing homologous recombination of the yeast selection marker. From this I obtained stable REPORTER strains with either single- or multi-copy insertions of the device. To test the Her1 parts, I transformed the REPRESSOR devices into the wild type W303 ADE⁺ and the REPORTER strains using standard transformation protocols. While the REPORTER strains can be cultured in standard YPD, all REPRESSOR devices require continued selection pressure and were therefore cultured in the respective drop out medium.

5.4.4 Part & Device Characterization

While we have identified a set of oscillator building blocks, described in Section 5.4.2, these parts are not well defined in the context of the yeast chassis. In order to generate oscillations, Her proteins need not only dimerize, translocate to the nucleus and bind DNA, but also activate the yeast's repression machinery at the targeted promoter region. In addition, modelling and construction of the Goodwin oscillator showed that short repressor half-lives are essential for sustained cyclic expression in negative feedback networks. Therefore, I designed simple REPRESSOR and REPORTER devices to test the Her part expression patterns and functional properties in yeast.

Her1 localization in yeast

First, I assessed whether the Her1 repressor parts are properly expressed in yeast (summarized in Figure 5.10). For this I visually inspected the expression of each REPRESSOR device in W303 ADE+ yeast strains at a screening microscope and checked whether the fluorescent YFP tag is localized to the nucleus as is observed for Her1-YFP in zebrafish (Figure 5.2). To maximize expression levels, the strong inducible and constitutive promoters, *pGAL* and *pGPD*, were used to screen localization patterns.

In *pGAL*-H1Y REPRESSOR cultures, most cells were negative for YFP expression and the remaining cells displayed YFP accumulation in spots in the area of the nucleus. While 'nuclear' spots were also observed in PSM cells, the typical diffusive signal throughout the nucleus is completely missing in yeast. Furthermore, the transformation of constitutively expressing REPRESSOR devices, containing *pGPD*-H1Y, yielded no colonies. This indicates that Her1-YFP is somehow toxic to yeast cell growth. This is further supported by the low levels of YFP expressing cells in the induced cultures as well as the slowed growth of these cells in comparison to other *pGAL* containing devices (data not shown). In addition, the absence of a clear nuclear localization pattern in these cells indicates that zebrafish derived *her1-yfp* is not properly expressed or processed in the yeast.

The expression of yeast codon optimized HWY, HYW and YHW resulted in similar phenotypes: no clones were obtained for constitutively expressing transformants

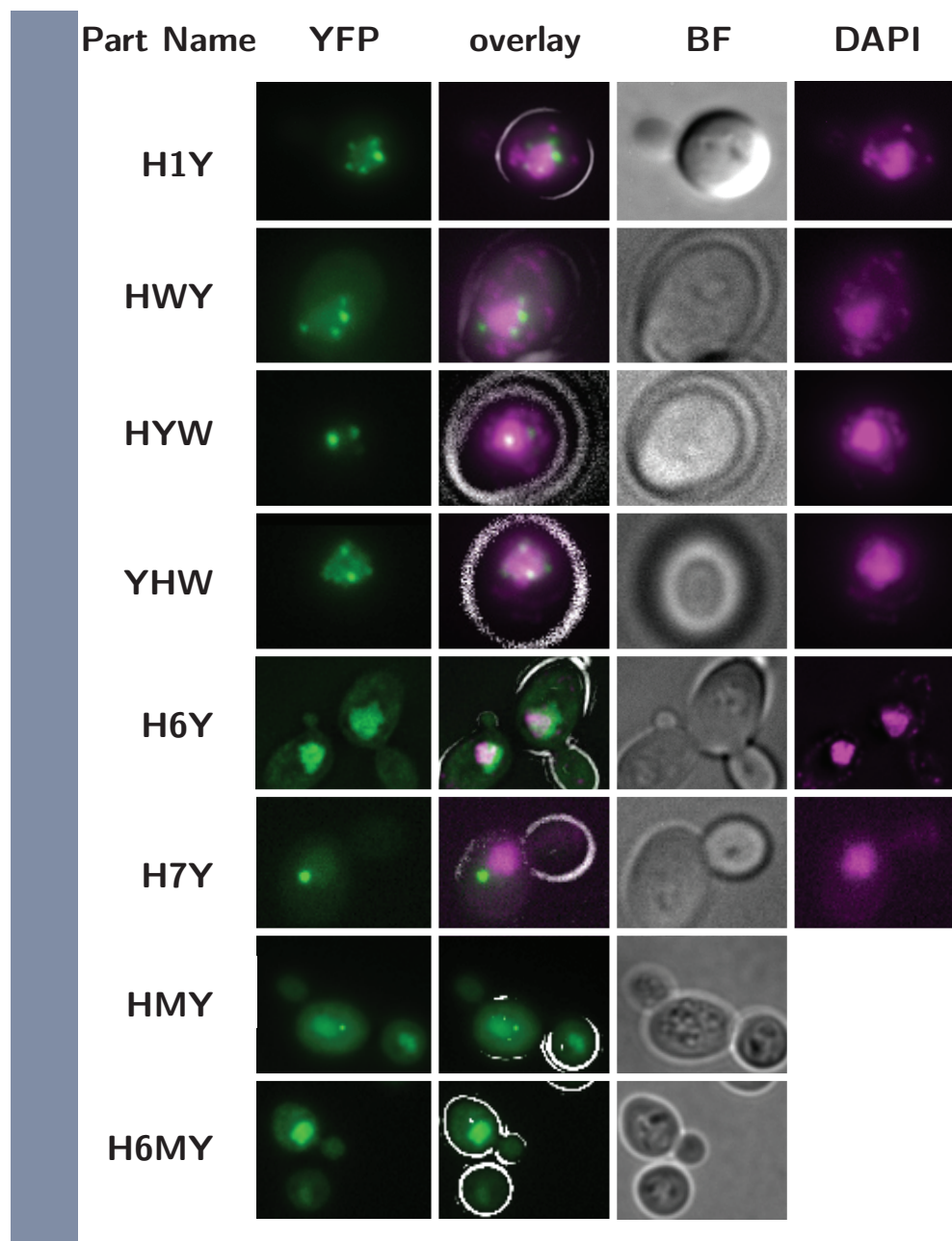


Figure 5.10 Heterologous expression of hairy genes in yeast. Expression patterns of hairy gene variants in fixed single yeast cells. The first column shows the YFP tagged Her parts (H1Y = fish codon Her1-YFP, HWY = yeastized Her1-WRPW-YFP, HYW = yeastized Her1-YFP-WRPW, YHW = yeastized YFP-Her1-WRPW, H6Y = fish codon Hes6-YFP, H7Y = fish codon Her7-YFP, HMY = yeastized Her1-MigED-YFP, H6MY = yeastized Hes6-MigED-YFP). The last column shows the DAPI stained nucleic acids and the second column is an overlay of fluorescent channels with the yeast cell outlines. All expressed Her proteins localize to the nucleus in yeast and tend to aggregate in nuclear spots.

and induced expression resulted in YFP accumulation in 'nuclear' spots. Double labeling with nuclear markers and 3D deconvolution revealed that these spots localize at the nuclear periphery, but it was unclear whether the signal was inside or outside of the nucleus (data not shown). This indicates that translation deficiencies due to codon usage is not a factor of H1Y expression efficiency in yeast.

In contrast, both constitutive and inducible REPRESSOR strains were obtained for the control parts H6Y and H7Y, indicating that their effect on cell growth is not as severe as in the Her1 repressor parts. However, for both H6Y and H7Y cultures only a few cells were positive for YFP expression and the overall signal intensity appeared to be lower in comparison to H1Y devices (not quantified). For H7Y typically a singular 'nuclear' spot was present and enrichment in the nucleus was detectable in only a few cells. In contrast, a homogenous nuclear signal was detected in all H6Y transformants. In rare cases a singular 'nuclear' spot formed in the H6Y expressing cells as well.

The expression of the MigED domain modified repressor controls, HMY and H6MY, was also successfully induced in yeast. Both HMY and H6MY are clearly localized within the nucleus. While HMY still aggregates into nuclear spots, it is the only Her1 part that is clearly distributed throughout the nucleus.

Expression levels affect Her1 localization in yeast

The slowed growth and cellular deformation of yeast cells upon Her part induction are signs of increased cellular stress. Indeed, the appearance of nuclear aggregates may be the accumulation of waste products, such as miss-folded proteins, in stress-induced compartments [Kaganovich et al., 2008]. Stress has drastic effects on a cell's metabolism, resulting in unique adaptations and increasing cell-cell variability within one culture. While this was not investigated explicitly here, it is clear that increased cell-cell variability reduces predictability and reproducibility of our system designs.

In addition, the inhomogeneous expression of Her proteins indicates that cells within one transformed culture are indeed adapting uniquely to Her-induced stresses. Therefore, it is essential to eliminate sources of additional cellular stresses. One such potential source, the strong *pGAL* promoter, may contribute to these effects two-fold. Firstly, *pGAL* can be induced with switch-like precision, quickly transitioning

from zero to high levels of protein expression (Figure 5.11), possibly overloading the yeast's expression machinery. Secondly, *pGAL* is induced using galactose, essentially a change in sugar source and therefore also a change in metabolism and related pathways.

To counter these effects, the copper inducible promoter *pCUP* was tested, which is associated with lower expression levels (but potentially leaky and less tightly regulated). As anticipated, the induction levels of Her parts was reduced approximately 10-fold with respect to background noise, a level at which H7Y no longer accumulates to a measurable level. Interestingly, copper induction leads to pulsatile expression levels of Her parts in these transformants. More specifically, the oscillations in protein expression are coordinated with cell division, therefore linking the *pCUP* promoter to the cell cycle. As a consequence, it became apparent that the localization of Her proteins, in particular HMY, is in fact related to its expression level. At low levels of HMY, corresponding to low cumulative YFP signals per cell, the protein is distributed evenly in the nucleus. However, when the YFP signal increases accumulation into nuclear spots also increases (Figure 5.11.A.). This accumulation is either a result of DNA binding to Her binding sites, which is consistent with the absence of spots in H6Y and H6MY transformants, or it reflects increased aggregation of protein in degradation compartments.

While the copper induction of *pCUP* transformants resulted in inhomogeneous expression within the culture (Figure 5.11.B.), it generally did not lead to changes in cell morphology. Therefore, the switch to *pCUP* induction seems to eliminate at least some cellular strains and was therefore used in subsequent part characterization experiments. Furthermore, Hes6 based constructs were chosen as primary control parts, due to their nuclear localization, the low occurrence of nuclear spots and the measurable expression levels in both *pGAL* and *pCUP* transformants.

SWITCH-OFF: Her1 repression in yeast

To characterize the repressor function of Her1 parts in yeast, I tracked reporter signals in single cells containing the SWITCH-OFF system over time. In this system, both REPRESSOR devices and REPORTER device are present in individual cells. Initially, the REPRESSOR device is turned off and therefore transcription should proceed freely from the REPORTER device, leading to an accumulation

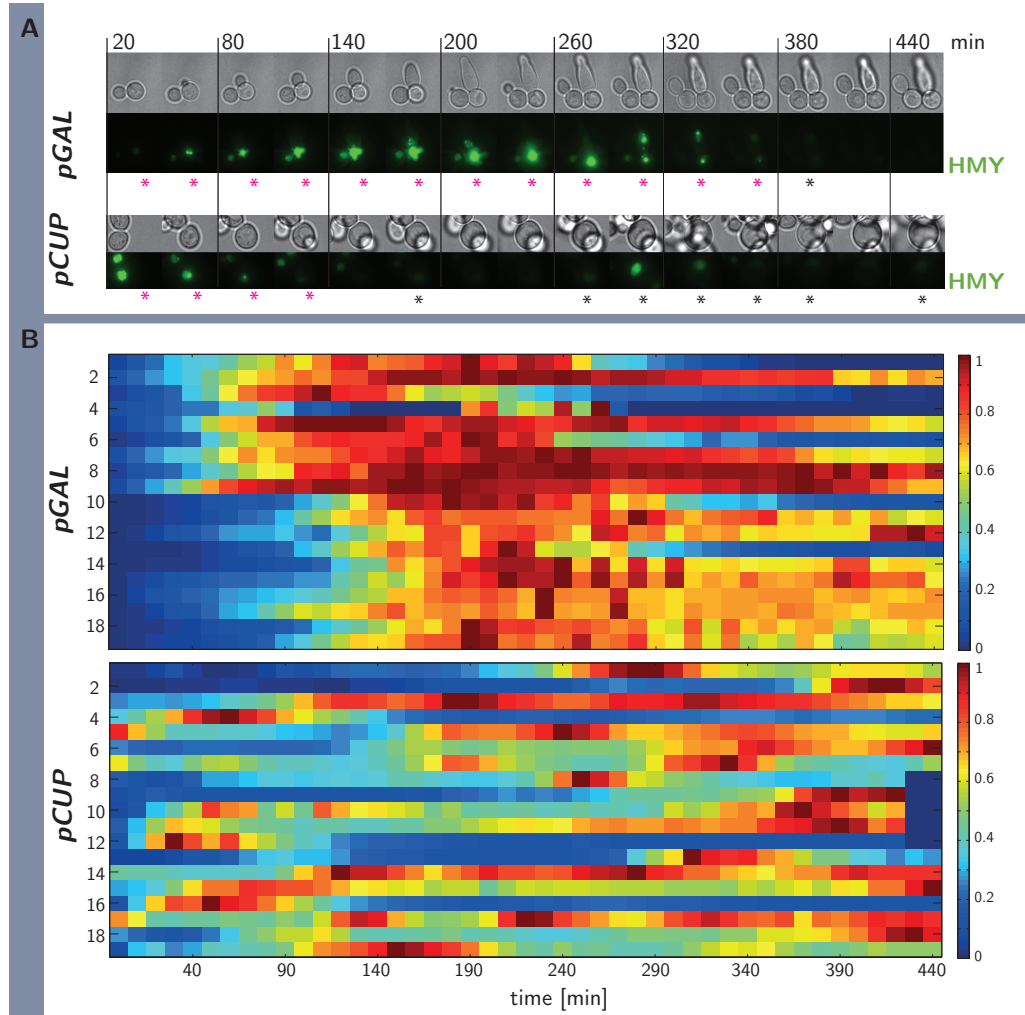


Figure 5.11 Inducible Promoters: *pGAL* versus *pCUP*. *pGAL* and *pCUP* are positively regulated yeast promoters that can be activated by the addition of diffusible substances in the medium (galactose and copper, respectively). In this Figure, the expression of HMY, 15min-30min after induction, under *pGAL* and *pCUP* is compared. **A.** Typical cell tracks of *pGAL* and *pCUP* controlled induction. Asterisks mark imaging frames in which HMY is detectable in cells. Magenta asterisks (*) mark HMY signals that accumulate in nuclear spots or have reached saturation. **B.** Sample sets of tracked YFP signals per cell over time for *pGAL* and *pCUP* inductions. Each cell track is normalized to its own maximum signal for cell-cell comparison. *pGAL* results in large transcriptional increase, often leading to signal saturation and HMY aggregation in nuclear spots. *pGAL* is switch like, sharp transition curve from off to on state. *pCUP* is variable, oscillatory in nature, fluctuating between off and on states, likely connected to cell-cycle rhythms. *pCUP* expression levels are lower than those of *pGAL*. For *pCUP* nuclear spots only occur at high signal levels.

5 Results and Discussion

of reporter fluorophores in the cell. I then induced the REPRESSOR device and monitored Her part accumulation in the system. If the Her part is able to bind to the REPORTER's promoter region and recruit the yeast's repression machinery, the reporter fluorescence is expected to decrease over time - or in other words: a SWITCH-OFF.

Similarly to Her1 part expression, I first screened fluorescent reporters visually for homogeneous, bright signals in single copy REPORTER strains. For most reporter fluorophores, either low signal strength, cell-cell variability, or bleed-through into the YFP channel was detected. Therefore, I selected the brightest dimer, 2xCFP, in combination with the strong *pTEF* yeast promoter and the 6mer of high affinity binding sites, 100BS, as the core REPORTER strain for testing Her1 repression in the SWITCH-OFF assay. The low copy HIS3 vectors containing *pCUP* were selected for controlled Her1 part expression in the REPRESSOR devices.

For long-term imaging, yeast cells were seeded onto glass-bottom imaging dishes and continuously cultured in SD-HIS drop out medium. At the beginning of each imaging run copper sulfate was added to the cultures to induce repressor expression. Each REPRESSOR-REPORTER strain was imaged at single cell resolution for up to eight hours, typically at 10min intervals, in multiple fields. A reference brightfield image was recorded at each time point, however both YFP and CFP fluorescence signals were recorded in several z-stacks to compensate for slight shifts in focus over time.

For image analysis, max projections were generated for each imaging field and fluorescence channel. Then individual cells were tracked over time using the bright-field reference images and Fiji's COI plugin was used to extract the mean fluorescent signals per cell at each time point. Typically, six YFP positive (Her part expressing) cells and three non-expressing cells (negative) were tracked per imaging field. In addition, the background signal of each channel was subtracted as baseline from each cell's measurement.

For visual comparison, single cell traces of YFP-REPRESSOR and CFP-REPORTER signals were normalized to each cell's maximum fluorescent signal. In Figure 5.12.A, I show typical cell traces obtained for H1Y, HMY and H6MY, as well as signal traces of negative cells. The normalized YFP signal of negative cells results in a speckled pattern, which reflects noise fluctuations of auto-fluorescent

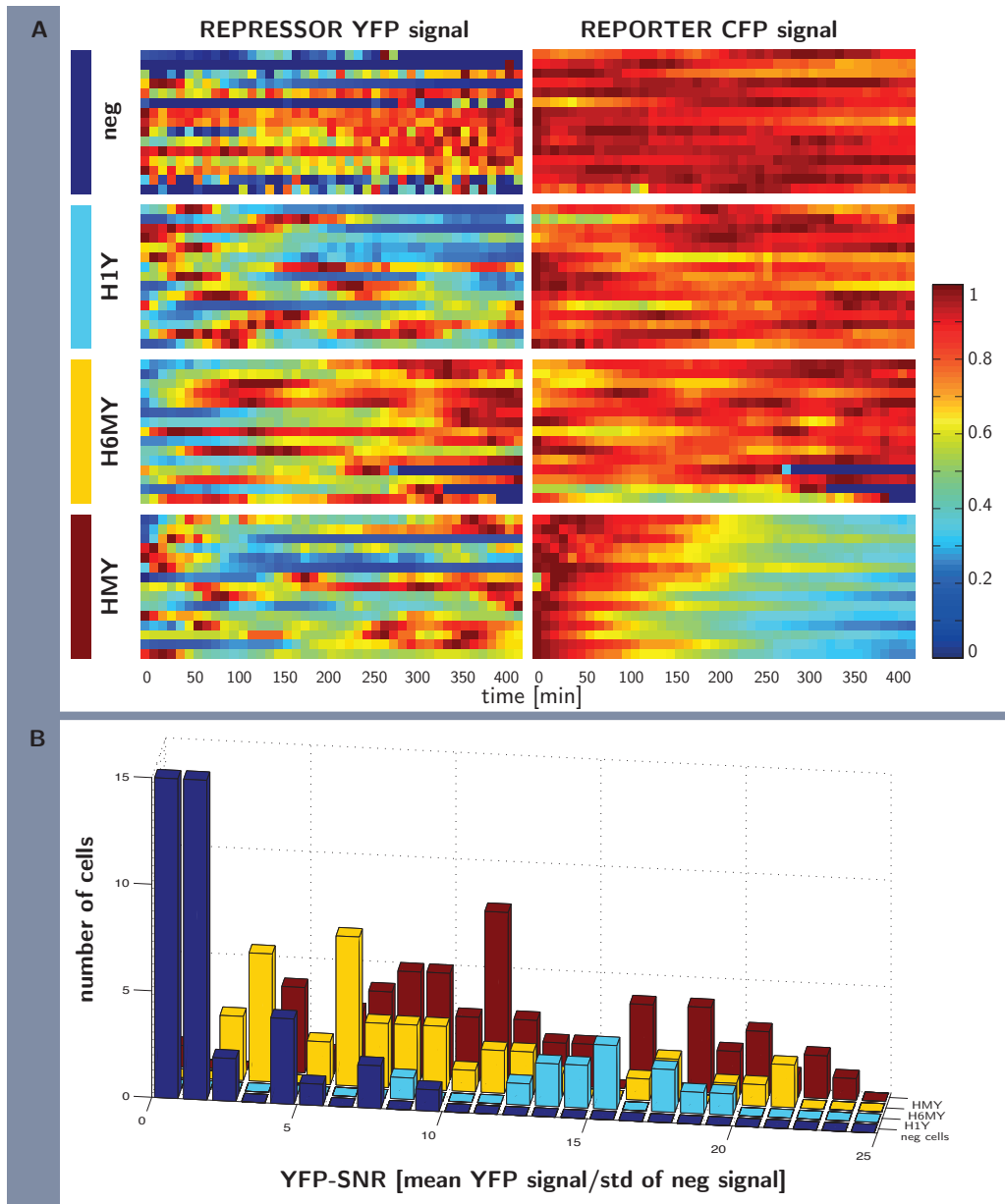


Figure 5.12 SWITCH-OFF: Single Cell Traces. **A.** Typical single cell traces of YFP REPRESSOR (left column) and CFP REPORTER (right column) signal for Her repressor parts H1Y (cyan), H6MY (yellow) and HMY (red), as well as non-REPRESSOR negative cells (blue). The fluorescent signal was normalized to each cell trace’s maximum, resulting in red color for high signal values and blue color for low signal values. The YFP signal for Her proteins fluctuates rhythmically over time, while it is speckled around background levels for negative cells. The CFP REPORTER signal remains high everywhere, except for the cells also expressing HMY. **B.** A histogram of Signal to Noise Ratios (SNR) of mean YFP signal per cell divided by the mean standard deviation of negative cells. The REPORTER signal was only analyzed for cells with SNR greater than 5. The SNR analysis provides a non-biased method for distinguishing Her part expressing from non-expressing cells in the nonhomogeneous yeast cultures. This graph also shows that the YFP signal of negative cells (blue) is close to zero (background values).

background levels in these cells. In contrast, the copper induced transcription of REPRESSOR parts generates pulsatile expression of YFP signal over time and the signal dynamics vary between individual cell traces for all tested parts.

As expected, the REPORTER signal in HMY induced cells decreases, or switches off, steadily over time. In contrast, the REPORTER signal of H1Y and H6MY cells fluctuates over time. Since the negative samples show similar variability, this fluctuation is not coupled to the REPRESSOR expression dynamics of H1Y and H6MY. Therefore, these fluctuations could simply represent general expression noise in this biological system. However, similarly to cell-cycle linked *pCUP* expression, these patterns could indicate that the REPORTER device is not fully independent from other cellular processes. For instance, the *pTEF* could be responsive to periodic cell-cycle cues, the CFP dimer concentration may get diluted during growth phases and cell division events, or endogenous yeast transcription factors interact with expression levels through interactions with the Her1 binding sites.

In order to quantify REPORTER response for each tested part, two parameters were calculated for each cell trace: 1. YFP-SNR and 2. CFP-SFC. The first parameter, the signal to noise ratio (SNR) of YFP induction, determines whether a REPRESSOR part was expressed in a cell. YFP-SNR is obtained by dividing each cells mean YFP signal by the standard deviation of noise calculated from the cell tracks of negative cells. A low SNR value indicates that the recorded signal cannot be distinguished from background or noise fluctuations. While most REPRESSOR devices were clearly activated, a number of cells were not identified clearly (overlapping region of blue bars in Figure 5.12). Therefore, only cell tracks with YFP-SNR values greater than 5 were used in subsequent analysis of REPORTER response.

The second parameter calculates the CFP signal fold change (SFC) over time and therefore determines whether a reporter concentration is increasing ($\text{CFP-SFC} > 1$) or decreasing ($\text{CFP-SFC} < 1$) after REPRESSOR induction. To compare reporter response between independent experiments, each CFP-SFC was normalized to the mean CFP-SFC value of negative cells. The ANOVA statistical test for multiple comparison showed that reporter response in duplicate experiments were not significantly different and were therefore pooled for further analysis. The pooled data for Her parts H1Y, H6Y, HMY, HYM and H6MY is shown in Figure 5.13 alongside the CFP-SFC values obtained for negative cells. The REPORTER response to Her parts

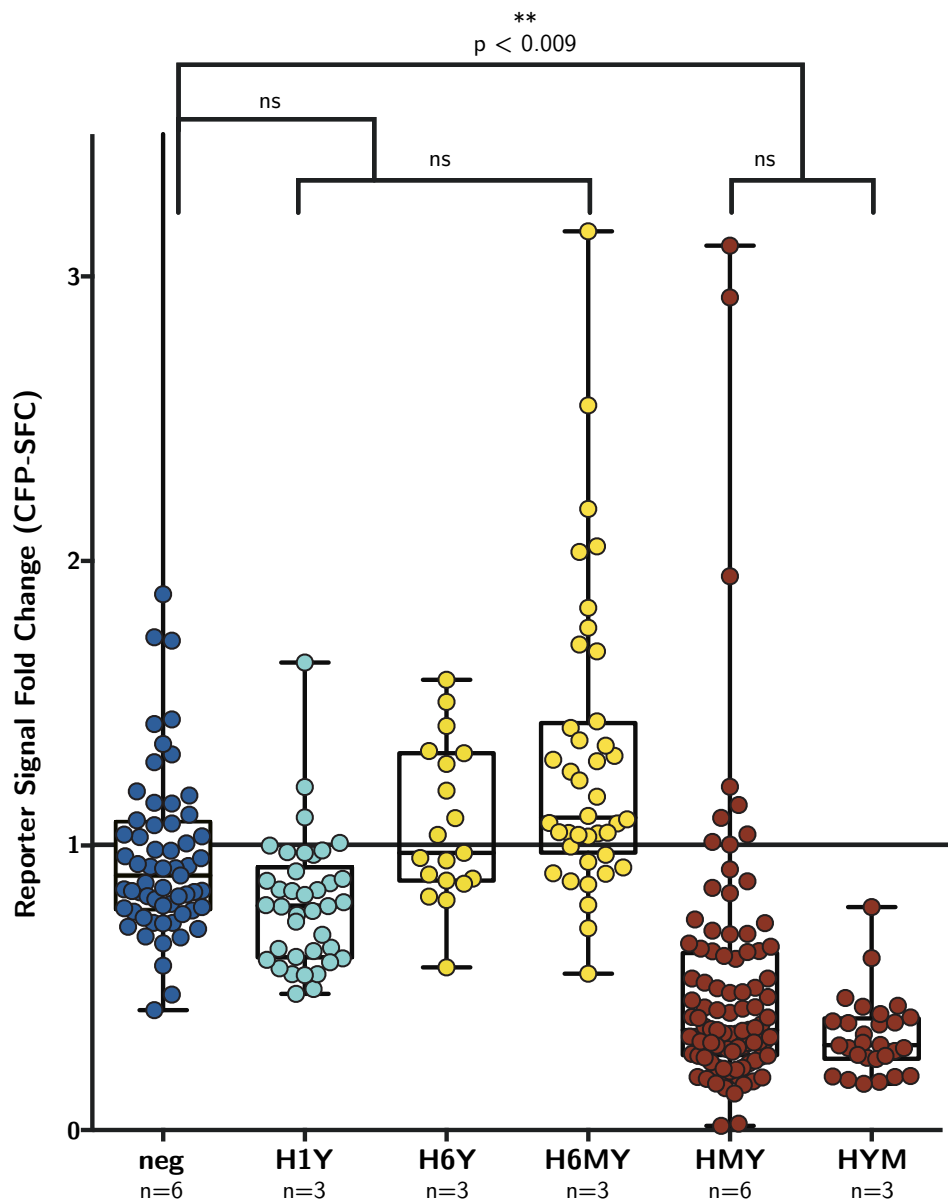


Figure 5.13 Switch Assay - Reporter Response. This graph shows all calculated CFP-signal fold change values (CFP-SFC). The fold change of reporter signal upon induction of Her parts was calculated using $SFC = CFP_{final}/CFP_{initial}$. A SFC value around one is expected for constant expression levels and $SFC < 1$ implies a reduction in REPORTER signal. Her part induction levels were scored by calculating the signal to noise ratio (SNR) of YFP signal in induced and uninduced cells. Traces for which the $SNR < 5$ were excluded from final analysis. The CFP-SFC values of each cell are shown in the plot. For analysis only the mean values of each independent measurement (the number of independent experiments, n , is shown at the bottom of the graph) was used. Each Her part SFC was then compared to that of non-expressing cells using ANOVA statistics. For the parts H1Y, H6Y and H6MY the REPORTER signal does not change significantly. Only MigED containing Her1 parts, HMY and HYM, result in a reduction of REPORTER signal.

5 Results and Discussion

H1Y, H6Y, and H6MY is not significantly different from REPORTER behavior in negative cells. In contrast, the reporter CFP-SFC significantly drops for Her1 fused with the Mig repressor domain, HMY and HYM. Therefore, HMY and HYM can function as transcriptional repressor in yeast, while H1Y, H6Y and H6MY cannot.

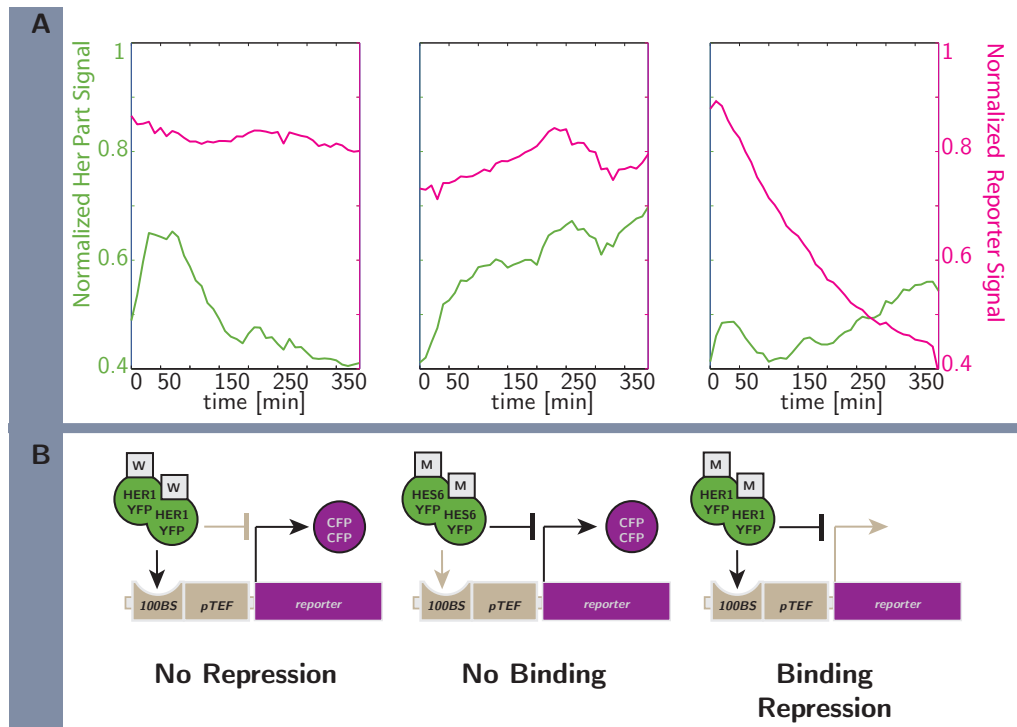


Figure 5.14 SWITCH-OFF in yeast: MigED vs. WRPW. In the SWITCH-OFF assay, Her parts in REPRESSOR devices are expressed in yeast strains carrying a CFP-REPORTER device. Here the data of parts H1Y (left column), H6MY (middle column) and HMY (right column) are summarized. **A.** These plots show the normalized average of all cell traces (see individual traces in Figure 5.12) for each induced Her part (green curve) and resulting CFP signal (magenta curve). Across a culture, the expression level of Her parts fluctuates around 50%. This is consistent with cell-cycle dependent fluctuations of the *pCUP* devices in non-synchronized cultures. The expression level the CFP reporter is constant for H1Y and H6MY devices and decreases over time in HMY devices. Therefore, only HMY can repress CFP transcription. **B.** Both DNA binding and repressor function are necessary to switch-off the REPORTER device. H1Y homodimers can bind H-box motifs (100BS), but its WRPW domain (W) recruit repressor machinery in yeast. H6MY has the functioning repressor domain MigED (M), but cannot bind to the promoter region.

Repression activity requires three steps, first Her dimerization, second DNA binding and third the recruitment of a yeast co-repressor. Recently, Schröter et al. [2012] not only showed that both Her1 and Hes6 form homodimers, but also that Her1 homodimers are able to bind the Her binding site, 100BS, used in this reporter con-

struct. This indicates that the zebrafish WRPW repressor domain in H1Y is not able to interact with Groucho homolog TUP1 in yeast (Figure 5.14.B). While it is possible that the C-terminal YFP tag interferes with WRPW - TUP1 interaction, the repressor activity of HMY shows that MigED can interact with TUP1 despite the presence of the tag. Therefore, the replacement of the WRPW domain with the yeast MigED repressor domain is sufficient to functionalize Her1 in yeast and does not interfere with Her1 dimerization or DNA binding activity. Finally, the inability of H6MY to repress, despite the presence of MigED repression domain, shows that binding at the high affinity H-box, 100BS, is specific.

Her1 Yeast Half-Life

Next, I measured the half-life (HL) of the selected Her1-repressor part, HMY, to determine whether its degradation rate is similar to the 10min half-life estimated for Her1-YFP in zebrafish cells (unpublished data, Phillipp Knyphausen, MPI-CBG). In order to stop protein synthesis, I used the chemical cycloheximide to block translation. Due to the inhomogeneous expression levels of cells within a yeast culture, I again tracked Her part concentration in individual cells by measuring YFP signal over time in single cell microscopy. Similar to the SWITCH-OFF assay, the mean YFP signal per cell was calculated and plotted over time (Figure 5.15.A, first column). The half-life was then calculated by fitting a "one phase decay" curve to each cell trace using PRISM software (Figure 5.15.B, first column).

The half-life of HMY, determined by the translation block using 35 $\mu\text{g}/\text{ml}$ cycloheximide is 35min ($\pm 7\text{min}$ SD) and ranges from 25min to 60min. These HL values were consistently measured when protein synthesis was blocked with cycloheximide concentrations from 5 to 75 $\mu\text{g}/\text{ml}$, with the majority of half-lives ranging from 29min to 56min (Figure 5.16). Even though the added cycloheximide clearly inhibited cell growth and division, which is expected when protein synthesis is blocked globally, the cell-cell variability of half-life measurements indicates that translation was not blocked sufficiently or that protein degradation rates vary greatly in individual yeast cells. The first issue can be addressed by eliminating sources of variability in the experimental set-up. On the other hand, the second issue has substantial effects on the oscillator design and measurement considerations, because cells within a single culture will fall in different parameter spaces of the oscillator.

5 Results and Discussion

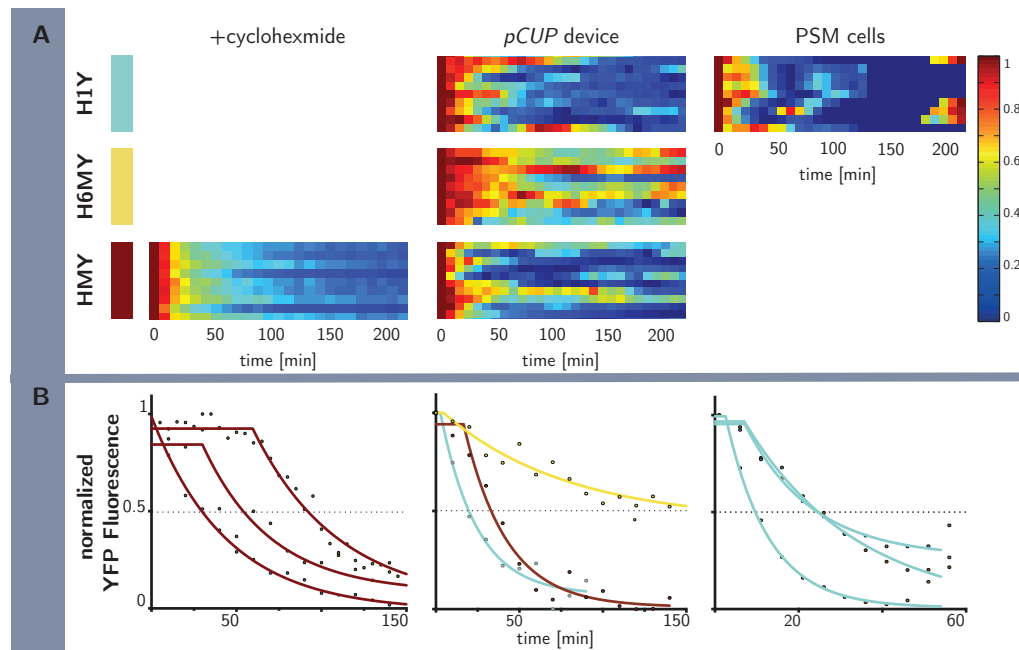


Figure 5.15 Her Part Degradation Curves. The half-life of HMY, H6MY and H1Y was estimated from single cell traces in which protein synthesis was inhibited via translation block (cycloheximide) or transcription block (*pCUP* device, PSM cells). **A.** For analysis the first expression peak of *pCUP* and PSM traces were shifted to the initial time point, $t = 0$. The graphs show typical cell traces with YFP fluorescent signals normalized to 1. **B.** Degradation was approximated using the 'plateau followed by one phase decay' model. The half-life of each part corresponds to the time it takes for the normalized decay curves to drop from 1 to 0.5 (dotted line). The half-life values were calculated from the decay curve fit and are shown in Figure 5.16.

In either case, the median HMY protein half-life of 36min is not only longer than the 10min half-life estimated for zebrafish Her1-YFP but also exceeds the maximal half-life predicted for the stable oscillations of the fast zebrafish segmentation clock [Giudicelli et al., 2007]. This means, that the selected HMY part may be too stable to generate oscillations in yeast. However, the cyclic expression of HMY from the *pCUP* REPRESSOR device showed that HMY is degraded rapidly within the 1.5hour period of the yeast cell-cycle. Since HMY does not fluctuate during divisions in *pGAL* devices its protein decay in *pCUP* is likely a result of blocked transcription at the promoter site rather than other cell-cycle activated degradation pathways.

Based on this assumption I calculated an approximate HMY half-life in the *pCUP* REPRESSOR strains by fitting a "one phase decay" to the decreasing portion of fluorescence peaks (Figure 5.15). Similarly, I obtained half-life estimates for H6MY and H1Y in yeast and an approximate half-life of the reporter protein Her1-YFP

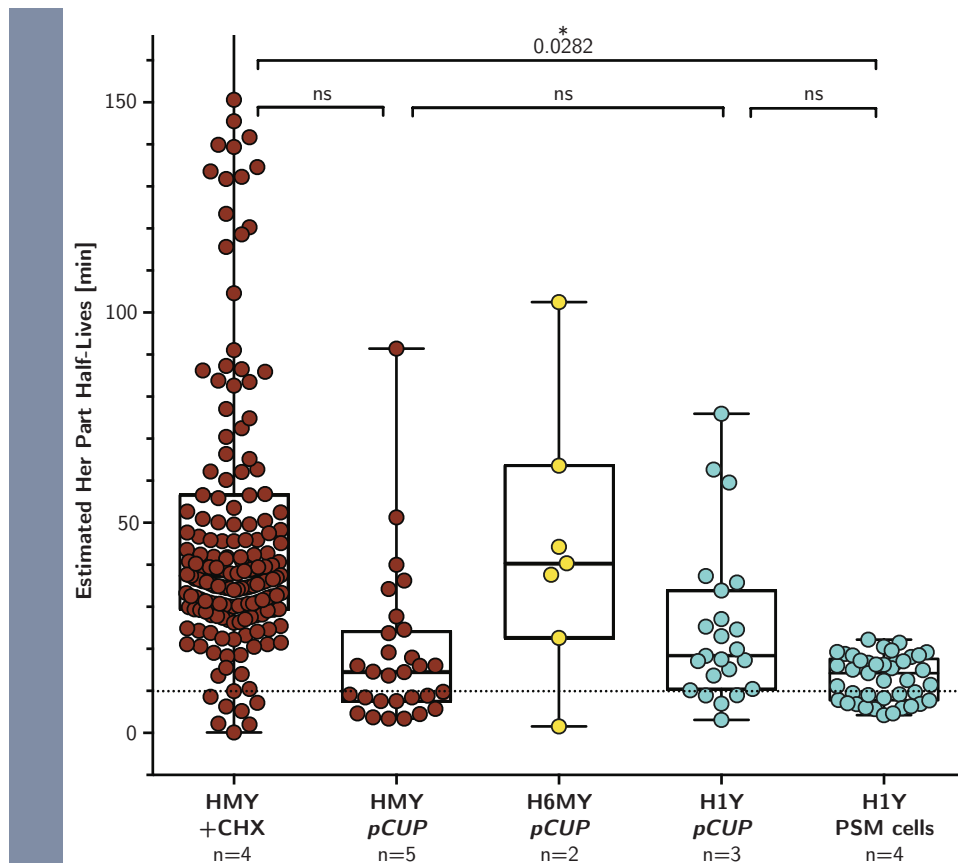


Figure 5.16 Half Life Values of Her parts. HMY+CHX are HMY half-life (HL) measurements upon blocking protein synthesis using cycloheximide. HMY *pCUP*, H6MY *pCUP*, H1Y *pCUP* are the half-life estimates obtained from oscillating Her part cultures in yeast. H1Y-PSMCELLS shows the apparent half-life of H1Y in zebrafish cells. The calculated HL values of each cell is shown in this Figure, but only the mean values of each independent experiment, *n*, were used for statistical analysis. The following HL values were calculated: HMY+CHX = 35min (± 7 min SD), HMY *pCUP* = 17min (± 10 min SD), H6MY *pCUP* = 58min (± 48 min SD), H1Y *pCUP* = 27min (± 16 min SD), H1Y-PSMCELLS = 13min (± 5 min SD). Due to the variability of HL values, the effective degradation rates are similar in yeast and zebrafish for all measured Her parts.

from the expression peaks measured in single PSM cells (Figure 5.3). The effective half-life of HMY in *pCUP* REPRESSOR devices is 17min (± 10 min SD), which is comparable to the 27min (± 16 min SD) half life of H1Y, but significantly faster than the 58min (± 48 min SD) half-life of H6MY. The difference in degradation rates between Her1 parts and H6MY is consistent with the accumulating fluorescence signal of induced H6MY REPRESSOR devices (Figure 5.12) and is in agreement with the longer Hes6-YFP half-life measured in the lab previously (unpublished data, Philipp Knyphausen, MPI-CBG). In addition, the effective half-life of Her1-YFP in zebrafish cells is 13min (± 5 min SD), which is not only close to the previously measured 10min, but is also on the same order as HMY and H1Y half-life in yeast. Despite the large variability of half-lives obtained from translation block experiments, I have verified that Her1 proteins degrade at comparable rates in both yeast and zebrafish.

5.5 PART2: Discussion

5.5.1 Implications of Part Properties on OSCILLATOR Design

The characterization of Her parts in yeast showed that zebrafish derived oscillator components can function in yeast. While Schröter et al. [2012] successfully expressed Her proteins in the yeast one hybrid assay to test DNA binding, this work is the first to look at Her expression dynamics over time using YFP tags and high resolution microscopy in individual yeast cells. I showed that the three core oscillator proteins, Her1, Hes6 and Her7 are localized to the nucleus in yeast, which means that their internal nuclear localization signal is sufficient for translocation between subcellular compartments in yeast. In addition, the accumulation of nuclear spots at high concentrations and the half-life of Her1-YFP are consistent with the observations made in zebrafish PSM cells. Finally, I identified the functional network parts required for OSCILLATOR construction, a Her1 repressor part, HMY, and a Her responsive promoter part, 100BS-*pTEF*, using the SWITCH-OFF assay. Unfortunately, assembly and integration of this particular OSCILLATOR device did not lead to detectable oscillations in single yeast cells (data not shown) indicating that further analysis and optimization is required.

It is possible that the 100BS-*pTEF*-HMY network is not able to generate stable oscillations because the network parts do not fulfil the requirements of time delay,

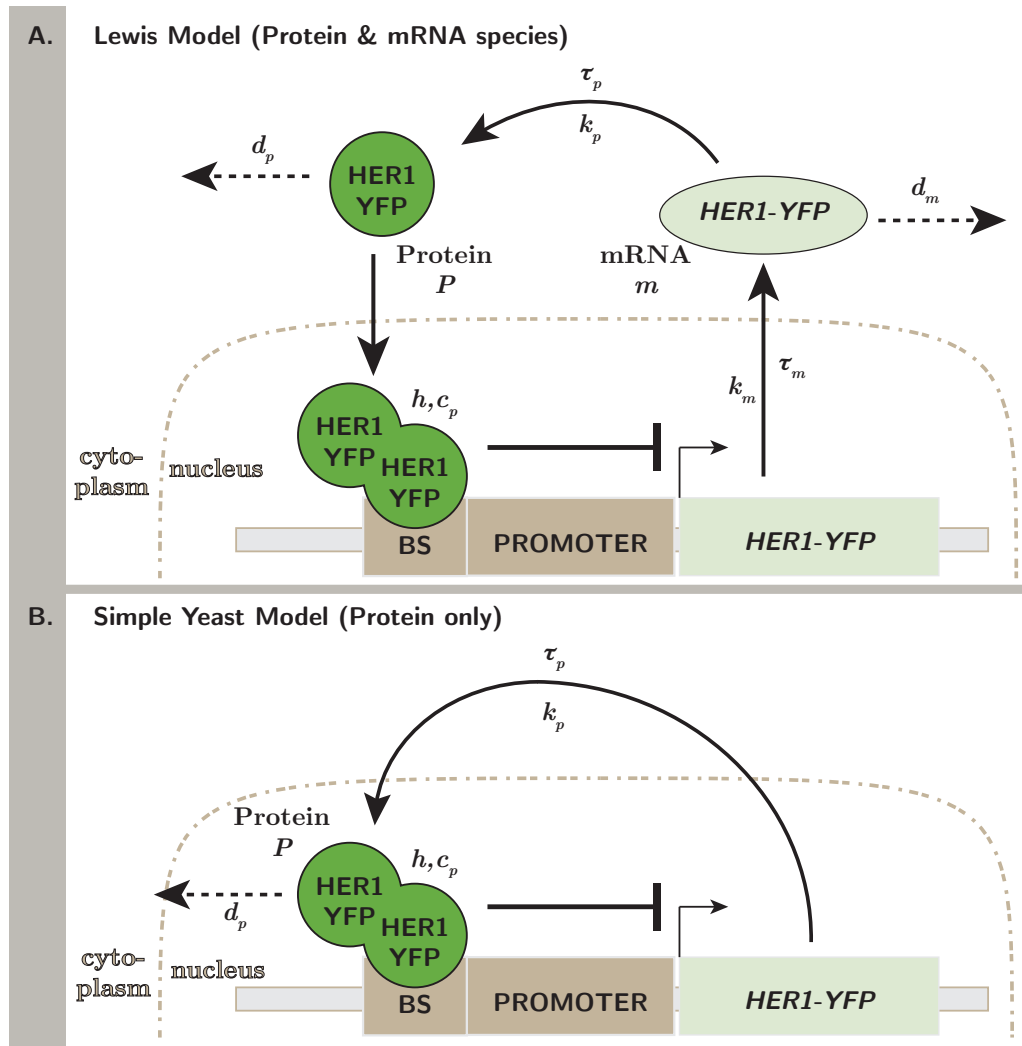


Figure 5.17 Her1 Oscillator Model. **A.** The parameters used by Lewis [2003] to model a minimal zebrafish single cell oscillator are: k - species production rates, τ - time delay of process, d - degradation rates, c_p - critical repressor concentration, h - Hill coefficient. These parameters describe the dynamics of transcription, translation and molecular activity of the mRNA and protein species of the *her1-yfp* gene. **B.** The simplified oscillator model for the synthetic network in yeast eliminates the *her1-yfp* mRNA species since its associated parameters are difficult to measure or control/alter in the current network design. Nonetheless, the dynamics of mRNA production are not neglected but are instead reflected in changes of the remaining model parameters, such as τ_p .

5 Results and Discussion

non-linearity and balanced time-scales. To explore these possibilities, and to investigate strategies for optimization, I developed a simplified mathematical model of the circuit. Lewis [2003] has previously estimated the oscillatory requirements of the minimal oscillator by modelling the zebrafish oscillator network using Her1 alone (Figure 5.17.A). Lewis used two mass balance equations, describing the rate of change of Her1 mRNA (m') and Her1 protein (P') concentrations over time, and included delay terms for transcription and translation as well as dimerization kinetics at the repressor binding site. As a result, the requirements for sustained oscillations can be summarized in the following three equations:

$$\frac{k_P}{d_P d_m} > 2c_P \quad (5.1)$$

$$d_P, d_m \geq \frac{1.7}{(\tau_m + \tau_P)} \quad (5.2)$$

The first condition means that the maximal rates of mRNA and protein synthesis must be sufficiently high to raise the protein concentration above the critical value of repressor activity, c_P . The other requirements state that the half-life of mRNA and protein, the inverses of d_m and d_P , need to be short or at least proportional to the sum of transcriptional and translational delays, τ_m and τ_P .

In this model, Her1 half-life is estimated at 3min in order to generate stable oscillations, when the sum of delays, $\tau_m + \tau_P$, equals 13min (Table 5.1). The main issue of this analysis is that the model parameters were not constrained by experimental measurements, but rather estimated to obtain a short oscillator period. Whereas other terms were simply given 'reasonable' values, such as the 10^{-9} M critical protein concentration for repression in the nucleus. This corresponds to $c_P = 40$ molecules in zebrafish but only $c_P = 2$ in the small yeast cells. In fact, the estimated Her1 half-life of 17min in yeast fulfils oscillatory requirements for all of these parameters as long as the time delay is lengthened to approximately 30min ($\tau_m + \tau_P = 1.7 * 17$ min). As a consequence the period of oscillations will of course be longer. This is consistent with the oscillatory period of Her proteins in the *pCUP* expression devices and even with the long periods measured in single PSM cells (Figure 5.1.2). In addition, if we assume that the onset of REPORTER repression in the HMY SWITCH-OFF

assay (Figure 5.14) is the timepoint at which HMY becomes active then the sum of delays can be estimated as 25min-40min, a permissible range for oscillations.

Another issue of the Lewis model is the inclusion of mRNA concentrations. The measurements of RNA concentrations in single yeast cells over time is difficult and the inhomogeneous expression of Her proteins eliminates the use of standard RNA extraction protocols. In addition, the control elements of RNA degradation in the 3'UTR regions of genes are not well defined and in our assay the same terminal sequence, *tCYC*, is used throughout. Therefore, it is sensible to ignore mRNA species and use a single species negative feedback network with delay (Figure 5.17.B) to estimate the OSCILLATOR's parameter space in yeast. The Her1 oscillator model, illustrated in Figure 5.17, is thereby reduced to a single mass balance equation:

$$\begin{aligned}
 P'(t) &= \text{protein synthesis rate} && -\text{protein degradation rate} \\
 &= \frac{k_P}{1 + \left[\frac{P(t - \tau_P)}{c_P} \right]^h} && -d_P P(t)
 \end{aligned} \tag{5.3}$$

This simple model contains only a few parameters which can be measured in yeast cell experiments or tuned using different library parts. For instance, the protein decay rate, d_P , can be inferred from protein half-life measurements ($d_P = \ln(2)/HL$) and the rate of protein production, k_P , is directly linked to the promoter strength. In addition, the time delay, τ_P , represents the time difference between initiation of transcription and the emergence of mature protein species and can therefore be calculated from SWITCH-OFF experiments. The protein synthesis rate is described by a Hill equation, which represents the inhibitory action of Her1 proteins at the promoter. Both the Hill coefficient, h , and c_P are tightly linked to the inherent dimerization, DNA and co-repressor binding properties of Her1 and are therefore difficult to manipulate in this system. The parameters defining the oscillatory regime of this model are listed in Table 5.1 alongside the parameters used in the Lewis Model.

Matlab simulations of this simple network (see Appendix for the code used) illustrate how low production rates and short time-delays can reduce the amplitude of oscillations when the three parameters, d_P , h , c_P , describing innate properties of

5 Results and Discussion

Parameter [units]	Fish	Yeast	
	[Lewis, 2003]	value	source
k_m [$\frac{\text{mRNA molecules}}{\text{cell min}}$]	33		
k_P [$\frac{\text{protein molecules}}{\text{mRNA molecule min}}$]	4.5	[1,4.5,20] > .1	for HL < 27min
d_m [$\frac{\text{molecules}}{\text{min}}$]	0.23		
d_P [$\frac{\text{molecules}}{\text{min}}$]	0.23	0.1 – [0.04] – 0.03	HLs 7min-[17min]-27min
τ_m [min]	10.2 – 31.5		
τ_P [min]	2.8	12 – [29] – 46	minimum delays estimated for HLs 7min-[17min]-27min
c_P [molecules]	40	2+	10^{-9}M
h	2	2	dimer repression at promoter

Table 5.1 Parameters used for Theoretical Oscillator Model. *HL* - half-life

Her1 in yeast are kept constant (Figure 5.18). Indeed, low signal-to-noise ratios are a possible source of undetected oscillations, particularly in single cell microscopy of yeast. Therefore, the OSCILLATOR signal should be improved by implementing both stronger constitutive promoter parts and strategies to extend time-delay. One possibility for extending time-delays is the insertion of artificial introns into Her parts, which are essential for generating oscillations in the mouse [Takashima et al., 2011].

The time-delay of cyclic genes in zebrafish is estimated between 7min and 16min [Giudicelli et al., 2007]. Therefore, it is possible that the delay associated with the intron-less HMY is in fact shorter than the 30min required for sustained oscillations. In this case, it is necessary to either increase the degradation rate of HMY or to push the OSCILLATOR away from its equilibrium to record transient, or damped, signal oscillations. In yeast, proteins have typically been destabilized by either adding PEST sequences or using an N-end rule degron. While these approaches can dramatically reduce the half-life proteins, they are neither well-defined nor tunable. For this reason, the synthetic protein degradation network constructed by Grilly et al. [2007] could be implemented alongside the OSCILLATOR device. This gene network utilizes controlled expression of the ClpXP protease, derived from *E. coli*, to tune the degradation of ssrA tagged proteins. However, the lowest half-life documented for

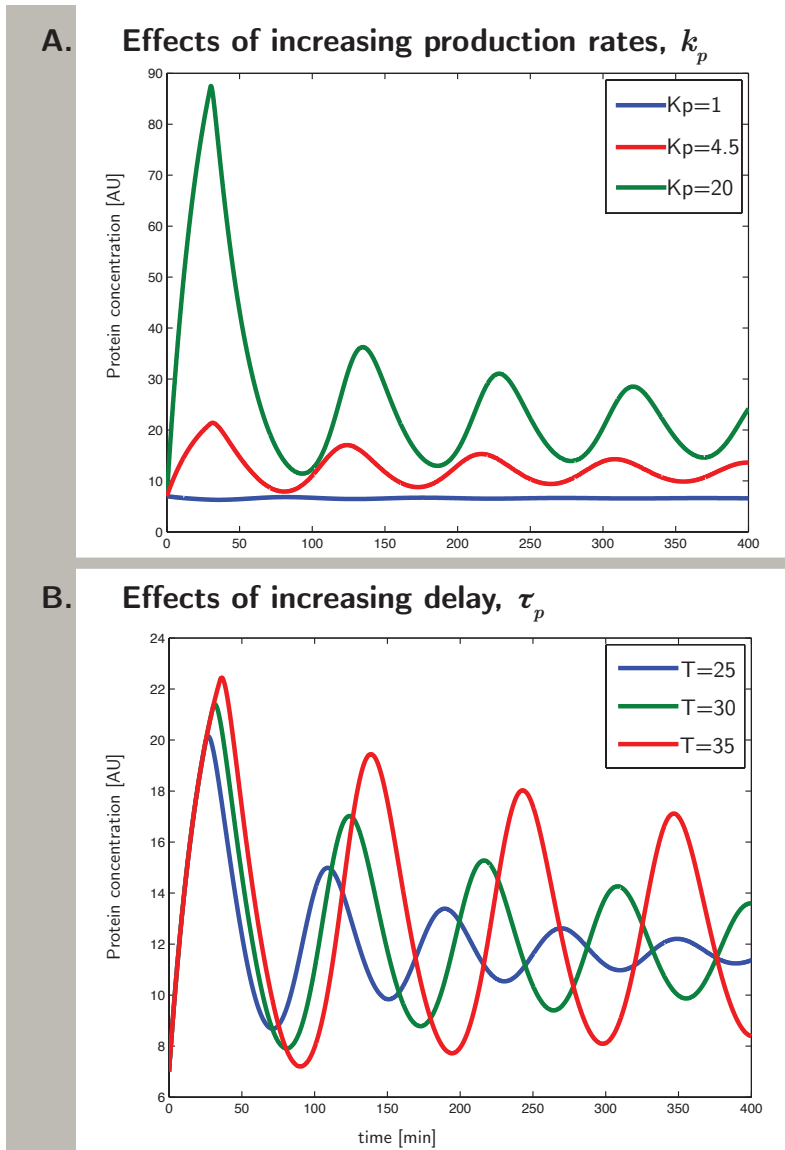


Figure 5.18 Effects of Model Parameters on OSCILLATOR expression. Matlab simulations of the simplified yeast OSCILLATOR model, when $d_P = 0.04$ (Her1 HL of 17min), $h = 2$ (dimer binding at Her BS), $c_P = 2$ (High affinity binding of Her1 at promoter site) show the effects of **A.** protein production rates, k_P , and **B.** time-delay, τ_P , on oscillator amplitude, periodicity and stability. Both increased production rates and longer time-delays result in better signal to noise ratios by increasing the oscillator amplitude. In addition, time-delays which are shorter than the critical value ($\tau_P < 30$ min for Her1 HL=17min, blue curve in B) generate damped oscillations.

this system ranges around 20min, which would not be a sufficient improvement in degradation rate.

Therefore, it may be necessary to push the OSCILLATOR device out of equilibrium even for 'destabilized' HMY networks. One option is to use an inducible promoter, in place of the constitutive *pTEF*, in the OSCILLATOR device to initiate transcription at a user-defined moment. The *pGAL* promoter part may be an optimal choice, since it provides strong expression level and appears to function independently of cell-cycle oscillations. Another option is the integration of an additional REPRESSOR device in parallel with the OSCILLATOR. Then transcription in the oscillator network can be pushed from homeostasis by providing a pulse of extra HMY repressor proteins from the inducible REPRESSOR device. We have coined this method the OSCILLATOR-RELEASE assay.

5.5.2 Synthetic Oscillator Applications and Considerations

In this work, I showed that standardized assembly of synthetic her networks in yeast is a unique tool to systematically implement and test the design principles underlying the zebrafish segmentation clock oscillator. In contrast to previously built synthetic oscillators, where standardized parts were used to build abstract network topologies, this network is designed to mimic the natural system as closely as possible, including the use of original Her protein parts. A similar strategy was used to study the transcriptional elements regulating the day and night rhythms of the circadian clock in mammalian fibroblast cells [Ukai-Tadenuma et al., 2008]. However, they did not attempt to build a circadian clock oscillator *de novo*, but instead used synthesized transcriptional circuits that contained clock responsive promoter elements. Essentially, Ukai-Tadenuma et al. [2008] used synthetic circuitry to read-out the rhythms generated in these cells. In contrast, the 'bottom-up' construction of the segmentation oscillator in the yeast chassis is intended to function in the absence of interfering components from the natural system.

Even though the presence of redundant segmentation clock oscillators can be excluded in yeast, the complete separation from endogenous yeast circuits is difficult. While the cell-cycle linked expression of the *pCUP* promoter part is an obvious example, interactions with other cellular components is not always visible. For example, Her proteins were found to dimerize promiscuously with other Her/Hes

proteins, indicating that Her proteins may also interact with other bHLH proteins in yeast, which in turn could influence their effective half-lives in yeast [Schröter et al., 2012]. Another major draw-back of working with heterogeneous expression is the need for modifications of building parts to generate functionality in foreign systems, especially since well-defined synthetic parts are not yet available in yeast [Blount et al., 2012]. In combination with the limitations of single cell microscopy, screening of network topologies and components can be tedious in yeast. Therefore, it will be pertinent to implement high through put methods, such as FACS sorting, to characterize new parts in the future.

The preliminary analysis of the SWITCH-OFF assay and part characterization revealed that precise measurements of protein synthesis or degradation rates and time-delays are needed to properly constrain the simple oscillator model. In addition to the proposed changes to the OSCILLATOR device and the implementation of an OSCILLATOR-RELEASE assay, the single cell microscopy protocol needs to be improved. For example, the use of a flow-chamber allows the controlled exchange of media and inducers during imaging and therefore time-delays can be measured more accurately. In combination with the predictions from the yeast oscillator model, the parameter space of each HMY oscillator device could then be defined more precisely. Nonetheless, the successful expression of zebrafish derived parts in yeast and the identification of functional Her repressors demonstrate that the yeast chassis is suitable for studying segmentation clock inspired gene networks.

5.6 PART2: Conclusion

In the second part of this thesis, a 'bottom-up' approach was developed for studying synthetic *her* gene networks, based on the zebrafish segmentation oscillator model, in single yeast cells. This protocol incorporates new concepts and workflows to allow the yeast chassis to accommodate original zebrafish clock components and enables the testing of various network motifs. I showed that the core zebrafish segmentation oscillator parts, Her1, Hes6 and Her7, can be expressed in yeast and established a single cell microscopy protocol to track network dynamics over time. A SWITCH-OFF assay was successfully implemented to show that HMY, a yeast codon optimized Her1 enhanced with the Mig1 effector domain (MigED), functions

5 Results and Discussion

as a transcriptional repressor in yeast. Even though a functional OSCILLATOR device could not be built from the characterized parts 100BS, *pTEF* and HMY, the properties of these parts do not prohibit oscillations completely. Therefore, I proposed several optimization strategies based on my mathematical modeling of the OSCILLATOR circuit, including an OSCILLATOR-RELEASE assay, the implementation of a synthetic protein degradation device and high throughput FACS screening, to tune and scan a variety of network parameters. At this stage, the young field of synthetic biology requires the creation of novel methods and infrastructure that allow the quick re-iteration between design, construction and optimization of user-defined networks. This work pioneers in establishing yeast as a chassis for the somitogenesis clock by generating libraries, testing assays, and characterizing parts for standardized assembly of synthetic *hairly* networks.

Matlab Code

```
% Simple Yeast Oscillator Model
% single protein species and negative feedback
%*****
function [time,ysol] = minloop
%set the time-delay of the system
tau =30; % delay - transcription + translation + translocation [min]
%set the time for which system is solved
dt=0.1;
tmax=400;
time=0:dt:tmax;
%solve the system of delay differential equations
sol = dde23(@dde, [tau], @history, [0, tmax]);
ysol = deval(sol, time);
%define the function for the history
function h = history(t)
h = zeros(1,1); h(1)=7;%initial start values of HMY protein h(1)
%define the system of delay differential equations
function ydot = dde(t,y,Z)
%define all constants - all in minutes
HL_prot = 17; % protein half-life [min]
cm = 4; % critical concentration at promoter
h = 2; % hill coefficient, promoter dimer binding
% set degradation and synthesis rates
dp = log(2)/HL_prot; % protein degradation rate
Km = 1; % protein synthesis rate
ylag = Z(:,1); % protein activity delay
% Mass Balance Equation of Single Protein Species
ydot = Km/(1+(ylag(1)/cm)h) - dp*y(1);
```

List of Companies

Company	Website	Address
Fermentas	http://www.thermoscientificbio.com/	
Invitrogen	http://www.invitrogen.com/	
Sigma-Aldrich	http://www.sigmaaldrich.com/	
Biomers	http://www.biomers.net/en/index.html	
PAA	http://www.paa.com/	
QIAGEN	http://www.qiagen.com	

List of Software Programs

Software	Purpose	Website
Matlab	data display and processing, model simulations	http://www.mathworks.de/products/matlab/
FIJI	image processing	http://fiji.sc/
PRISM	Statistical evaluation, decay curve fitting and data analysis	http://www.graphpad.com/scientific-software/prism/
L ^A T _E X	Generation of text documents such as this Thesis	http://www.latex-project.org/

Acknowledgements

I would like to express my gratitude towards my supervisor, Andy C. Oates, who thought up this exciting and innovative project. Thanks for sharing your enthusiasm of science, letting me try out so many fascinating technologies and always being supportive. I want to thank all the members of the Oates lab for a friendly and scientifically stimulating environment; in particular, the people who were instrumental in teaching me new techniques: Dani for showing me how to dissect zebrafish embryos, Daniele for generating the incredible Looping transgenic line, Phillip for generating convenient GW vectors, Christina for discussions on cloning strategies and the theory boys for simplifying. In addition, I am grateful for the advice and support that I have been given by Simon Alberti (MPI-CBG) and all the people of his lab, it has been instrumental for all the work in yeast.

A very special thanks goes out to my parents and sister for supporting me almost unconditionally throughout my entire life, during ups and downs and in times of special need. I would also like to thank Colin for understanding, nurturing and simply being there throughout the past years and last months specifically.

I must also acknowledge that this work would not have been possible without the financial support from the DIGS-BB and the NIMR .

Bibliography

- S. Alberti, A. D. Gitler, and S. Lindquist. A suite of Gateway cloning vectors for high-throughput genetic analysis in *Saccharomyces cerevisiae*. *Yeast*, 24(10):913–919, Oct. 2007.
- M. R. Atkinson, M. A. Savageau, J. T. Myers, and A. J. Ninfa. Development of genetic circuitry exhibiting toggle switch or oscillatory behavior in *Escherichia coli*. *Cell*, 113(5):597–607, May 2003.
- A. Aulehla and O. Pourquié. Signaling gradients during paraxial mesoderm development. *Cold Spring Harbor perspectives in biology*, 2(2):a000869, Feb. 2010.
- A. Aulehla, C. Wehrle, B. Brand-Saberi, R. Kemler, A. Gossler, B. Kanzler, and B. G. Herrmann. Wnt3a plays a major role in the segmentation clock controlling somitogenesis. *Developmental Cell*, 4(3):395–406, Mar. 2003.
- A. Aulehla, W. Wiegand, V. Baubet, M. B. Wahl, C. Deng, M. Taketo, M. Lewandoski, and O. Pourquié. A beta-catenin gradient links the clock and wavefront systems in mouse embryo segmentation. *Nature cell biology*, 10(2):186–193, Feb. 2008.
- R. E. Baker, S. Schnell, and P. K. Maini. A clock and wavefront mechanism for somite formation. *Developmental Biology*, 293(1):116–126, May 2006.
- A. Becskei and L. Serrano. Engineering stability in gene networks by autoregulation. *Nature*, 405(6786):590–593, June 2000.
- Y. Bessho, R. Sakata, S. Komatsu, K. Shiota, S. Yamada, and R. Kageyama. Dynamic expression and essential functions of Hes7 in somite segmentation. *Genes & development*, 15(20):2642–2647, Oct. 2001.
- Y. Bessho, H. Hirata, Y. Masamizu, and R. Kageyama. Periodic repression by the bHLH factor Hes7 is an essential mechanism for the somite segmentation clock. *Genes & development*, 17(12):1451–1456, June 2003.
- B. A. Blount, T. Weenink, and T. Ellis. Construction of synthetic regulatory networks in yeast. *FEBS Letters*, 586(15):2112–2121, July 2012.

- D. Bratsun, D. Volfson, L. S. Tsimring, and J. Hasty. Delay-induced stochastic oscillations in gene regulation. *Proceedings of the National Academy of Sciences of the United States of America*, 102(41):14593–14598, Oct. 2005.
- M. Buscarlet and S. Stifani. The ‘Marx’ of Groucho on development and disease. *Trends in Cell Biology*, 17(7):353–361, July 2007.
- I. Cantone, L. Marucci, F. Iorio, M. A. Ricci, V. Belcastro, M. Bansal, S. Santini, M. di Bernardo, D. di Bernardo, and M. P. Cosma. A Yeast Synthetic Network for In Vivo Assessment of Reverse-Engineering and Modeling Approaches. *Cell*, 137(1):172–181, Apr. 2009.
- D. L. Cheo. Concerted Assembly and Cloning of Multiple DNA Segments Using In Vitro Site-Specific Recombination: Functional Analysis of Multi-Segment Expression Clones. *Genome Research*, 14(10b):2111–2120, Oct. 2004.
- O. Cinquin. Repressor dimerization in the zebrafish somitogenesis clock. *PLoS Computational Biology*, 3(2):e32, Feb. 2007.
- J. Cooke and E. C. Zeeman. A clock and wavefront model for control of the number of repeated structures during animal morphogenesis. *Audio and Electroacoustics Newsletter, IEEE*, 58(2):455–476, May 1976.
- T. Danino, T. Danino, O. Mondragón-Palomino, O. Mondragón-Palomino, L. Tsimring, L. Tsimring, J. Hasty, and J. Hasty. A synchronized quorum of genetic clocks. *Nature*, 463(7279):326–330, Jan. 2010.
- E. A. Delaune, P. François, N. P. Shih, and S. L. Amacher. Single-cell-resolution imaging of the impact of Notch signaling and mitosis on segmentation clock dynamics. *Developmental Cell*, 23(5):995–1005, Nov. 2012.
- J. Dubrulle and O. Pourquié. fgf8 mRNA decay establishes a gradient that couples axial elongation to patterning in the vertebrate embryo. *Nature*, 427(6973):419–422, Jan. 2004.
- J. Dubrulle, M. J. McGrew, and O. Pourquié. FGF Signaling Controls Somite Boundary Position and Regulates Segmentation Clock Control of Spatiotemporal Hox Gene Activation. *Cell*, 106(2):14–14, July 2001.
- A. Eldar and M. B. Elowitz. Functional roles for noise in genetic circuits. *Nature*, 467(7312):167–173, Sept. 2010.
- M. B. Elowitz and S. Leibler. A synthetic oscillatory network of transcriptional regulators. *Nature*, 403(6767):335–338, Jan. 2000.

Bibliography

- D. Endy. Foundations for engineering biology. *Nature*, 438(7067):449–453, Nov. 2005.
- Z. Ferjentsik, S. Hayashi, J. K. Dale, Y. Bessho, A. Herreman, B. De Strooper, G. del Monte, J. L. de la Pompa, and M. Maroto. Notch is a critical component of the mouse somitogenesis oscillator and is essential for the formation of the somites. *PLoS Genetics*, 5(9):e1000662, Sept. 2009.
- A. L. Fisher and M. Caudy. Groucho proteins: transcriptional corepressors for specific subsets of DNA-binding transcription factors in vertebrates and invertebrates. *Genes & development*, 12(13):1931–1940, July 1998.
- E. Fung, W. W. Wong, J. K. Suen, T. Bulter, S.-g. Lee, and J. C. Liao. A synthetic gene-metabolic oscillator. *Nature*, 435(7038):118–122, May 2005.
- M. Gajewski, D. Sieger, B. Alt, C. Leve, S. Hans, C. Wolff, K. B. Rohr, and D. Tautz. Anterior and posterior waves of cyclic her1 gene expression are differentially regulated in the presomitic mesoderm of zebrafish. *Development (Cambridge, England)*, 130(18):4269–4278, Sept. 2003.
- T. S. Gardner, T. S. Gardner, C. R. Cantor, C. R. Cantor, J. J. Collins, and J. J. Collins. Construction of a genetic toggle switch in *Escherichia coli*. *Nature*, 403(6767):339–342, Jan. 2000.
- D. G. Gibson, L. Young, R.-Y. Chuang, J. C. Venter, C. A. Hutchison, and H. O. Smith. Enzymatic assembly of DNA molecules up to several hundred kilobases. *Nature methods*, 6(5):343–345, May 2009.
- F. Giudicelli, E. M. Ozbudak, G. J. Wright, and J. Lewis. Setting the Tempo in Development: An Investigation of the Zebrafish Somite Clock Mechanism. *PLoS biology*, 5(6):e150, 2007.
- C. Gomez, E. M. Ozbudak, J. Wunderlich, D. Baumann, J. Lewis, and O. Pourquié. Control of segment number in vertebrate embryos. *Nature*, 454(7202):335–339, July 2008.
- C. Grilly, C. Grilly, J. Stricker, J. Stricker, W. L. Pang, W. L. Pang, M. R. Bennett, M. R. Bennett, J. Hasty, and J. Hasty. A synthetic gene network for tuning protein degradation in *Saccharomyces cerevisiae*. *Molecular Systems Biology*, 3: 127, 2007.
- C. A. Henry, M. K. Urban, K. K. Dill, J. P. Merlie, M. F. Page, C. B. Kimmel, and S. L. Amacher. Two linked hairy/Enhancer of split-related zebrafish genes, her1 and her7, function together to refine alternating somite boundaries. *Development (Cambridge, England)*, 129(15):3693–3704, July 2002.

- L. Herrgen, S. Ares, L. G. Morelli, C. Schröter, F. Jülicher, and A. C. Oates. Intercellular Coupling Regulates the Period of the Segmentation Clock. *Current biology : CB*, 20(14):10–10, July 2010.
- S. D. Hester, J. M. Belmonte, J. S. Gens, S. G. Clendenon, and J. A. Glazier. A multi-cell, multi-scale model of vertebrate segmentation and somite formation. *PLoS Computational Biology*, 7(10):e1002155, Oct. 2011.
- H. Hirata, S. Yoshiura, T. Ohtsuka, Y. Bessho, T. Harada, K. Yoshikawa, and R. Kageyama. Oscillatory expression of the bHLH factor *Hes1* regulated by a negative feedback loop. *Science (New York, NY)*, 298(5594):840–843, Oct. 2002.
- H. Hirata, Y. Bessho, H. Kokubu, Y. Masamizu, S. Yamada, J. Lewis, and R. Kageyama. Instability of *Hes7* protein is crucial for the somite segmentation clock. *Nature genetics*, 36(7):750–754, July 2004.
- S. A. Holley, R. Geisler, and C. Nüsslein-Volhard. Control of *her1* expression during zebrafish somitogenesis by a delta-dependent oscillator and an independent wave-front activity. *Genes & development*, 14(13):1678–1690, July 2000.
- S. A. Holley, D. Jülich, G.-J. Rauch, R. Geisler, and C. Nüsslein-Volhard. *her1* and the notch pathway function within the oscillator mechanism that regulates zebrafish somitogenesis. *Development (Cambridge, England)*, 129(5):1175–1183, Mar. 2002.
- K. Horikawa, K. Ishimatsu, E. Yoshimoto, S. Kondo, and H. Takeda. Noise-resistant and synchronized oscillation of the segmentation clock. *Nature*, 441(7094):719–723, June 2006.
- Huppert, Ilagan, and Kopan. Analysis of Notch Function in Presomitic Mesoderm Suggests a @c-Secretase-Independent Role for Presenilins in Somite Differentiation. *Developmental Cell*, 8(5):12–12, Apr. 2005.
- Invitrogen. Gateway Technology. pages 1–72, 2003.
- M. Itoh, C.-H. Kim, G. Palardy, T. Oda, Y.-J. Jiang, D. Maust, S.-Y. Yeo, K. Lorick, G. J. Wright, L. Ariza-McNaughton, A. M. Weissman, J. Lewis, S. C. Chandrasekharappa, and A. B. Chitnis. Mind bomb is a ubiquitin ligase that is essential for efficient activation of Notch signaling by Delta. *Developmental Cell*, 4(1): 67–82, Jan. 2003.
- Y. J. Jiang, B. L. Aerne, L. Smithers, C. Haddon, D. Ish-Horowicz, and J. Lewis. Notch signalling and the synchronization of the somite segmentation clock. *Nature*, 408(6811):475–479, Nov. 2000.

- D. Jülich, C. Hwee Lim, J. Round, C. Nicolaije, J. Schroeder, A. Davies, R. Geisler, J. Lewis, Y.-J. Jiang, S. A. Holley, and Tübingen 2000 Screen Consortium. beamter/deltaC and the role of Notch ligands in the zebrafish somite segmentation, hindbrain neurogenesis and hypochord differentiation. *Developmental Biology*, 286(2):391–404, Oct. 2005.
- D. Kaganovich, R. Kopito, and J. Frydman. Misfolded proteins partition between two distinct quality control compartments. *Nature*, 454(7208):1088–1095, Aug. 2008.
- A. Kawamura, S. Koshida, H. Hijikata, T. Sakaguchi, H. Kondoh, and S. Takada. Zebrafish hairy/enhancer of split protein links FGF signaling to cyclic gene expression in the periodic segmentation of somites. *Genes & development*, 19(10):1156–1161, May 2005.
- W. Kim, T. Matsui, M. Yamao, M. Ishibashi, K. Tamada, T. Takumi, K. Kohno, S. Oba, S. Ishii, Y. Sakumura, and Y. Bessho. The period of the somite segmentation clock is sensitive to Notch activity. *Molecular Biology of the Cell*, 22(18):3541–3549, Sept. 2011.
- C. B. Kimmel, W. W. Ballard, S. R. Kimmel, B. Ullmann, and T. F. Schilling. Stages of embryonic development of the zebrafish. *Developmental dynamics : an official publication of the American Association of Anatomists*, 203(3):253–310, Feb. 2005.
- A. J. Krol, D. Roellig, M.-L. Dequéant, O. Tassy, E. Glynn, G. Hattem, A. Mushegian, A. C. Oates, and O. Pourquié. Evolutionary plasticity of segmentation clock networks. *Development (Cambridge, England)*, 138(13):2783–2792, July 2011.
- Y. Kuramoto. *Chemical Oscillations, Waves, and Turbulence*. Courier Dover Publications, 2003.
- E. C. Lai. Notch signaling: control of cell communication and cell fate. *Development (Cambridge, England)*, 131(5):965–973, Mar. 2004.
- J. Lewis. Autoinhibition with Transcriptional Delay - A Simple Mechanism for the Zebrafish Somitogenesis Oscillator. *Current biology : CB*, 13(16):11–11, Aug. 2003.
- T. M. Malavé and S. Y. R. Dent. Transcriptional repression by Tup1–Ssn6 This paper is one of a selection of papers published in this Special Issue, entitled 27th International West Coast Chromatin and Chromosome Conference, and has undergone the Journal’s usual peer review process. *Biochemistry and Cell Biology*, 84(4):437–443, Aug. 2006.

- M. Maroto, J. K. Dale, M.-L. Dequéant, A.-C. Petit, and O. Pourquié. Synchronised cycling gene oscillations in presomitic mesoderm cells require cell-cell contact. *The International journal of developmental biology*, 49(2-3):309–315, 2005.
- Y. Masamizu, T. Ohtsuka, Y. Takashima, H. Nagahara, Y. Takenaka, K. Yoshikawa, H. Okamura, and R. Kageyama. Real-time imaging of the somite segmentation clock: revelation of unstable oscillators in the individual presomitic mesoderm cells. *Proceedings of the National Academy of Sciences of the United States of America*, 103(5):1313–1318, Jan. 2006.
- M. J. McGrew, J. K. Dale, S. Fraboulet, and O. Pourquié. The lunatic fringe gene is a target of the molecular clock linked to somite segmentation in avian embryos. *Current biology : CB*, 8(17):979–982, Aug. 1998.
- C. Miller, B. Schwalb, K. Maier, D. Schulz, S. Dümcke, B. Zacher, A. Mayer, J. Sydow, L. Marcinowski, L. Dölken, D. E. Martin, A. Tresch, and P. Cramer. Dynamic transcriptome analysis measures rates of mRNA synthesis and decay in yeast. *Molecular Systems Biology*, 7:458, Jan. 2011.
- O. Mondragón-Palomino, T. Danino, J. Selimkhanov, L. Tsimring, and J. Hasty. Entrainment of a population of synthetic genetic oscillators. *Science (New York, NY)*, 333(6047):1315–1319, Sept. 2011.
- N. A. M. Monk. Oscillatory expression of Hes1, p53, and NF-kappaB driven by transcriptional time delays. *Current biology : CB*, 13(16):1409–1413, Aug. 2003.
- L. G. Morelli, S. Ares, L. Herrgen, C. Schröter, F. Jülicher, and A. C. Oates. Delayed coupling theory of vertebrate segmentation. *HFSP journal*, 3(1):55–66, Jan. 2009.
- T. A. Moreno and C. Kintner. Regulation of Segmental Patterning by Retinoic Acid Signaling during *Xenopus* Somitogenesis. *Developmental Cell*, 6(2):14–14, Feb. 2004.
- D. Mumberg, R. Müller, and M. Funk. Regulatable promoters of *Saccharomyces cerevisiae*: comparison of transcriptional activity and their use for heterologous expression. *Nucleic acids research*, 22(25):5767–5768, Dec. 1994.
- D. Mumberg, R. Müller, and M. Funk. Yeast vectors for the controlled expression of heterologous proteins in different genetic backgrounds. *Gene*, 156(1):119–122, Apr. 1995.
- B. Novak and J. J. Tyson. Design principles of biochemical oscillators. *Nature Reviews Molecular cell biology*, 9(12):981–991, Dec. 2008.

- A. C. Oates and R. K. Ho. Hairy/E(spl)-related (Her) genes are central components of the segmentation oscillator and display redundancy with the Delta/Notch signaling pathway in the formation of anterior segmental boundaries in the zebrafish. *Development (Cambridge, England)*, 129(12):2929–2946, June 2002.
- A. C. Oates, L. G. Morelli, and S. Ares. Patterning embryos with oscillations: structure, function and dynamics of the vertebrate segmentation clock. *Development (Cambridge, England)*, 139(4):625–639, Feb. 2012.
- J. Ostling, M. Carlberg, and H. Ronne. Functional domains in the Mig1 repressor. *Molecular and Cellular Biology*, 16(3):753–761, Mar. 1996.
- I. Palmeirim, D. Henrique, D. Ish-Horowicz, and O. Pourquié. Avian hairy gene expression identifies a molecular clock linked to vertebrate segmentation and somitogenesis. *Cell*, 91(5):639–648, Nov. 1997.
- A. Picker, D. Roellig, O. Pourquié, A. C. Oates, and M. Brand. Tissue micromanipulation in zebrafish embryos. *Methods in molecular biology (Clifton, NJ)*, 546:153–172, 2009.
- O. Purcell, N. J. Savery, C. S. Grierson, and M. Di Bernardo. A comparative analysis of synthetic genetic oscillators. *Journal of The Royal Society Interface*, 7(52):1503–1524, Sept. 2010.
- I. H. Riedel-Kruse, C. Müller, and A. C. Oates. Synchrony dynamics during initiation, failure, and rescue of the segmentation clock. *Science (New York, NY)*, 317(5846):1911–1915, Sept. 2007.
- M. A. Romanos, C. A. Scorer, and J. J. Clare. Foreign gene expression in yeast: a review. *Yeast*, 8(6):423–488, May 1992.
- Y. Saga and H. Takeda. The making of the somite: molecular events in vertebrate segmentation. *Nature reviews Genetics*, 2(11):835–845, Nov. 2001.
- A. Sawada, A. Fritz, Y. J. Jiang, A. Yamamoto, K. Yamasu, A. Kuroiwa, Y. Saga, and H. Takeda. Zebrafish Mesp family genes, *mesp-a* and *mesp-b* are segmentally expressed in the presomitic mesoderm, and *Mesp-b* confers the anterior identity to the developing somites. *Development (Cambridge, England)*, 127(8):1691–1702, Mar. 2000.
- A. Sawada, M. Shinya, Y. J. Jiang, A. Kawakami, A. Kuroiwa, and H. Takeda. Fgf/MAPK signalling is a crucial positional cue in somite boundary formation. *Development (Cambridge, England)*, 128(23):4873–4880, Dec. 2001.

- C. Schröter, L. Herrgen, A. Cardona, G. J. Brouhard, B. Feldman, and A. C. Oates. Dynamics of zebrafish somitogenesis. *Developmental dynamics : an official publication of the American Association of Anatomists*, 237(3):545–553, Mar. 2008.
- C. Schröter, S. Ares, L. G. Morelli, A. Isakova, K. Hens, D. Soroldoni, M. Gajewski, F. Jülicher, S. J. Maerkl, B. Deplancke, and A. C. Oates. Topology and dynamics of the zebrafish segmentation clock core circuit. *PLoS biology*, 10(7):e1001364, July 2012.
- T. Sekiya and K. S. Zaret. Repression by Groucho/TLE/Grg Proteins: Genomic Site Recruitment Generates Compacted Chromatin In Vitro and Impairs Activator Binding In Vivo. *Molecular Cell*, 28(2):291–303, Oct. 2007.
- S. S. Shankaran, D. Sieger, C. Schröter, C. Czepe, M.-C. Pauly, M. A. Laplante, T. S. Becker, A. C. Oates, and M. Gajewski. Completing the set of h/E(spl) cyclic genes in zebrafish: her12 and her15 reveal novel modes of expression and contribute to the segmentation clock. *Developmental Biology*, 304(2):615–632, Apr. 2007.
- R. P. Shetty, D. Endy, and T. F. Knight. Engineering BioBrick vectors from BioBrick parts. *Journal of Biological Engineering*, 2(1):5, 2008.
- D. Sieger, D. Tautz, and M. Gajewski. her11 is involved in the somitogenesis clock in zebrafish. *Development genes and evolution*, 214(8):393–406, Aug. 2004.
- D. Sieger, B. Ackermann, C. Winkler, D. Tautz, and M. Gajewski. her1 and her13.2 are jointly required for somitic border specification along the entire axis of the fish embryo. *Developmental Biology*, 293(1):242–251, May 2006.
- P. A. Silver, A. Chiang, and I. Sadler. Mutations that alter both localization and production of a yeast nuclear protein. *Genes & development*, 2(6):707–717, June 1988.
- D. Soroldoni and A. C. Oates. Live transgenic reporters of the vertebrate embryo's Segmentation Clock. *Current Opinion in Genetics & Development*, 21(5):600–605, Oct. 2011.
- M. Spingola, L. Grate, D. Haussler, and M. Ares. Genome-wide bioinformatic and molecular analysis of introns in *Saccharomyces cerevisiae*. *RNA*, 5(2):221–234, Feb. 1999.
- J. Stricker, S. Cookson, M. R. Bennett, W. H. Mather, L. S. Tsimring, and J. Hasty. A fast, robust and tunable synthetic gene oscillator. *Nature*, 456(7221):516–519, Nov. 2008.

Bibliography

- I. A. Swinburne, D. G. Miguez, D. Landgraf, and P. A. Silver. Intron length increases oscillatory periods of gene expression in animal cells. *Genes & development*, 22(17):2342–2346, Sept. 2008.
- Y. Takashima, T. Ohtsuka, A. González, H. Miyachi, and R. Kageyama. Intronic delay is essential for oscillatory expression in the segmentation clock. *Proceedings of the National Academy of Sciences*, 108(8):3300–3305, Feb. 2011.
- C. Takke and J. A. Campos-Ortega. *her1*, a zebrafish pair-rule like gene, acts downstream of notch signalling to control somite development. *Development (Cambridge, England)*, 126(13):3005–3014, July 1999.
- C. Takke, P. Dornseifer, E. von Weizsäcker, and J. A. Campos-Ortega. *her4*, a zebrafish homologue of the *Drosophila* neurogenic gene *E(spl)*, is a target of NOTCH signalling. *Development (Cambridge, England)*, 126(9):1811–1821, Apr. 1999.
- M. Tigges, T. T. Marquez-Lago, J. Stelling, and M. Fussenegger. A tunable synthetic mammalian oscillator. *Nature*, 457(7227):309–312, Jan. 2009.
- A. Trofka, J. Schwendinger-Schreck, T. Brend, W. Pontius, T. Emonet, and S. A. Holley. The *Her7* node modulates the network topology of the zebrafish segmentation clock via sequestration of the *Hes6* hub. *Development (Cambridge, England)*, Jan. 2012.
- M. Ukai-Tadenuma, T. Kasukawa, and H. R. Ueda. Proof-by-synthesis of the transcriptional logic of mammalian circadian clocks. *Nature cell biology*, 10(10):1154–1163, Sept. 2008.
- B. Varnum-Finney, L. Wu, M. Yu, C. Brashem-Stein, S. Staats, D. Flowers, J. D. Griffin, and I. D. Bernstein. Immobilization of Notch ligand, Delta-1, is required for induction of notch signaling. *Journal of Cell Science*, 113 Pt 23:4313–4318, Dec. 2000.
- J. Vermot, J. Gallego Llamas, V. Fraulob, K. Niederreither, P. Chambon, and P. Dollé. Retinoic acid controls the bilateral symmetry of somite formation in the mouse embryo. *Science (New York, NY)*, 308(5721):563–566, Apr. 2005.
- O. Wartlick, A. Kicheva, and M. G. I.-G. n. Morphogen gradient formation. *Cold Spring Harbor perspectives in biology*, 1(3):a001255–a001255, Aug. 2009.
- M. Westerfield. *The Zebrafish Book: A Guide for the Laboratory Use of Zebrafish (Brachydanio Rerio)*. University of Oregon Press, Eugene, 2nd edition, 1993.
- A. T. Winfree. Biological rhythms and the behavior of populations of coupled oscillators. *Journal of Theoretical Biology*, 16(1):15–42, July 1967.

Erklärung entsprechend §5.5 der Promotionsordnung/ Declaration according to §5.5 of the doctorate regulations

PhD Thesis "Hairy Switches and Oscillators – Reconstructing the Zebrafish Segmentation Clock" submitted by Annelie Oswald

Hiermit versichere ich, dass ich die vorliegende Arbeit ohne unzulässige Hilfe Dritter und ohne Benutzung anderer als der angegebenen Hilfsmittel angefertigt habe; die aus fremden Quellen direkt oder indirekt übernommenen Gedanken sind als solche kenntlich gemacht. Die Arbeit wurde bisher weder im Inland noch im Ausland in gleicher oder ähnlicher Form einer anderen Prüfungsbehörde vorgelegt.

Die Dissertation wurde im Zeitraum vom 1. März 2009 bis 7. August 2013 verfasst, am 30. Januar 2014 verteidigt und von Prof. Dr. Andrew C. Oates , MPI-CBG (Dresden, Germany) & UCL/MRC-NIMR (London, UK seit Oktober 2012) betreut.

Meine Person betreffend erkläre ich hiermit, dass keine früheren erfolglosen Promotionsverfahren stattgefunden haben.

Ich erkenne die Promotionsordnung der Fakultät für Mathematik und Naturwissenschaften, Technische Universität Dresden an.

I herewith declare that I have produced this paper without the prohibited assistance of third parties and without making use of aids other than those specified; notions taken over directly or indirectly from other sources have been identified as such. This paper has not previously been presented in identical or similar form to any other German or foreign examination board.

The thesis work was conducted from *March 1st 2009 to August 7th 2013 and defended on January 30th 2014* under the supervision of *Prof. Dr. Andrew C. Oates at MPI-CBG (Dresden, Germany) & UCL /MRC-NIMR (London, UK - since Oktober 2012).*

I declare that I have not undertaken any previous unsuccessful doctorate proceedings.

I declare that I recognize the doctorate regulations of the *Fakultät für Mathematik und Naturwissenschaften* of the *Technische Universität Dresden*.

02.05.2014

Date


Annelie Oswald